



Classe di Scienze Matematiche, Fisiche e Naturali  
*Corso di Perfezionamento in Scienze Chimiche*

**“The chemistry of unsaturated hydrocarbyl  
ligands bridging coordinated in  
diiron or diruthenium complexes”**



*Adriano Boni*

*Pisa, anno accademico 2010/2011*

## Index

1. Abstract.....	3
2. Introduction.....	5
2.1 Allenyl ligand: types of coordination.....	7
2.2 Synthesis of dinuclear $\mu$ -allenyl complexes.....	13
2.3 Chemistry of dinuclear $\mu$ -allenyl complexes.....	17
2.4 Vinyl ligand: types of coordination.....	25
2.5 Synthesis of dinuclear $\mu$ -vinyl complexes.....	31
2.6 Chemistry of dinuclear $\mu$ -vinyl complexes.....	36
2.7 Objective.....	42
3. Results and Discussion.....	43
3.1 Dimetallacyclopentenones: Synthesis and characterization.....	43
3.2 Chemistry of the Cationic diruthenium $\mu$ -allenyl complexes.....	47
3.3 Chemistry of the cationic diiron $\mu$ -allenyl complexes.....	69
3.4 Chemistry of the cationic diriron $\mu$ -vinyl complexes.....	78
4. Conclusions.....	102
5. Experimental.....	106
6. Crystallographic Appendix.....	120
7. Bibliography.....	126

## 1. Abstract

The reactivity of the previously reported diruthenium  $\mu$ -allenyl complex  $[\text{Ru}_2(\text{Cp})_2(\text{CO})_2(\mu\text{-CO})\{\mu\text{-}\eta^1\text{:}\eta^2_{\alpha,\beta}\text{-C(H)=C=C(Me)}_2\}][\text{BF}_4]$  (**4a**) and of the new one  $[\text{Ru}_2(\text{Cp})_2(\text{CO})_2(\mu\text{-CO})\{\mu\text{-}\eta^1\text{:}\eta^2_{\alpha,\beta}\text{-C(H)=C=C(Ph)}_2\}][\text{BF}_4]$  (**4b**) have been investigated. The reaction of **4b** with Brönsted base results in formation of the  $\mu$ -allenylidene derivative  $[\text{Ru}_2\text{Cp}_2(\text{CO})_2(\mu\text{-CO})\{\mu\text{-}\eta^1\text{:}\eta^1\text{-C=C=C(Ph)}_2\}]$  (**10**). The nitrile adducts  $[\text{Ru}_2\text{Cp}_2(\text{CO})(\text{NCMe})(\mu\text{-CO})\{\mu\text{-}\eta^1\text{:}\eta^2\text{-C(H)=C=C(R)}_2\}]^+$  (R = Me, **6a**; R = Ph, **6b**), prepared by treatment of **4a,b** with MeCN/Me<sub>3</sub>NO, react with N<sub>2</sub>CHCO<sub>2</sub>Et/NEt<sub>3</sub> at room temperature affording the butenolide-substituted carbene complexes  $[\text{Ru}_2\text{Cp}_2(\text{CO})(\mu\text{-CO})\{\mu\text{-}\eta^1\text{:}\eta^3\text{-C}_\alpha\text{(H)}\overline{\text{C}_\beta\text{C}_\gamma\text{(R)}_2\text{OC(=O)C(H)}}\}]$  (R = Me, **13a**; R = Ph, **13b**). The intermediate cationic  $[\text{Ru}_2\text{Cp}_2(\text{CO})(\mu\text{-CO})\{\mu\text{-}\eta^1\text{:}\eta^3\text{-C}_\alpha\text{(H)}\overline{\text{C}_\beta\text{C}_\gamma\text{(Me)}_2\text{OC(OEt)C(H)}}\}]^+$  (**12**) has been detected in the course of the reaction leading to **13a**. Alternatively, the addition of N<sub>2</sub>CHCO<sub>2</sub>Et/NHEt<sub>2</sub> to **4a** gives the 2-furaniminium-carbene  $[\text{Ru}_2\text{Cp}_2(\text{CO})(\mu\text{-CO})\{\mu\text{-}\eta^1\text{:}\eta^3\text{-C}_\alpha\text{(H)}\overline{\text{C}_\beta\text{C}_\gamma\text{(Me)}_2\text{OC(NEt}_2\text{)C(H)}}\}]^+$  (**14**). The X-Ray structures of **4a**][BPh<sub>4</sub>], **4c**][BPh<sub>4</sub>], **13a**, **13b** and **14**][BF<sub>4</sub>] have been determined.

The novel cationic diiron  $\mu$ -allenyl complexes  $[\text{Fe}_2(\text{Cp})_2(\text{CO})_2(\mu\text{-CO})\{\mu\text{-}\eta^1\text{:}\eta^2_{\alpha,\beta}\text{-C(H)=C=C(R)}_2\}][\text{BF}_4]$  (R = Me, **7a**; R = Ph, **7b**) have been obtained in good yields by a two-step reaction starting from  $[\text{Fe}_2\text{Cp}_2(\text{CO})_4]$ . The solid state structures of **7a**][CF<sub>3</sub>SO<sub>3</sub>] has been ascertained by X-Ray diffraction studies. The reaction of **7a** with Brönsted bases yields the dimetallacyclopentenone  $[\text{Fe}_2\text{Cp}_2(\text{CO})(\mu\text{-CO})\{\mu\text{-}\eta^1\text{:}\eta^3\text{-$

C(H)=C(C(Me)CH<sub>2</sub>)C(=O))}] (**16**). The reactions of **7a,b** with MeCN/Me<sub>3</sub>NO result in prevalent decomposition to mononuclear iron species.

The diiron  $\mu$ -vinyl complex [Fe<sub>2</sub>Cp<sub>2</sub>(CO)( $\mu$ -CO){ $\mu$ - $\mu^1$ : $\mu^2$ -CH=CH(Ph)}][BF<sub>4</sub>], **9**, undergoes reduction by means of CoCp<sub>2</sub> affording selectively the C–C coupling Fe<sub>4</sub> compound [Fe<sub>2</sub>Cp<sub>2</sub>(CO)<sub>2</sub>( $\mu$ -CO){ $\mu$ - $\mu^2$ -CHCH(Ph)}] **16**. The cation [**9**]<sup>+</sup> has been regenerated from **16** in good yield upon treatment with I<sub>2</sub>. Electrochemical studies have outlined that the reduction of **9** to **16**, occurring at -0.92V, is reversible and proceeds with intermediate formation of the radical species [Fe<sub>2</sub>Cp<sub>2</sub>(CO)<sub>2</sub>( $\mu$ -CO){ $\mu$ -CHCH(Ph)}], **17**. This latter has been characterized by EPR spectroscopy. The structures of **9**, **16** and **17** have been optimized for the gas phase by DFT calculations; the computed enthalpy related to the equilibrium **17**  $\rightleftharpoons$  **16** is  $\Delta H = -12.25 \text{ KJ}\cdot\text{mol}^{-1}$ . The reaction of **9** with CoCp<sub>2</sub> in the presence of excess PhSSPh affords the mononuclear complex [Fe<sub>2</sub>Cp<sub>2</sub>(CO)<sub>2</sub>( $\mu$ -CO){ $\mu$ - $\mu^2$ -CHCH(Ph)(SPh)}], **18**, in 70% yield. The new compounds **16** and **18** have been fully characterized by IR and NMR spectroscopy, elemental analysis and X-Ray diffraction studies.

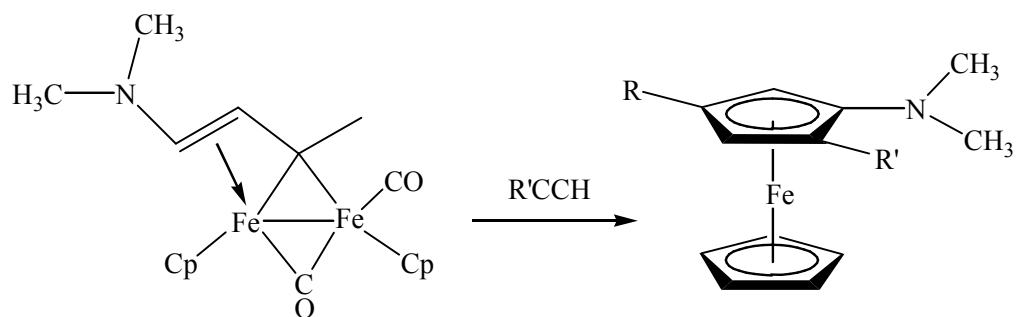
## 2. Introduction

The addition of organic reactants to unsaturated hydrocarbyl fragments, promoted by transition metal species, is a topic arousing great interest, due to the wide applications both in laboratory synthesis and in industrial processes<sup>1</sup>. In this context, the activation of hydrocarbyl units, bridged coordinated in dinuclear iron or ruthenium complexes bearing ancillary cyclopentadienyl and/or carbonyl ligands, has been widely investigated<sup>2</sup>. Indeed, dinuclear metal species often provide unconventional reactivity patterns to bridging ligands, as consequence of the cooperativity effects due to the two metal centres working in concert<sup>3</sup>. Therefore, metal-bound hydrocarbyl groups may be converted into unusual organic species, which could not be attainable through common organic procedures. Furthermore, the bimetallic core may play a key role in the stabilization of the new species, offering the possibility of different coordination fashions.

These reactions, particularly those leading to carbon-carbon bond formation, have attracted interest because they may act as models for heterogeneously catalyzed processes occurring on metal surfaces<sup>4</sup>.

As a noticeable example, several papers have appeared in the last decade on the chemistry of diiron complexes containing a bridging vinyliminium ligand,  $[-C(R)=C(R')C=N(Me)(R'')]^{+}$ , held by the frame  $[Fe_2Cp_2(CO)_2]$ . These metal compounds have revealed to be convenient starting materials for the preparation of unusual “organic architectures” in mild conditions, by stepwise functionalization of the  $C_3$  chain<sup>5</sup>. Interesting examples of the potentiality of these materials are the following: *i)*

synthesis of a selenophene-functionalized carbene complex<sup>5a</sup>; *ii*) synthesis of ferrocenes substituted at one Cp ring only, *via* alkyne cycloaddition to the vinyliminium (Scheme 1).



*Scheme 1: Formation of a tetrasubstituted ferrocenyl complex from a bridging vinyliminium dinuclear complex.*

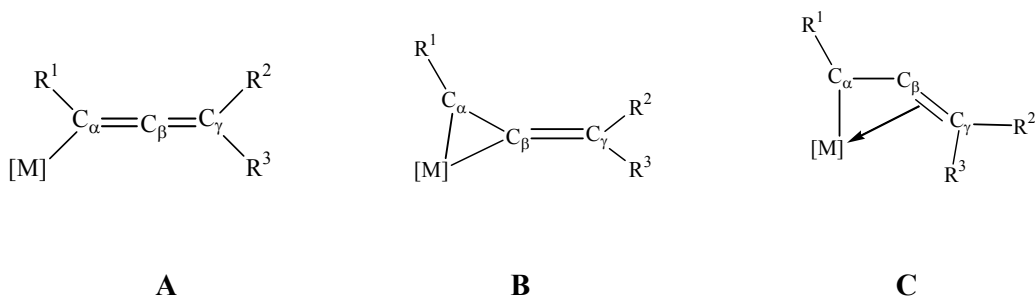
## 2.1 Allenyl ligand: types of coordination

Among the unsaturated hydrocarbyl species, allenyl ligands  $[-C(H)=C=CRR']$  in mono-, di- and poly-nuclear complexes have attracted increased attention, since their coupling reactions with unsaturated organics may provide interesting derivatives<sup>6</sup>. In particular, di- and poly-nuclear species have attracted considerable attention: the unsaturated  $C_3$  chain, similarly to the vinyliminium one, readily undergoes coupling reactions with organic fragments, providing an easy route for the synthesis of new multisite-bound hydrocarbyl ligands.

Allenyls possess diverse bonding capabilities, and each can provide host metal centre(s) with up to 5 electrons through  $\sigma$  and  $\pi$  interactions upon further complexation.

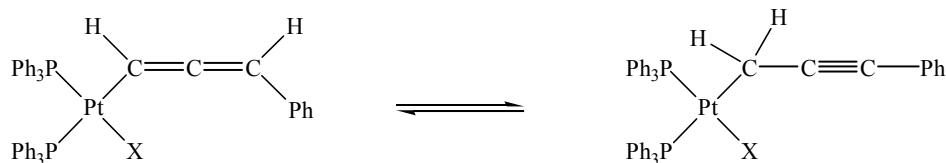
### 2.1.1 Mononuclear complexes

In mono-nuclear complexes three modes are possible, depending on the number of carbons involved (Scheme 2):



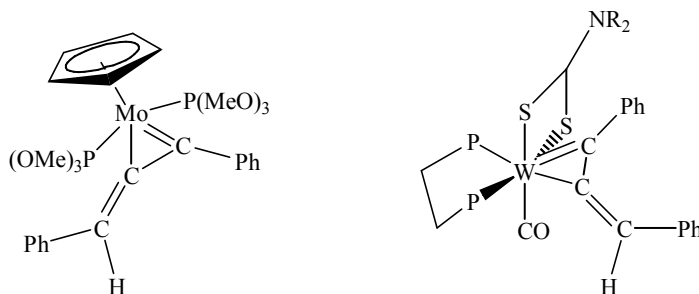
*Scheme 2: Coordination modes observed in mononuclear allenyl complexes.*

The simple  $\eta^1$  coordination, **A**, involves only the  $C_\alpha$  of the ligand, which is  $\sigma$ -bound to the metal. A noticeable example<sup>7</sup> is depicted in Scheme 3; As in many cases,  $\eta^1$ -allenyl complexes exhibit slow tautomerization to yield an equilibrium mixture with the  $\eta^1$ -propargyl isomer.



*Scheme 3: Reversible interconversion between  $\eta^1$ -allenyl and  $\eta^1$ -propargyl platinum complexes.*

Mononuclear  $\eta^2$ -allenyl or metallamethylenecyclopropene complexes represent a small group of compounds in which the (neutral) organic ligand behaves as a 3-electron donor. The  $\eta^2$  coordination, **B**, involves two metal-carbon interactions:  $\pi$ -interaction with  $C_\alpha$  and  $\sigma$ -interaction with  $C_\beta$ . Two structures<sup>8,9</sup> are reported as an example (Scheme 4).

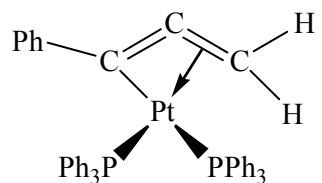


*Scheme 4: Molybdenum (a) and tungsten (b)  $\eta^2$ -allenyl complexes.*

The  $\eta^3$  coordination mode, **C**, is the most common one found in mononuclear complexes, as is the case of  $[\text{Os}(\text{PMe}_3)_4(\eta^3\text{-C}(\text{Ph})=\text{C}=\text{C}(\text{H})(\text{Ph}))]\text{PF}_6$ <sup>10</sup> and



$[\text{Pt}(\text{PPh}_3)_2(\eta^3\text{-C}(\text{Ph})=\text{C}=\text{CH}_2)]\text{PF}_6$  (see Scheme 5).<sup>11</sup> This type of coordination consists of three metal-carbon interactions:  $\sigma$  (through  $\text{C}_\alpha$ ), and  $\pi$  (through the  $\text{C}_\alpha=\text{C}_\beta$  double bond).

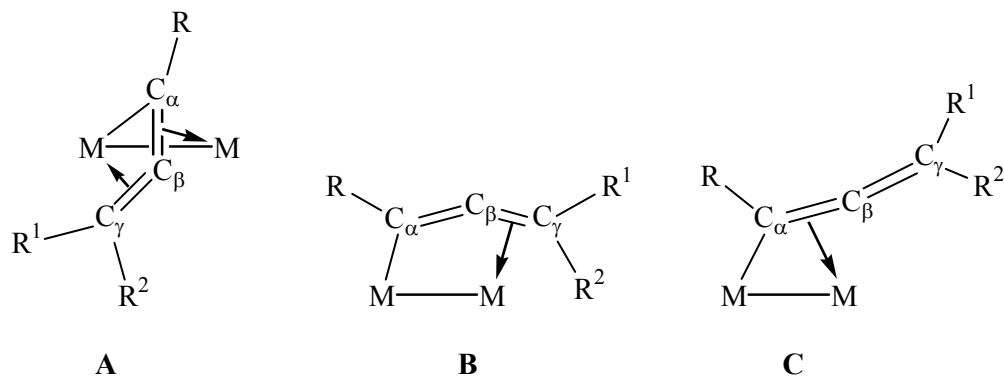


*Scheme 5:  $\eta^3$ -allenyl platinum complex.*

### 2.1.2 Dinuclear complexes

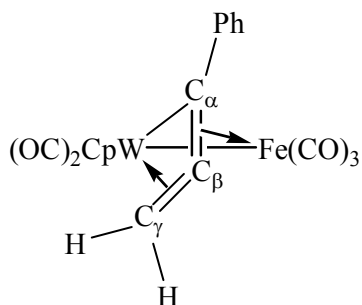
Dinuclear complexes, as well as mononuclear ones, exhibit three possible coordination fashions, which are represented in

Scheme 6.



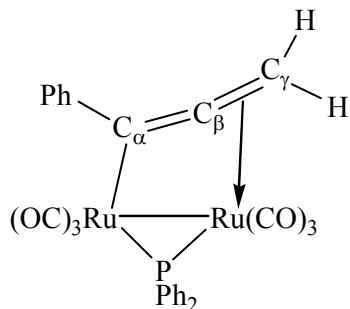
*Scheme 6: Coordination modes in mononuclear allenyl complexes.*

A  $\eta^3$ -allenyl ligand can become a 5-electron  $\eta^2:\eta^3$  donor upon coordination to two metal centres, as showed for **A**. Dinuclear compounds containing such  $\eta^2:\eta^3$ -allenyl ligand have been known for over a decade, and here one example is reported<sup>12</sup>.



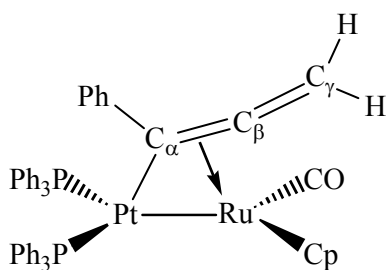
*Scheme 7:  $\mu\text{-}\eta^2:\eta^3$ -allenyl iron-tungsten complex.*

The only case of type **B** coordination mode complex is  $\text{Ru}_2(\text{CO})_6(\mu\text{-PPh}_2)(\mu\text{-}\eta^1:\eta^2\text{-C(Ph)=C=CH}_2)$ , reported by Carty and coworkers<sup>13</sup> in 1986. This compound, as well as its  $\text{Os}_2$  analogue, show unusual  $\mu\text{-}\eta^1:\eta^2_{\beta,\gamma}$ -allenyl coordination<sup>14</sup> (Scheme 8). In fact, allenyls in  $\text{M}_2(\text{CO})_6(\mu\text{-PPh}_2)(\mu\text{-}\eta^1:\eta^2\text{-C(R)=C=CR}'_2)$  complexes behave as 3-electron donors binding the metal atoms through the  $\text{C}_\alpha=\text{C}_\beta$  bond;<sup>15</sup>



*Scheme 8:  $\mu\text{-}\eta^1:\eta^2_{\beta,\gamma}$ -diruthenium complex.*

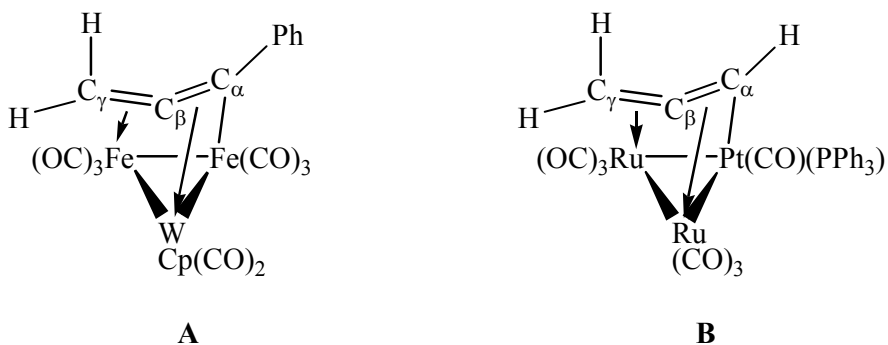
The solid state structures of several  $\mu\text{-}\eta^1\text{:}\eta^2_{\alpha,\beta}$ -allenyl complexes, **C**, have been elucidated by X-ray diffraction<sup>1,2,16</sup>. Thus, the allenyl fragment is differently bent, with the C–C–C angle ranging between 143 and 157°. The  $\text{C}_\alpha\text{=C}_\beta$  bond distance (1.36÷1.40 Å) is somewhat lengthened compared to the free C=C double bond, whereas the  $\text{C}_\beta\text{=C}_\gamma$  bond distance (1.31÷1.35 Å) resembles that of an unperturbed C=C double bond. For homometallic complexes, the  $\text{M}_\beta\text{--C}_\alpha$  and  $\text{M}_\beta\text{--C}_\beta$  bonds are longer than the  $\text{M}_\alpha\text{--C}_\alpha$  bond, as expected for  $\pi$  and  $\sigma$  interactions respectively (see Scheme 9).<sup>15b</sup>



*Scheme 9:  $\mu\text{-}\eta^1\text{:}\eta^2_{\alpha,\beta}$ -platinum-ruthenium complex.*

### 2.1.3 Trinuclear complexes

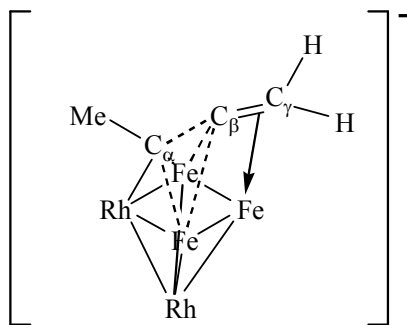
In the case of trinuclear allenyl compounds, only one type of coordination has been reported in the literature. These complexes contain an allenyl ligand that is  $\eta^1$ –bonded to one metal centre through  $\text{C}_\alpha$  and  $\eta^2$ –bonded to the remaining metal atoms through  $\text{C}_\alpha\text{=C}_\beta$  and  $\text{C}_\beta\text{=C}_\gamma$ . Thus the allenyl behaves as a overall 5-electron donor (see Scheme 10<sup>12</sup>).



Scheme 10: Examples of trinuclear allenyl complexes.

#### 2.1.4 Polynuclear complexes

The anionic pentanuclear cluster  $[\text{Rh}_2\text{Fe}_3(\text{CO})_{10}(\mu_2\text{-CO})_3(\mu_4\text{-}\eta^1\text{:}\eta^2\text{:}\eta^2\text{-C}(\text{Me})=\text{C}=\text{CH}_2)]^-$ <sup>17</sup>, whose simplified structure is reported in Scheme 11, represents the unique case of allenyl metal compound with nuclearity higher than 3. As observed for trinuclear clusters, the allenyl ligand is  $\eta^1$ -coordinated through  $\text{C}_\alpha$  to one metal and  $\eta^2$ -coordinated through  $\text{C}_\beta=\text{C}_\gamma$  to the diagonally opposite metal; the  $\text{C}_\alpha=\text{C}_\beta$  double bond is coordinated also to both the remaining metals.



Scheme 11: pentanuclear allenyl compound,

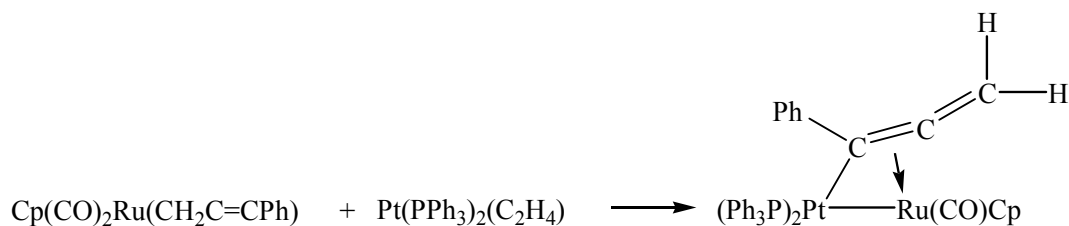
$[\text{Rh}_2\text{Fe}_3(\text{CO})_{10}(\mu_2\text{-CO})_3(\mu_4\text{-}\eta^1\text{:}\eta^2\text{:}\eta^2\text{-C}(\text{Me})=\text{C}=\text{CH}_2)]^-$ ,  
(carbonyl ligands are omitted for sake of clearness).

## 2.2 Synthesis of dinuclear $\mu$ -allenyl complexes

Four synthetic procedures have been reported for the preparation of dinuclear bridging allenyl complexes, and they are described in the following.

### 2.2.1 Reaction of mononuclear metal $\eta^1$ -allenyls or $\eta^1$ -propargyls with low-valent metal complexes

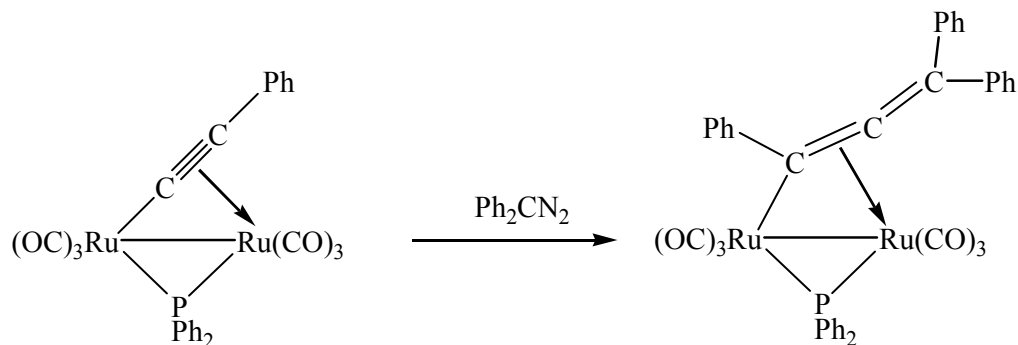
This method<sup>15a,1816a</sup> is useful for the synthesis of heterometallic  $\mu$ - $\eta^1:\eta^2_{\alpha,\beta}$ -allenyl complexes. The unattached carbon-carbon multiple bond(s) of the reacting allenyl or propargyl complex is (are) employed in coordination to another metal, thus initiating a sequence of steps leading to a higher nuclearity product (example in Scheme 12).



Scheme 12: Synthesis of  $[\text{Pt(PPh}_3)_2\text{Ru(CO)(Cp)}](\mu\text{-}\eta^1:\eta^2\text{-PhC=C=CH}_2)$

### 2.2.2 Reaction of dinuclear metal acetylides with diazomethane

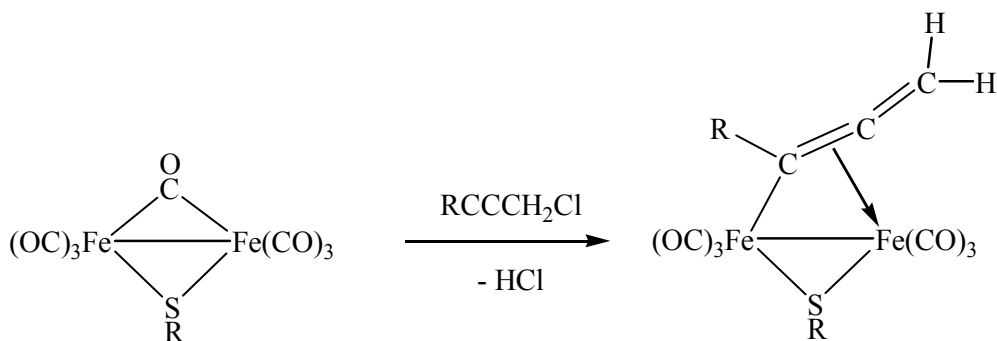
This method was developed by Carty<sup>13,15b</sup> and coworkers and has been applied to homobimetallic complexes. Reaction of dinuclear metal acetylides with diazomethane results in nucleophilic attack occurring regiospecifically at  $\text{C}_\alpha$ , to afford a bridging allenyl complex (see Scheme 13).<sup>15b</sup>



Scheme 13: Synthesis of  $[Ru_2(CO)_6(\mu-PPh_2)(\mu-\eta^1:\eta^2-PhC=C=CPh_2)]$ .

### 2.2.3 Reaction of binuclear metal carbonyl anions with propargyl halides

This procedure consists of nucleophilic attack of metal carbonyl anions on propargyl cations. For example<sup>19</sup>, the generic complex  $[Fe_2(CO)_6(\mu-SR)(\mu-CO)]^-$  reacts with a variety of propargyl halides affording the corresponding dinuclear bridging allenyl complex  $[Fe_2(CO)_6(\mu-SR)(\mu-\eta^1:\eta^2-RC=C=CH_2)]$  (Scheme 14).

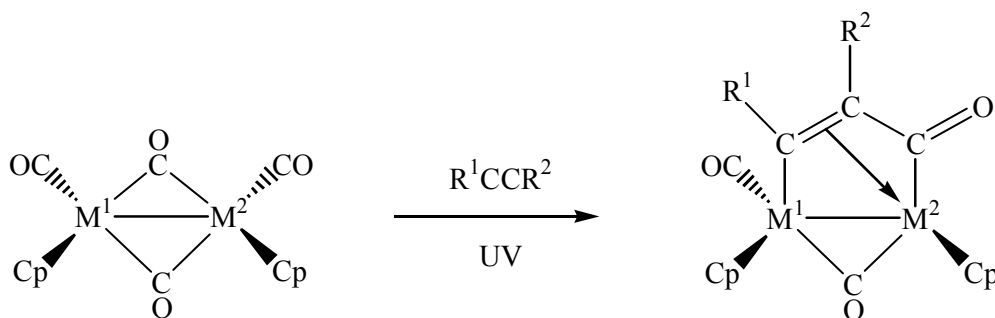


Scheme 14: Synthesis of  $[Fe_2(CO)_6(\mu-SR)(\mu-\eta^1:\eta^2-RC=C=CH_2)]$ .

### 2.2.4 Alkyne exchange and Dehydration

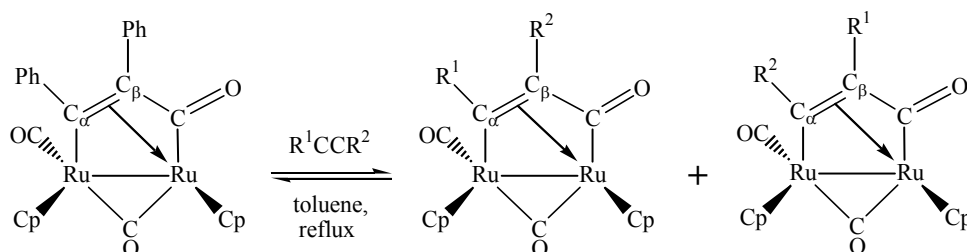
Knox and coworkers discovered that a convenient route to  $\mu-\eta^1:\eta^2_{\alpha\beta}$ -allenyl complexes is the photolytic reaction of an alkyne with  $[M^1M^2(CO)_2(\mu-CO)_2(Cp)_2]$

( $M^1=M^2=Fe$ ;  $M^1=Fe$ ,  $M^2=Ru$ ;  $M^1=M^2=Ru$ ) to afford the dimetallacyclopentenone  $[M^1M^2(CO)(\mu-CO)_2\{\mu-\eta^1:\eta^3-C(R^1)C(R^2)C(O)\}(Cp)_2]$  ( $M^1=M^2=Ru$ , **1**;  $M^1=M^2=Fe$ , **2**;  $M^1=Fe$ ,  $M^2=Ru$ , **3**) in good yield<sup>20</sup> (Scheme 15).



*Scheme 15: Photolytic insertion of an alkyne into the M–CO bond of  $[M^1M^2(CO)_2(\mu-CO)_2(Cp)_2]$  ( $M^1=M^2=Ru$ , **1**;  $M^1=M^2=Fe$ , **2**;  $M^1=Fe$ ,  $M^2=Ru$ , **3**).*

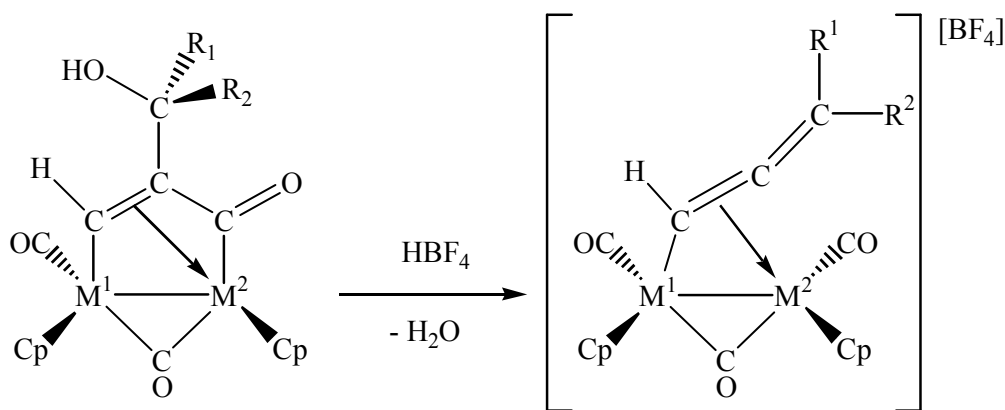
While in the case of the mixed iron-ruthenium dimetallacyclopentenone<sup>2d</sup> a large variety of alkynes undergo insertion in the Ru–CO bond of  $[RuFe(CO)_2(\mu-CO)_2(Cp)_2]$ , the same reaction involving the diruthenium complex  $[Ru_2(CO)_2(\mu-CO)_2(Cp)_2]$  is limited to diphenylacetylene<sup>20a</sup>, affording **1**. However, **1** gives alkyne exchange when heated at reflux in toluene with an excess of  $R^1C\equiv CR^2$ <sup>21</sup>; it is important to notice that this reaction may produce an inseparable mixture of two regioisomers, with either  $R^1$  or  $R^2$  being the substituent at  $C_\alpha$  (Scheme 16).



*Scheme 16: Alkyne exchange reaction of  $[Ru_2(CO)_2(\mu-CO)_2(Cp)_2]$ ,*

When the exchange process illustrated in Scheme 16 is carried out by using a terminal alkyne, the reaction is governed by steric factors so that the alkyne-hydrogen will be found at C<sub>α</sub>. On the other hand, the reaction is controlled by electronic factors in case of use of internal alkynes, with the most withdrawing substituent binding to the relatively electron-rich C<sub>β</sub>.

The facile exchange reaction makes complex **1** as a source of the highly reactive intermediate “[Ru<sub>2</sub>(CO)<sub>3</sub>(Cp)<sub>2</sub>]”. By this approach<sup>22</sup>, it has been possible to prepare the cationic μ-allenyl complexes [M<sup>1</sup>M<sup>2</sup>Cp<sub>2</sub>(CO)<sub>2</sub>(μ-CO) {μ-η<sup>1</sup>:η<sup>2</sup>-C(H)=C=C(Me)(R)}] [BF<sub>4</sub>] (M<sup>1</sup>=M<sup>2</sup>=Ru: R=Me, **4a**; R=Ph, **4b**; M<sup>1</sup>=Ru, M<sup>2</sup>=Fe: R=Me, **5**) in good yields; the synthesis includes a protonation followed by dehydration step starting from dimetallacyclopentenone species obtained by insertion of an alkynol of general formula HC≡C-C(R<sup>1</sup>)(R<sup>2</sup>)OH (Scheme 17).



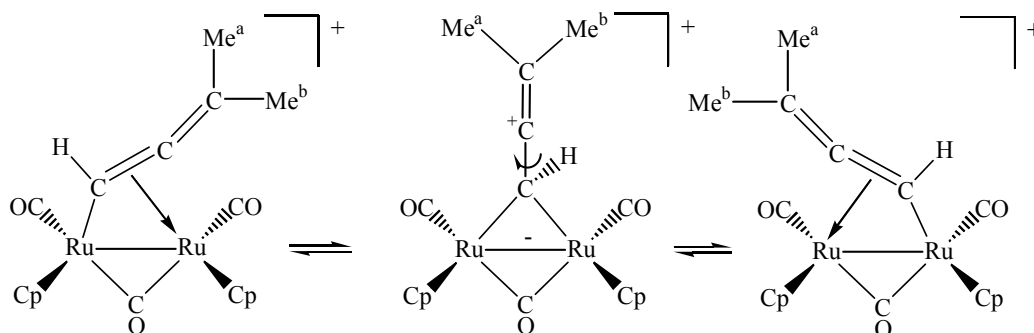
*Scheme 17: Dehydration step affording [M<sup>1</sup>M<sup>2</sup>Cp<sub>2</sub>(CO)<sub>2</sub>(μ-CO) {μ-η<sup>1</sup>:η<sup>2</sup>-C(H)=C=C(R<sup>1</sup>)(R<sup>2</sup>)}] [BF<sub>4</sub>].*



## 2.3 Chemistry of dinuclear $\mu$ -allenyl complexes

### 2.3.1 Fluxionality

NMR studies on the  $\mu$ - $\eta^1:\eta^2$ -allenyl complex  $[\text{Fe}_2(\text{CO})_6(\mu\text{-SR})(\mu\text{-}\eta^1:\eta^2\text{-HC=C=CH}_2)]$  carried out by Seyferth and coworkers showed that the methylene protons equivalent at room temperature on the NMR timescale<sup>19</sup>. It was determined that there was a close structural similarity between the allenyl bonding mode and that of a bridging  $\sigma$ - $\pi$  vinyl, both of which undergoing a fluxional process known as “windshield wiper” exchange<sup>23</sup>. This process consists of rapid exchange of the  $\sigma$  and  $\pi$  bonds of the bridging allenyl between the two metal centres. Analogous evidence has been found for the diruthenium cationic  $\mu$ -allenyl complex **4a** (Scheme 18) but not for **4b**. This has been attributed to the presence of a phenyl substituent on  $\text{C}_\gamma$  in the latter. The phenyl group, being sterically bulkier than the methyl, prefers axial orientation with respect to the Ru-Ru axis; a  $\sigma/\pi$  exchange would lead the phenyl substituent in a sterically unfavoured position<sup>21</sup>.

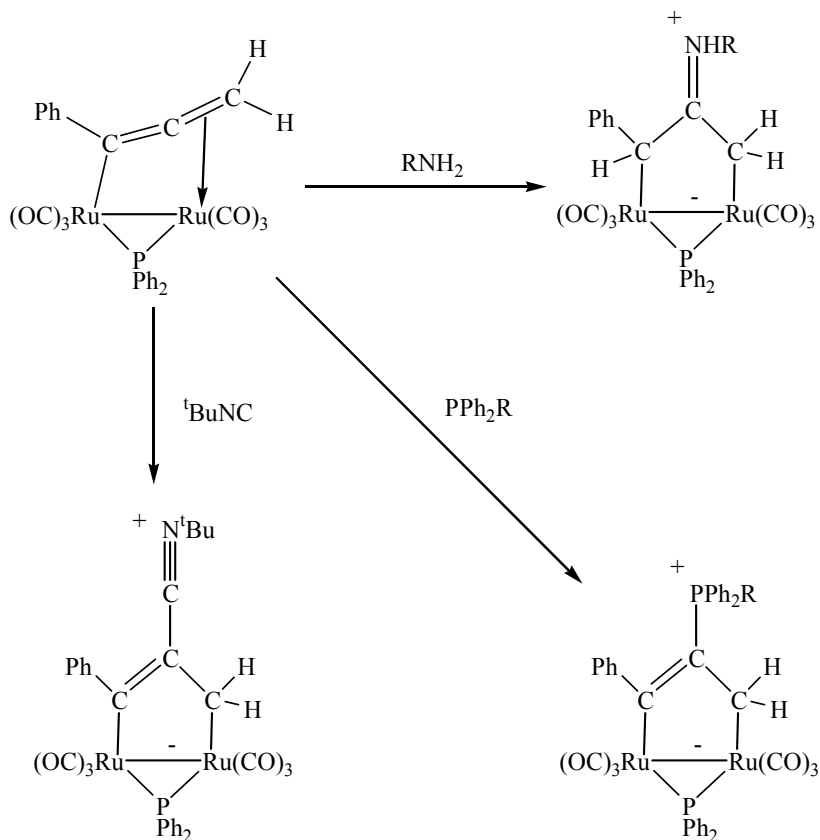


Scheme 18: Fluxionality in complex **4a**.

### 2.3.2 Reactivity with nucleophilic reagents

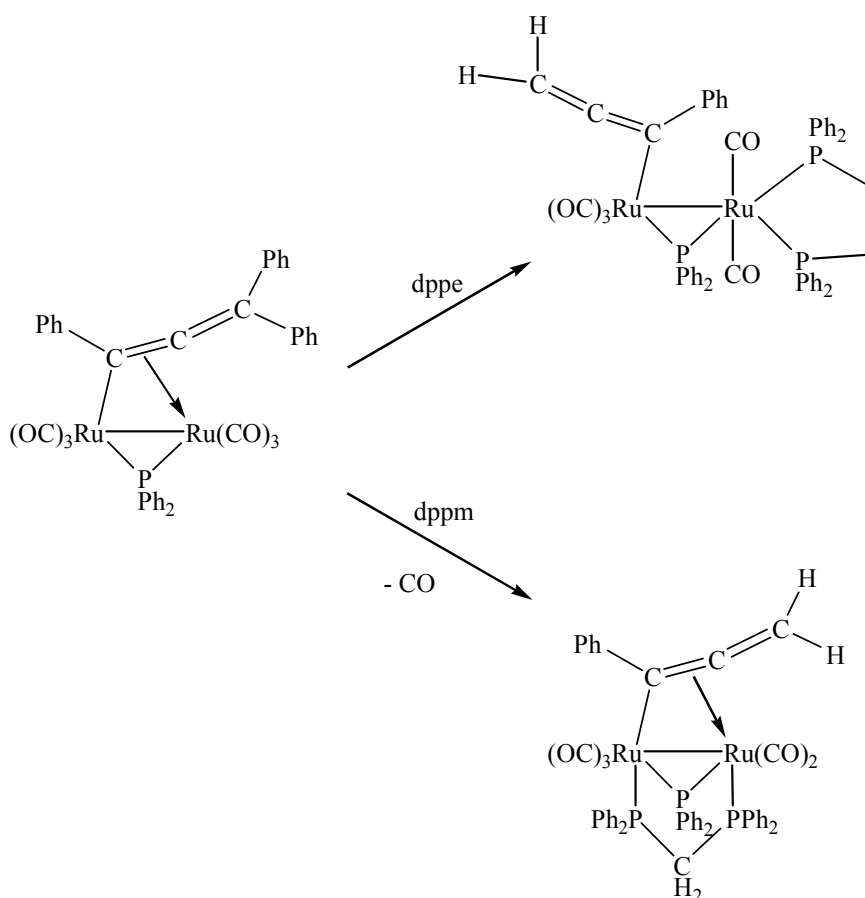
In principle, the  $\mu$ -allenyl ligand contains three sites susceptible of nucleophilic attack, *i.e.* the  $\alpha$ ,  $\beta$  and  $\gamma$  carbons. Actually, to date examples are dominated by the attack at the  $\beta$  carbon.

For example, Carty and coworkers<sup>24</sup> investigated the reaction of the diruthenium  $\mu$ - $\eta^1:\eta^2$ -allenyl complex  $[\text{Ru}_2(\text{CO})_6(\mu\text{-PPh}_2)(\mu\text{-}\eta^1:\eta^2\text{-PhC=C=CH}_2)]$  with carbon, phosphorus and nitrogen nucleophiles. All the latter attacked regioselectively at  $\text{C}_\beta$  to afford novel, zwitterionic five-membered dimetallacycles (Scheme 19).



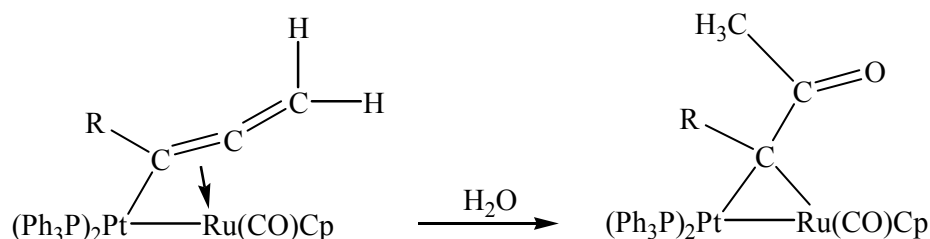
Scheme 19: Reactivity of  $[\text{Ru}_2(\text{CO})_6(\mu\text{-PPh}_2)(\mu\text{-}\eta^1:\eta^2\text{-PhC=C=CH}_2)]$  towards nucleophiles.

When a bidentate nucleophile is employed, the attack may occur at the metal centre, as it was observed in the reaction of  $[\text{Ru}_2(\text{CO})_6(\mu\text{-PPh}_2)(\mu\text{-}\eta^1:\eta^2\text{-PhC}\equiv\text{C}\equiv\text{CPh}_2)]$  with dppe and dppm<sup>25</sup>. The aptitude of dppe to behave as a bidentate ligand towards a single metal centre, makes the allenyl displacing from the  $\eta^2$ -coordination. In the case of dppm, the latter bridges the two metals to form a five-membered cycle without affecting the Ru-allenyl binding (Scheme 20).



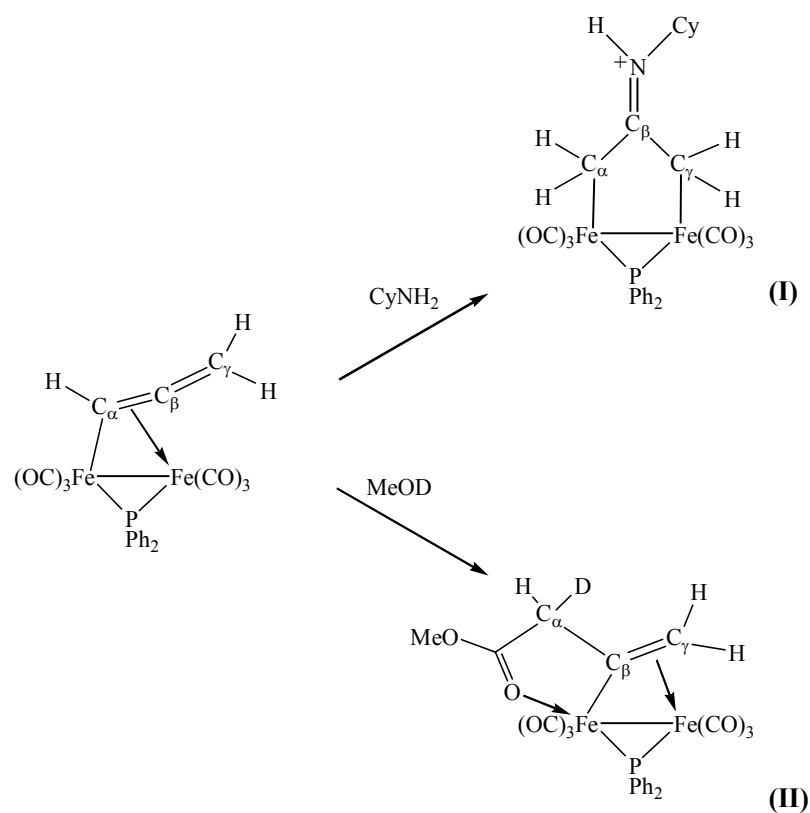
Scheme 20: Reaction of  $[\text{Ru}_2(\text{CO})_6(\mu\text{-PPh}_2)(\mu\text{-}\eta^1:\eta^2\text{-PhC}\equiv\text{C}\equiv\text{CPh}_2)]$  with dppe and dppm.

Further example<sup>26</sup> of nucleophilic attack occurring at the C<sub>β</sub> is given by the reaction of  $[(PPh_3)_2Pt(\mu-H)(\mu-\eta^1:\eta^2-C(R)=C=CH_2)Ru(CO)Cp]$  with water, promoted by acidic alumina, affording the hydrido-alkylidene complexes  $[(PPh_3)_2Pt(\mu-H)(\mu-\eta^1:\eta^1-C(R)C(O)CH_3)Ru(CO)Cp]$  (R = H, Ph) (Scheme 21).



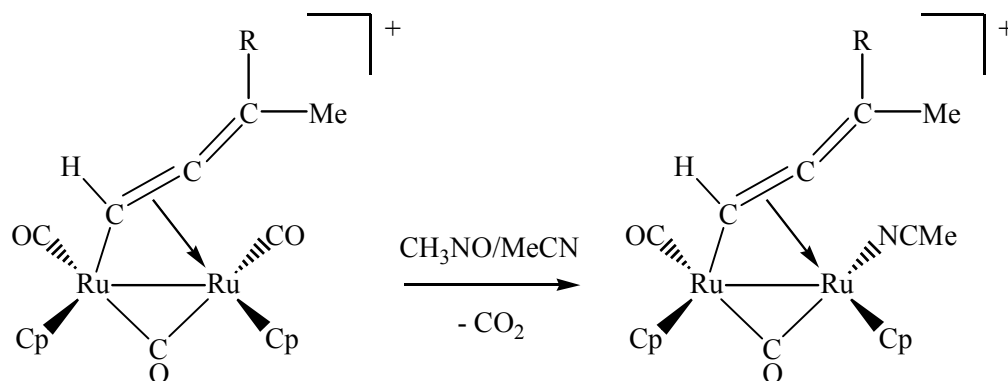
*Scheme 21: Reaction of  $[(PPh_3)_2Pt(\mu-H)(\mu-\eta^1:\eta^2-C(R)=C=CH_2)Ru(CO)Cp]$  with water.*

The reactions of homonuclear metal hexacarbonyl  $\mu$ -allenyl complexes have received considerable attention from Doherty and coworkers. They found that several diiron and diruthenium compounds of general formula  $[M_2(CO)_6(\mu-X)(\mu-\eta^1:\eta^2-C(R)=C=CR^1_2)]$  (X = PPh<sub>2</sub>, SBu-t; R = H, Ph; R<sup>1</sup><sub>2</sub> = H<sub>2</sub>, Ph<sub>2</sub>) were able to react readily with primary amines<sup>27</sup>, alcohols<sup>28</sup>, organolithium reagents<sup>16b</sup>, isocyanides<sup>29</sup>, phosphite esters<sup>6j</sup>, and monodentate and bidentate phosphines<sup>6i,6j,25,30</sup>. In most cases, the nucleophile added to the allenyl ligand, although additions to the metal and the carbonyl ligand have been described too. Examples of nucleophilic attack respectively at the allenyl C<sub>β</sub><sup>27b</sup> (Scheme 22, I) and at CO with consequent intramolecular rearrangement<sup>28</sup> (Scheme 22, II) are presented.



*Scheme 22: Reaction of  $[\text{Fe}_2(\text{CO})_6(\mu\text{-PPh}_2)(\mu\text{-}\eta^1:\eta^2\text{-C(H)=C=CH}_2)]$  with  $\text{CyNH}_2$  (I) and  $\text{MeOD}$  (II).*

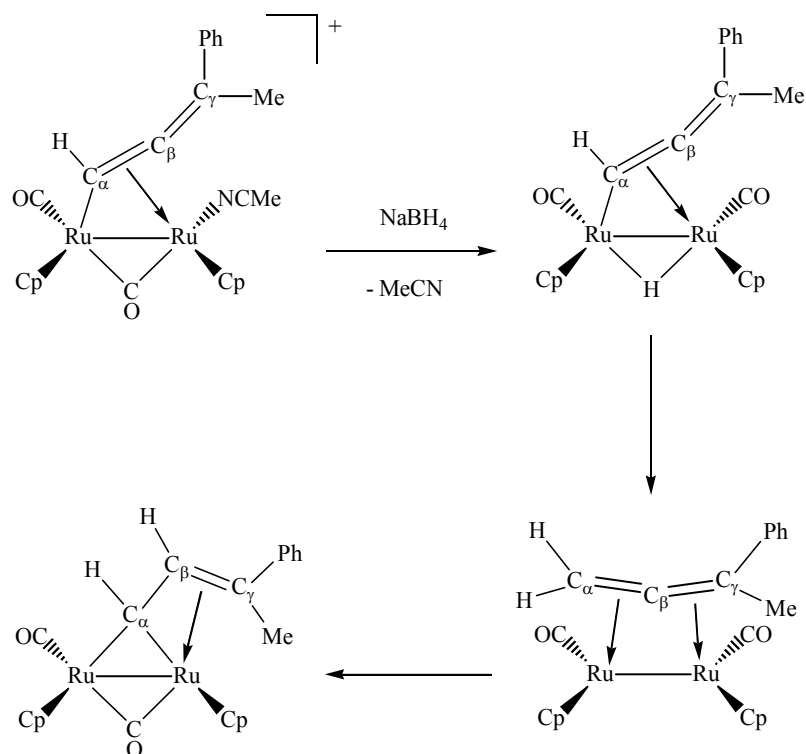
Preliminary studies on the chemistry of the diruthenium  $\mu$ -allenyl complex **4a** have shown that the allenyl ligand is reactive towards neutral organic molecules such as alkynes and diazocompounds<sup>21</sup>. Moreover, compounds **4a** and **4c** react readily with MeCN/Me<sub>3</sub>NO to give the acetonitrile adducts  $[\text{Ru}_2\text{Cp}_2(\text{CO})(\text{MeCN})(\mu\text{-CO})\{\mu\text{-}\eta^1:\eta^2\text{-C(H)=C=C(Me)(R)}\}][\text{BF}_4]$  (R=Me, **6a**; R=Ph, **6c**) (Scheme 23).



*Scheme 23: Reaction of  $[Ru_2Cp_2(CO)_2(\mu-CO)\{\mu-\eta^1:\eta^2-C(H)=C=C(Me)(R)\}][BF_4]$  with  $Me_3CN/Me_3NO$ .*

The chemistry of the derivatives **6** offers promise in that acetonitrile often acts as a labile ligand in transition metal chemistry. For dinuclear species, acetonitrile removal is a crucial step in allowing coordination, at one of the two metal centres, of either anionic nucleophiles such as hydride, halides and pseudo-halides<sup>31</sup>, or neutral organic fragments<sup>2g,2i,4a,4b,5e</sup>.

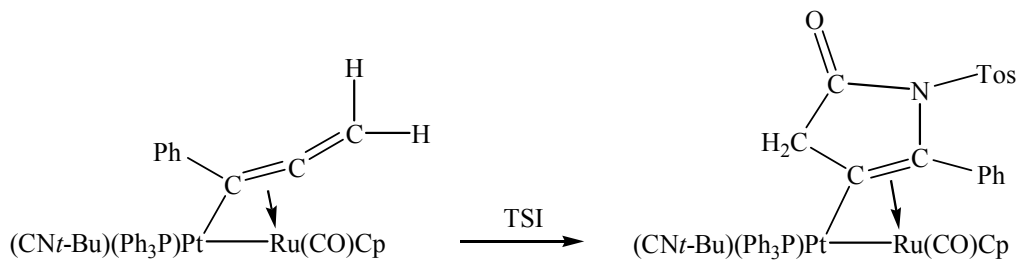
The substitution of a carbonyl ligand by an acetonitrile molecule in cationic diruthenium allenyl complexes allows the introduction of hydride and halide ions to the metal sites under mild conditions<sup>22</sup>. The resulting products undergo successive rearrangements involving the bridging allenyl ligand promoted by thermal treatment or filtration through alumina. Hydride migration from the metal site to the  $C_\alpha$  carbon of the allenyl moiety provides a  $\mu-\eta^1:\eta^2$ -allene product which is further convertible into a more stable vinyl-alkylidene derivative, by hydrogen migration from  $C_\alpha$  to  $C_\beta$  (Scheme 24).



Scheme 24: Reaction of **6b** with  $\text{NaBH}_4$ .

### 2.3.3 Reactivity with electrophilic reagents

Heterometallic  $\mu$ -allenyl complexes may react with the electrophilic  $p$ -TolSO<sub>2</sub>NCO (TSI) to generate [3+2] cycloaddition products<sup>6g</sup>, as illustrated in Scheme 25.

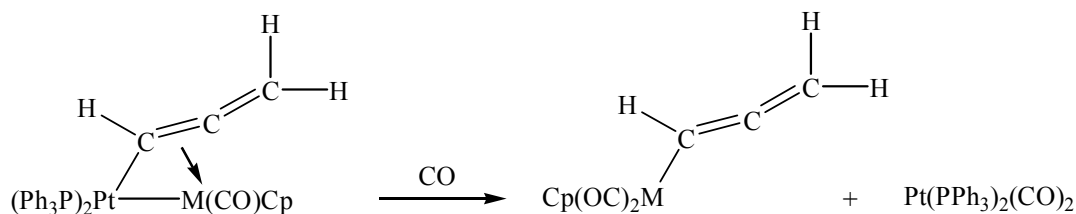


Scheme 25: Reaction of  $[(t\text{-BuNC})(\text{PPh}_3)_2\text{Pt}(\mu\text{-}\eta^1:\eta^2\text{-C(Ph)=C=CH}_2)\text{Ru(CO)Cp}]$  with TSI.

Other electrophilic alkenes, *e.g.* ClSO<sub>2</sub>NCO, TCNE and fumaronitrile, react with  $\mu$ -allenyl complexes by either  $M_\alpha$ – $M_\beta$  bond cleavage or uncharacterized decomposition<sup>6g</sup>. However, it has been reported that  $[\text{Au}(\text{PPh}_3)_2]^+$  adds to the  $\text{C}_\beta$  carbon of the allenyl ligand in  $[(\text{PPh}_3)_2\text{Pt}(\mu\text{-}\eta^1\text{:}\eta^2\text{-C(R)=C=CH}_2)\text{Ru}(\text{CO})\text{Cp}]$  ( $\text{R} = \text{H, Ph}$ ) to generate a  $\eta^3$ -allyl complex<sup>32</sup>.

#### 2.3.4 Other reactions

Bridging allenyl complexes sometimes display unusual propensity to fragmentation into mononuclear metal compounds upon treatment with CO<sup>16a</sup> (Scheme 26).



Scheme 26: Fragmentation of  $[(\text{PPh}_3)_2\text{Pt}(\mu\text{-}\eta^1\text{:}\eta^2\text{-C(H)=C=CH}_2)\text{Ru}(\text{CO})\text{Cp}]$ .

The observed fragmentation may be favoured by relatively weak Pt–M bond. Some of these reactions are reversed under Ar atmosphere.

Dinuclear  $\mu$ -allenyl complexes also serve as synthons for trinuclear metal  $\mu$ -allenyls<sup>16a</sup>.



## 2.4 Vinyl ligand: types of coordination

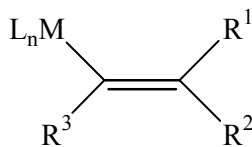
Metal vinyl complexes have attracted attention because of their significance in organometallic synthesis and catalysis<sup>33</sup>.

One area of great interest, in the light of the proposition that  $\mu$ -vinyl groups are involved in the initiation and propagation steps of the Fischer-Tropsch synthesis<sup>34</sup>, are the C–C bond forming reactions of the  $\mu$ -vinyl ligand with small organic molecules.

Due to the presence of a C–C double bond, the vinyl ligands exhibit different coordination modes in mono-, di- and polynuclear transition metal complexes.

### 2.4.1 Mononuclear complexes

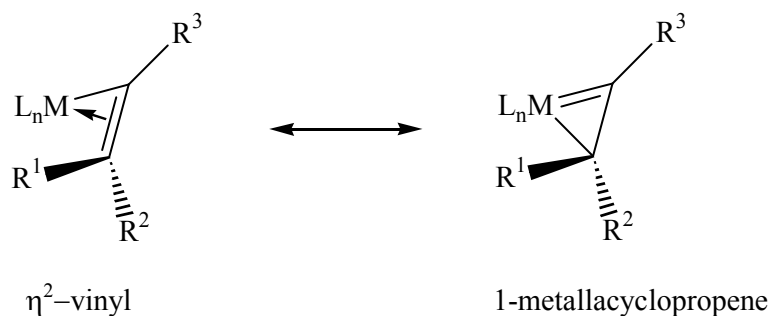
The organic vinyl fragment,  $[\text{CR}=\text{CR}_2]^-$ , can coordinate through one or both  $sp^2$  carbons. In the first case, the vinyl ligand acts as a simple  $\sigma$  donor, as highlighted in Scheme 27.



Scheme 27:  $\eta^1$ -vinyl /  $\sigma$ -vinyl.

Much more attractive is the second case, where the coordination of both carbons increases the electron count at the metal(s) by two electrons with respect to the situation of simple  $\sigma$ -bound vinyl ligand (Scheme 28). The discovery that the vinyl ligand could adopt this type of coordination led to the speculation that  $\eta^2$ -vinyl complexes could be

involved along catalytic pathways involving coordinatively unsaturated alkenyl species<sup>35</sup>.



*Scheme 28: Nomenclature and Labelling for  $L_nM(\eta^2\text{-C(R)=CR}_2)$ .*

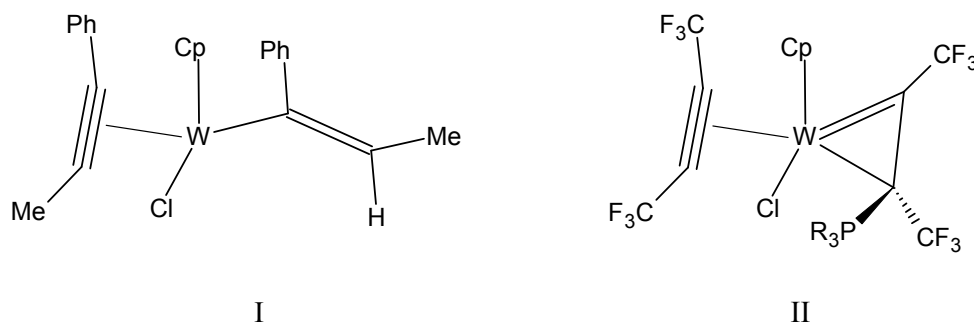
Two prominent geometrical features define the  $\eta^2$ -vinyl ligands. First, the ligand is bound asymmetrically to the metal(s) through both carbons. Second, the vinyl fragment is not planar. Conversely, the  $\text{CR}_2$  unit is rotated so that the carbon-carbon double bond characteristic of the vinyl unit is compromised in favor of double bond character between  $\text{C}_\alpha$  and the metal. The net result is that the substituents on the  $\beta$ -carbon are approximately orthogonal to the  $\text{MC}_2$  plane and the distinction between *cis* and *trans* sites associated with vinyl fragments is lost.

The  $[\eta^2\text{-C(R)=CR}_2)]^-$  ligand has been described as a  $\eta^2$ -vinyl ligand or as a  $\eta^2$ -alkenyl ligand, and the resulting product has been termed either a  $\eta^2$ -vinyl complex or a 1-metallacyclopropene complex (Scheme 28). However, the  $\eta^2$ -vinyl term has enjoyed widespread use in the literature, and the origin of the fragment and the reactivity patterns that yield and consume these ligands are intrinsically associated with the vinyl name. On the other hand, Casey has argued for adoption of the 1-

metallacyclopropene nomenclature<sup>36</sup>. Indeed, the 1-metallacyclopropene structural representation is congruent with the ground state structures and spectroscopic properties of these complexes.

It is important to remember that there are two components to the total metal-(C=C) bonding: (a) overlap of the  $\pi$ -electron density of the C=C bond with a  $\sigma$ -type acceptor orbital on the metal atom and (b) a “back bond” resulting from flow of electron density from the filled metal  $d_{xz}$  or other  $d\pi$ - $p\pi$  hybrid orbitals to *antibonding* orbitals of the carbon atoms. Of course, the donation of  $\pi$ -bonding electrons to the metal  $\sigma$  orbital and the introduction of the electrons into the  $\pi$ -antibonding orbital both weaken the  $\pi$  bonding in the C=C bond, so that the carbon atoms bound to the metal approach tetrahedral hybridization. Thus it is possible to formulate the bonding as involving two normal  $2c$ - $2e$  metal-carbon bonds in a metallacycle.

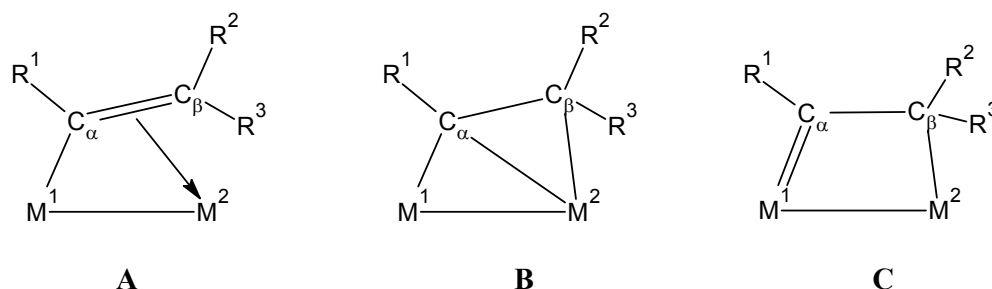
Thus, in vinyl complexes the preference of a  $\eta^2$ -coordination rather than a  $\eta^1$ - is driven by the electronic character of the ligands present in the coordination sphere. Strongly donating substituents force the vinyl ligand to adopt a  $\eta^1$  ( $2e^-$ ) binding mode rather than a  $\eta^2$  ( $4e^-$ ) binding mode, which is preferred when more withdrawing substituents are present, as highlighted by the examples<sup>37</sup> reported in Scheme 29.



Scheme 29: Examples of  $\eta^1$ -vinyl (I) and  $\eta^2$ -vinyl (II) complexes of tungsten.

#### 2.4.2 Dinuclear complexes

In the case of dinuclear complexes, only one coordination fashion is reported for the bridge vinyl ligand. The bonding in  $\mu$ -vinyl complexes has been described in terms of contribution from three Valence Bond structures (Scheme 30).

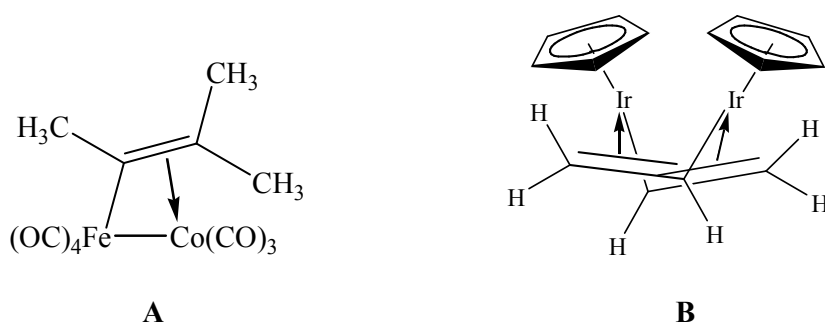


Scheme 30: VB structures of the bonding in  $\mu$ -vinyl complexes.

Cationic  $\mu$ -vinyl complexes undergo nucleophilic attack, including hydride addition, at the  $\beta$  carbon to generate  $\mu$ -alkylidene complexes<sup>44a,45b,48</sup>.

In most cases the metal-metal bond is preserved in the structure of dinuclear  $\mu$ -vinyl complexes (example<sup>38</sup> in Scheme 31, **A**), however Werner and coworkers<sup>39</sup> reported the

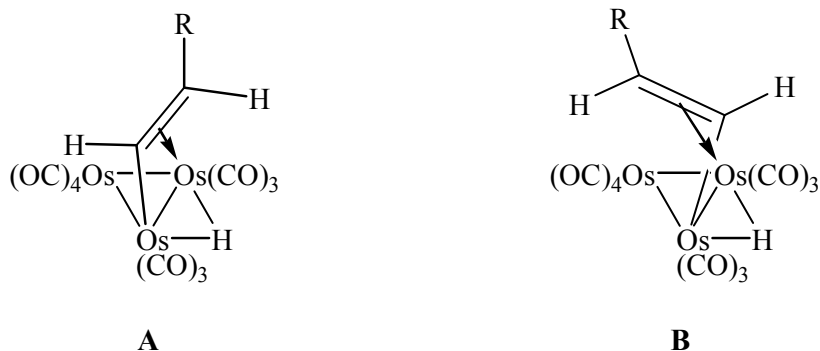
structure of dinuclear doubly vinyl-bridged iridium complexes where the two metal centres are not bonded to each other (Scheme 31, **B**).



Scheme 31: Examples of metal-metal bonded (**A**) and not bonded  $\mu$ -vinyl dinuclear complexes (**B**).

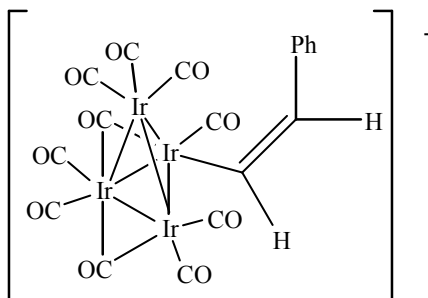
#### 2.4.3 Polynuclear complexes

Examples of trinuclear vinyl complexes are quite common; in these compounds the coordination mode of the vinyl ligand is analogous to the one adopted in dinuclear complexes, as the maximum number of carbons which can be involved in the metal-carbon bonds is two. An example<sup>40</sup> of a trinuclear  $\mu$ -vinyl complex is reported in Scheme 32. These compounds adopt the  $\mu$ - $\eta^2$ -vinyl structure (Scheme 32, **A**) with the *trans* configuration. The related *cis*-PhC=CHPh complex and the furyl complex are similar, except that they adopt the alternative configuration reported in Scheme 32, **B**, in which a clash of the 1-substituent with an axial CO at the Os(CO)<sub>4</sub> unit is avoided.



*Scheme 32: Structures of diosmium complexes of general formula  $[Os_3(CO)_{10}(\mu-H)(\mu-C(H)=CHR)]$ .*

To my knowledge, the only example of a vinyl-containing cluster with a nuclearity higher than 3 (three) is the tetranuclear anionic complex  $[Ir_4(CO)_{11}(\mu-C(Ph)=C(H)(Ph))]^{-41}$ . In this compound, the metallic framework is tetrahedral with the vinyl ligand being  $\eta^1$ -bound and pointing away from the core (Scheme 33).



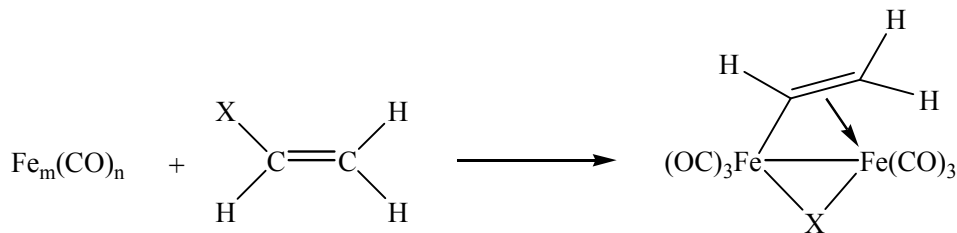
*Scheme 33: Structure of the anionic complex  $[Ir_4(CO)_{11}(\mu-C(Ph)=C(H)(Ph))]^-$ .*

## 2.5 Synthesis of dinuclear $\mu$ -vinyl complexes

There are numerous methods available for the preparation of bimetallic  $\mu$ -vinyl complexes: these include insertion of a metal into vinylic C–S<sup>42</sup> or C–halogen<sup>43</sup> bond, rearrangement of  $\mu$ -alkylidyne complexes and their reaction with alkenes<sup>44</sup>,  $\beta$ -hydride abstraction from  $\mu$ -alkylidene complexes<sup>45</sup>, addition of alkynes to transition metal carbonyl hydrides<sup>46</sup>, and protonation of alkyne-bridged bimetallic complexes<sup>47</sup> and dimetallacyclopentenones<sup>48</sup>.

### 2.5.1 Insertion of a metal into vinylic C–S or C–halogen bond

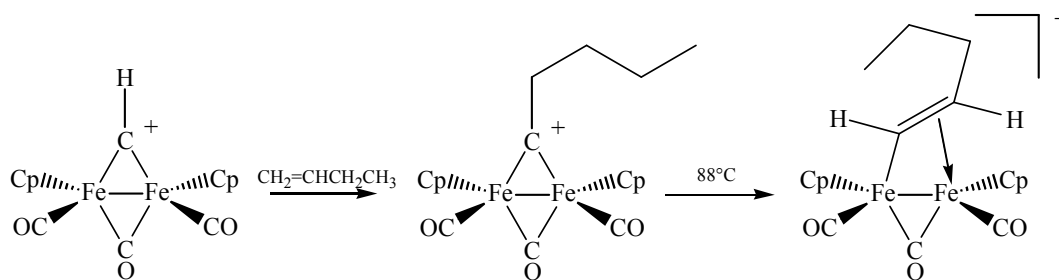
In 1961 King and coworkers<sup>42</sup> discovered that the reaction of triiron dodecacarbonyl with a vinyl sulfide resulted in insertion of two iron centres into the vinylic C–S bond of the sulfide, affording the vinyl diiron complexes  $[\text{Fe}_2(\mu\text{-SR})(\text{CO})_6(\mu\text{-CH=CH}_2)]$  ( $\text{R} = \text{Me, Et, CHCH}_2, ^i\text{Pr}$ ) (Scheme 34: Reaction of a). By a similar method, a vinyl diiron compound may be synthesized *via* insertion of the two iron centres of  $\text{Fe}_2(\text{CO})_9$  in the C–halogen bond of a haloalkene<sup>43</sup> (Scheme 34b).



*Scheme 34: Reaction of iron carbonyls with (a) vinyl sulfides ( $m=3$ ,  $n=12$ ,  $\text{X}=\text{RS}$ ) and (b) haloalkenes ( $m=2$ ,  $n=9$ ,  $\text{X} = \text{F, Br, I}$ ).*

### 2.5.2 Rearrangement of $\mu$ -alkylidyne complexes

A convenient way to prepare  $\mu$ -vinyl derivatives involves rearrangement of alkylidyne diiron complexes, such as  $[\text{Fe}_2\text{Cp}_2(\text{CO})_2(\mu\text{-CO})(\mu\text{-C}(\text{CH}_2)_3\text{CH}_3)][\text{PF}_6]^{44}$ , upon heating. The preparation of the alkylidyne is easily achieved by reacting the methylidyne complex  $[\text{Fe}_2\text{Cp}_2(\text{CO})_2(\mu\text{-CO})(\mu\text{-CH})][\text{PF}_6]$  with the appropriate alkene. This hydrocarbation reaction proceeds by a regioselective addition of the  $\mu\text{-C-H}$  bond across the  $\text{C}=\text{C}$  bond<sup>49</sup> (Scheme 35).



*Scheme 35: Reaction of diiron methylidyne complex with 1-butene and rearrangement of the alkylidyne product affording the corresponding  $\mu$ -vinyl species.*

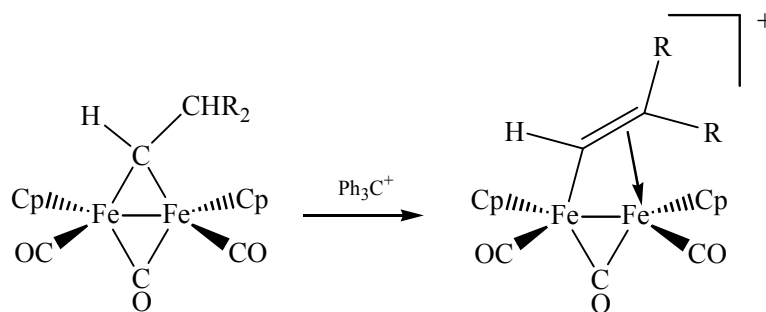
The conversion of  $\mu$ -alkylidene complexes to  $\mu$ -vinyl ones proceeds with net migration of a hydrogen atom from  $\text{C}_\beta$  to  $\text{C}_\alpha$ . Studies carried out with deuterated derivatives showed that the migration involved the  $\beta$ -carbon hydrogens<sup>49</sup>.

### 2.5.3 $\beta$ -Hydride abstraction from $\mu$ -alkylidene complexes

$\beta$ -Hydride abstraction from mononuclear metal alkyls, as well as the reverse reaction, are well known processes in organometallic chemistry<sup>50</sup>. This type of reaction may be used conveniently to prepare vinyl dinuclear complexes. For example<sup>45b</sup>, when the



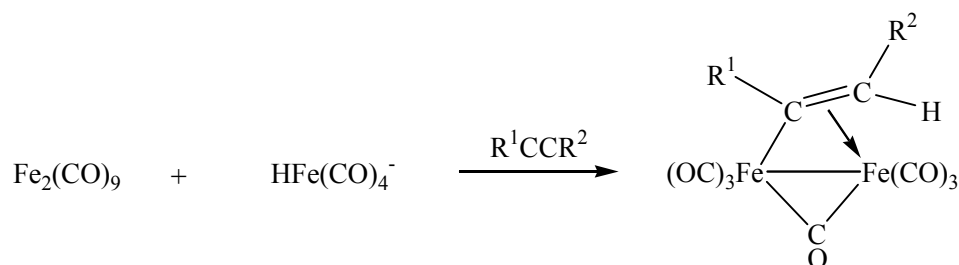
$\mu$ -alkylidene  $[\text{Fe}_2\text{Cp}_2(\text{CO})_2(\mu\text{-CO})(\mu\text{-CHCHR}_2)]$  are treated with the trityl cation  $\text{Ph}_3\text{C}^+$ , abstraction of a hydride from  $\text{C}_\beta$  takes place, affording the corresponding cationic vinyl complex, as highlighted in Scheme 36.



Scheme 36: Reaction of  $[\text{Fe}_2\text{Cp}_2(\text{CO})_2(\mu\text{-CO})(\mu\text{-CHCHR}_2)]$  with  $\text{Ph}_3\text{C}^+$ .

#### 2.5.4 Addition of alkynes to transition metal carbonyl hydrides

The reaction of metal hydrides with alkynes provides a general route to  $\mu$ -vinyl ligands. An equimolar mixture of  $\text{Fe}_2(\text{CO})_9$ ,  $\text{R}^1\text{C}\equiv\text{CR}^2$  and  $[\text{HFe}(\text{CO})_4]^-$  in THF affords the  $\mu$ -vinyl compounds of general formula  $[\text{Fe}_2(\text{CO})_6(\mu\text{-CO})(\mu\text{-CR}^1=\text{CHR}^2)]^-$ <sup>46</sup> (Scheme 37).



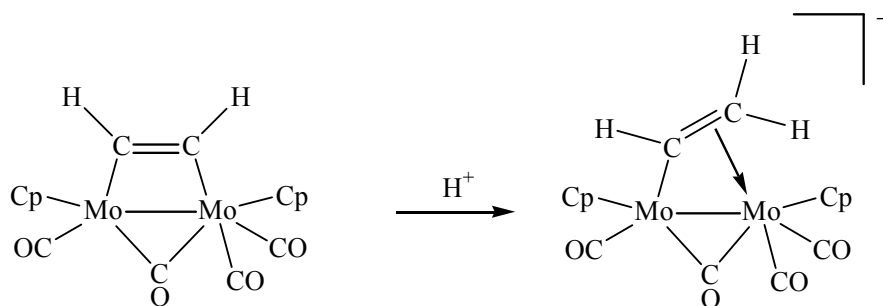
Scheme 37: Synthesis of  $[\text{Fe}_2(\text{CO})_6(\mu\text{-CO})(\mu\text{-CR}^1=\text{CHR}^2)]^-$ <sup>46</sup>.

The synthesis seems to occur with alkyne activation by  $\text{Fe}_2(\text{CO})_9$  followed by interaction with the metal hydride.

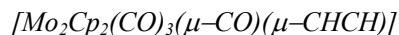
### 2.5.5 Protonation of alkyne-bridged bimetallic complexes and dimetallacyclopentenones

Insertion of alkynes into dinuclear species affords two kind of products, *i.e.* alkyne-bridged bimetallic complexes and dimetallacyclopentenones, which can be further protonated to obtain  $\mu$ -vinyl dinuclear complexes.

For example, the protonation of the  $\mu$ -alkyne dimolibdenum  $[\text{Mo}_2\text{Cp}_2(\text{CO})_3(\mu\text{-CO})(\mu\text{-CHCH})]$  yields the corresponding  $\mu$ -vinyl derivative  $[\text{Mo}_2\text{Cp}_2(\text{CO})_3(\mu\text{-CO})(\mu\text{-CHCH}_2)]^{47a}$  (see Scheme 38).

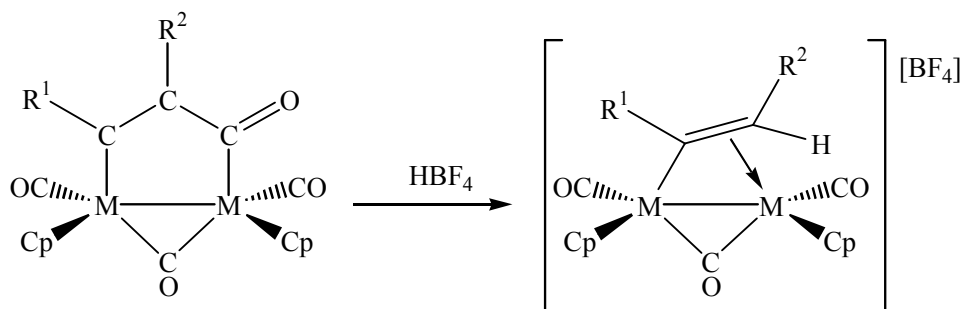


Scheme 38: Protonation of the  $\mu$ -alkyne dimolibdenum complex.

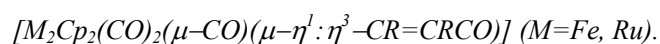


In a similar way, the dimetallacyclopentenone species  $[\text{M}_2\text{Cp}_2(\text{CO})_2(\mu\text{-CO})(\mu\text{-}\eta^1:\eta^3\text{-CR}^1\text{=CR}^2\text{C(O)})]$  ( $\text{M}=\text{Fe}, \text{Ru}$ )<sup>48</sup>, synthesized by photolytic insertion of alkynes into the  $\text{M-CO}$  bond (see paragraph 2.2.4), may be easily protonated upon treatment with  $\text{HBF}_4$ , resulting in immediate cleavage of the alkyne-CO bond. The “alkyne”

portion of the dimetallacycle is protonated to give the  $\mu$ -vinyl complexes  $[M_2Cp_2(CO)_2(\mu-CO)(\mu-CR^1=CHR^2)][BF_4]$  ( $M = Fe, Ru$ ), in which  $R^1$  and  $R^2$  are in relative *cis* position; as a result of the protonation, the acyl group is converted into a terminal carbonyl ligand.



*Scheme 39: Protonation of the dimetallacyclopentenone species*

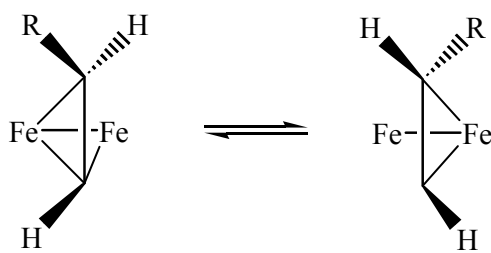


There is strong evidence that, whether preceded by metal protonation or not, the acyl moiety in the dimetallacyclopentenone undergoes protonation prior to the production of the  $\mu-CR^1=CHR^2$  unit. It is therefore apparent that the reaction proceeds with proton transfer from the  $\{C=O\}$  group to the  $\{C(R^2)\}$  carbon, with simultaneous C-C bond cleavage.

## 2.6 Chemistry of dinuclear $\mu$ -vinyl complexes

### 2.6.1 Fluxionality

As well as already highlighted for  $\mu$ - $\eta^1:\eta^2$ -allenyl complexes, also the  $\mu$ -vinyl ones exhibit fluxionality. In the  $^1\text{H}$  NMR spectra of  $[\text{Fe}_2\text{Cp}_2(\text{CO})_4(\mu\text{-CO})(\mu\text{-}\eta^1:\eta^2\text{-C(H)=CHR})]$  complexes, the non-equivalent cyclopentadienyl groups give rise to two resonances. Upon warming, the two peaks coalesce to a single averaged cyclopentadienyl resonance as first showed by Knox<sup>48</sup>. The fluxional process that exchanges the environment of the cyclopentadienyl groups involves movement of the  $\beta$ -carbon from one iron centre to the other. During this process,  $\text{C}_\alpha$  is always bonded to both iron centres while the  $\text{C}_\beta$  is bonded to only a single iron. A convenient way of describing the  $\mu$ -vinyl system is in terms of the 1,2-diiron bicyclop propane structure (Scheme 40).



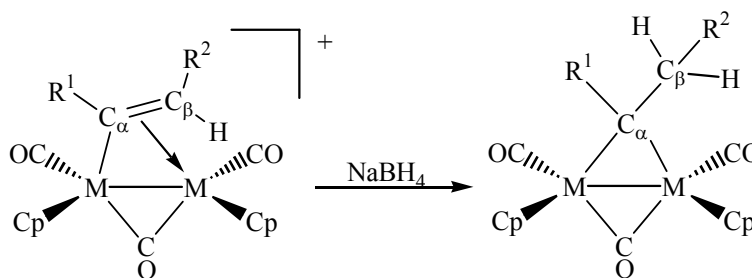
Scheme 40: Fluxionality of  $\mu$ -vinyl diiron cation.

### 2.6.2 Reactivity with nucleophilic reagents

The reactivity of  $\mu$ -vinyl dinuclear complexes with nucleophiles may involve attack at the  $\alpha$ - or  $\beta$ -carbon of the vinyl ligand, or at one of the two metal centres. The

reactivity of the previously described  $\mu$ -vinyl complexes of general formula  $[M_2Cp_2(CO)_2(\mu-CO)(\mu-CR^1=CHR^2)][BF_4]$  ( $M=Fe, Ru$ ) offers an interesting example of the chemical behavior of these systems in the presence of nucleophiles.

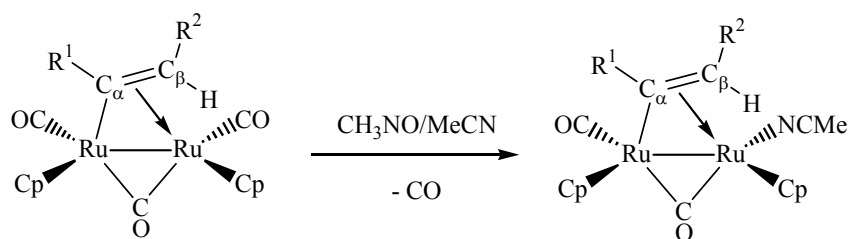
Both diruthenium and diiron  $\mu$ -vinyl complexes  $[M_2Cp_2(CO)_2(\mu-CO)(\mu-CR^1=CHR^2)][BF_4]$  are attacked by nucleophiles at the  $\beta$ -carbon to yield the corresponding  $\mu$ -carbene complexes. This reaction completes a sequence of transformation (see Scheme 15 and Scheme 39) by which an alkyne is converted to a carbene coordinated at a dinuclear metal centre. Interest in such complexes has been due to the fact that they may serve as models for metal surface-bound carbenes, which act as intermediate species in the Fischer-Tropsch synthesis of hydrocarbons<sup>51</sup>. For example, treatment of the  $\mu$ -vinyl  $[M_2Cp_2(CO)_2(\mu-CO)(\mu-CR^1=CHR^2)][BF_4]$  ( $M=Fe, Ru$ ) with  $NaBH_4$ <sup>48a</sup> determines rapid hydride addition to the  $\beta$ -carbon, generating the appropriate  $\mu$ -carbene complex (Scheme 41).



Scheme 41: Reaction of  $[M_2Cp_2(CO)_2(\mu-CO)(\mu-CR^1=CHR^2)][BF_4]$  ( $M=Fe, Ru$ ) with  $NaBH_4$ .

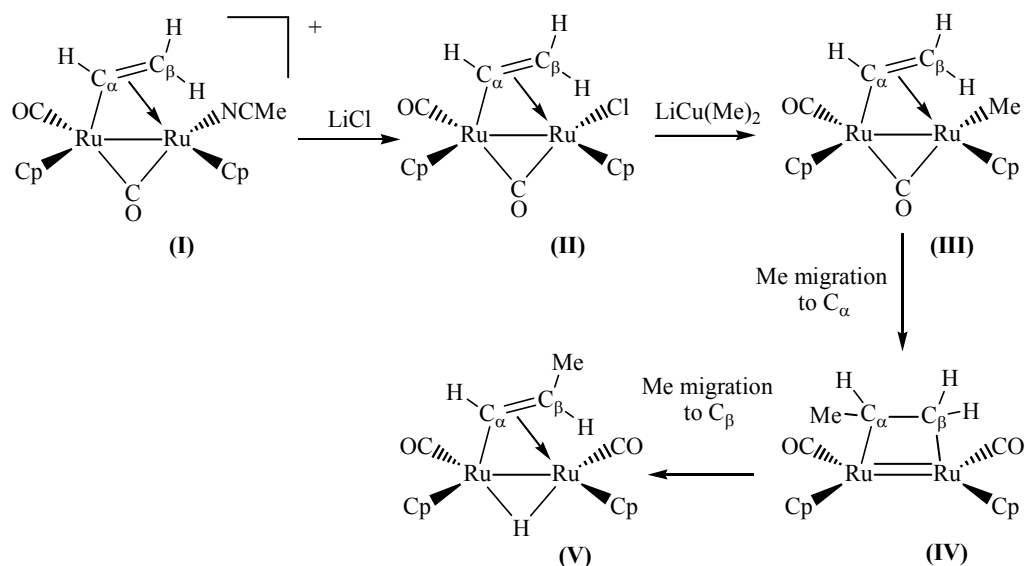
As previously described in paragraph 2.3.2 (Scheme 23) for analogous diruthenium  $\mu$ -allenyl complexes, also the diruthenium  $\mu$ -vinyl compounds show substitution of

one terminal CO with MeCN at one of the metal centres in the presence of Me<sub>3</sub>NO<sup>52</sup> (Scheme 42).



Scheme 42: Reaction of  $[Ru_2Cp_2(CO)_2(\mu-CO)(\mu-CR^1=CHR^2)][BF_4]$  with MeCN/Me<sub>3</sub>NO.

Knox and coworkers<sup>53</sup> (Scheme 43) highlighted how the complex  $[Ru_2Cp_2(CO)(MeCN)(\mu-CO)(\mu-CH=CH_2)]^+$ , (I), underwent nucleophilic attack of the chloride ion at one metal centre, to generate the chloro-derivative (II). Further treatment with LiCu(Me)<sub>2</sub> gave substitution of the chloride with a methyl group, resulting in formation of (III). Although quite stable in the solid state, (III) is unstable in solution due to slow methyl migration first to C<sub>α</sub>, (IV), and then to C<sub>β</sub>, (V).

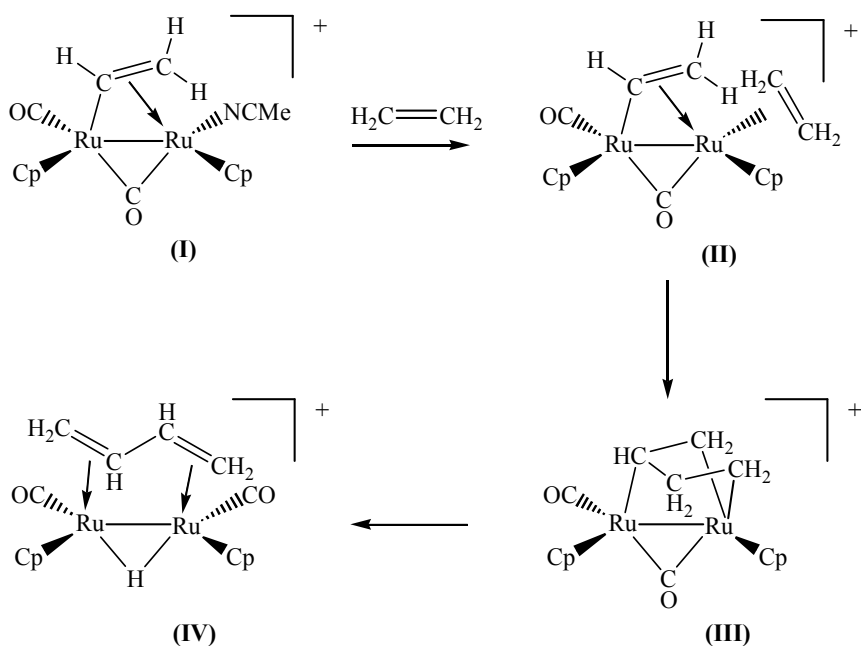


*Scheme 43: Progressive reactivity of  $[\text{Ru}_2\text{Cp}_2(\text{CO})(\text{MeCN})(\mu\text{-CO})(\mu\text{-CH=CH}_2)]^+$  with  $\text{LiCl}$  and  $\text{LiCu}(\text{Me})_2$ .*

### 2.6.3 Combination with alkenes

The reaction of  $[\text{Ru}_2\text{Cp}_2(\text{CO})(\text{MeCN})(\mu\text{-CO})(\mu\text{-CH=CH}_2)]^+$  with ethylene has been reported<sup>52</sup>. In the light of the mechanistic studies, it has been demonstrated that the first step is the displacement of the labile acetonitrile from **(I)** to give the transient  $\mu$ -vinyl/ethylene complex **(II)**, as shown in Scheme 44. Once ethylene is coordinated, carbon-carbon bond formation between it and the  $\alpha(\mu)$ -vinyl carbon occurs rapidly. The process can be viewed as a reductive elimination ( $2 \text{ Ru-C} \rightarrow \text{C-C}$ ), which generates the dimetallacycles **(III)** containing a sixteen-electron ruthenium centre. Then, the latter compound promotes  $\beta$ -elimination of one of the originally ethylenic hydrogen, so to restore the electronic saturation at the dimetal frame and afford **(IV)**. It is noteworthy that the  $\mu$ -vinyl precursor of **(I)** is obtained by oxidation of the ethylene

complex  $[\text{Ru}_2\text{Cp}_2(\text{CO})_3(\text{C}_2\text{H}_4)]^{54}$ , so that the overall scheme represents the sequence of reactions describing the coupling of two ethylene molecules at a dinuclear metal centre.

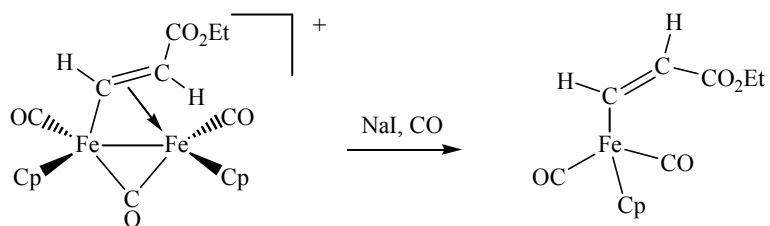


*Scheme 44: Combination of  $[\text{Ru}_2\text{Cp}_2(\text{CO})(\text{MeCN})(\mu\text{-CO})(\mu\text{-CH}=\text{CH}_2)]^+$  with ethylene.*

#### 2.6.4 Other Reactions

As stated for the  $\mu$ -allenyl complexes, also the  $\mu$ -vinyl ones may display sometimes propensity to fragmentation into mononuclear metal complexes. For example<sup>55</sup>, treatment of  $[\text{Fe}_2\text{Cp}_2(\text{CO})_2(\mu\text{-CO})(\mu\text{-CH}=\text{C}(\text{H})(\text{CO}_2\text{Et}))][\text{BF}_4]$  with NaI and CO results in Fe–Fe bond cleavage and formation of  $[\text{FeCp}(\text{CO})_2(\eta^1\text{-CH}=\text{C}(\text{H})(\text{CO}_2\text{Et}))]$  (Scheme 45).





*Scheme 45: Fragmentation of  $[Fe_2Cp_2(CO)_2(\mu-CO)(\mu-CH=C(H)(CO_2Et))] [BF_4]$ .*

Dinuclear  $\mu$ -vinyl complexes also serve as synthons for trinuclear metal  $\mu$ -vinyls<sup>56</sup>.

## 2.7 Objective

The object of the present Thesis is the study of the reactivity of diiron or diruthenium complexes containing the  $[M_2Cp_2(CO)_3]$  unit and a bridging unsaturated ligand (*i.e.* allenyl or vinyl), with the purpose to obtain novel organic fragments by functionalization of the bridging hydrocarbyl ligand, through selective synthetic pathways which may be favored by the dinuclear frame. Moreover, the study might give a contribution to the understanding of mechanistic aspects concerning industrial processes (*e.g.* Fischer-Tropsch).

On considering that the large majority of the known allenyl complexes are neutral, we have decided to focus our attention on the cationic  $[M_2Cp_2(CO)_2(\mu-CO)\{\mu-C(H)=C=CRR'\}]^+$  ( $M = Ru$ , **4**;  $M = Fe$ , **7**), whose positive charge should basically enhance the reactivity with nucleophiles.

In this Thesis the synthesis of the new diiron  $\mu$ -allenyl complexes  $[Fe_2(Cp)_2(CO)_2(\mu-CO)\{\mu-\eta^1:\eta^2_{\alpha,\beta}-C(H)=C=C(R)_2\}][BF_4]$  ( $R = Me$ , **7a**;  $R = Ph$ , **7b**) will be reported, and the chemistry of both diiron and diruthenium complexes will be discussed.

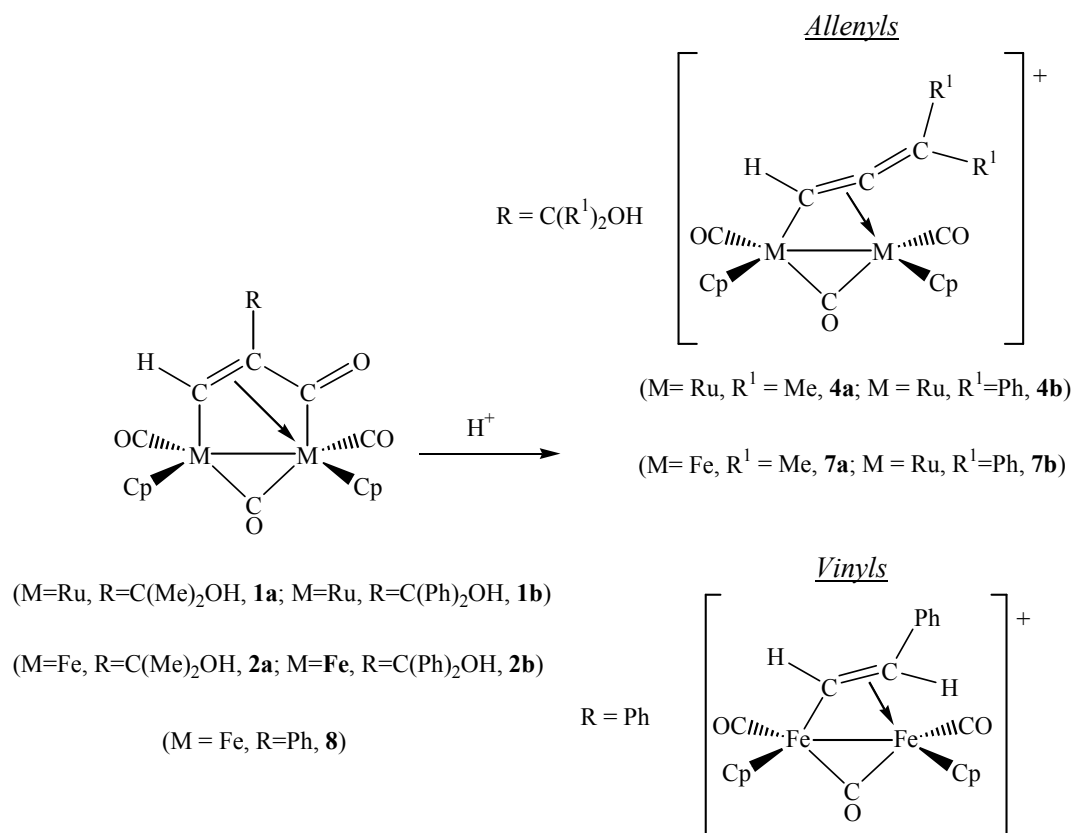
Then, we will extend the study to the  $\mu$ -vinyl complex  $[Fe_2Cp_2(CO)_2(\mu-CO)(\mu-CH=CHPh)]^+$ , **9**, which is easily prepared from the dimetallacyclopentenone precursor  $[Fe_2Cp_2(CO)_2(\mu-CO)(\mu-C(H)C(Ph)C(O))]$ , **8**. A particular attention will be devoted to the redox chemistry of **9**.

### 3 Results and Discussion

#### 3.1 Dimetallacyclopentenones: synthesis and characterization

Diiron and diruthenium dimetallacyclopentenone complexes represent convenient precursors for both  $\mu$ -allenyl and  $\mu$ -vinyl species, as previously stated in the introduction. Their synthesis is a well-known process, which involves alkyne insertion into the M–CO bond of  $[M_2Cp_2(CO)_4]$  ( $M = Fe, Ru$ ) under UV radiation. Photolytic insertion of alkynols (Scheme 46a) or alkynes (Scheme 46b) has been performed in order to obtain the desired products.

In the case of complexes **1** and **2**, addition of a proton results in dehydration of the inserted alkynol and formation of the allenyl ligand. Instead, in the case of complex **8**, proton attack occurs at  $C_\beta$ , resulting in formation of the vinyl ligand. In both cases the generation of the new hydrocarbyl moiety is accompanied by the cleavage of the C–C bond and the conversion of the acyl group into a terminal carbonyl ligand.



*Scheme 46: Dimetallacyclopentenone species as precursors for allenyl and vinyl complexes.*

Compounds **1**, **2** and **8** were characterized by IR, NMR and, in the case of **8**, by X-ray crystal structure.

Infrared spectra of the dimetallacyclopentenone species display peculiar bands due to the presence of a terminal-, a bridging carbonyl, and an acyl group at 1992-1969 (s), 1790-1805 (s) and 1731-1754  $cm^{-1}$  (m), respectively. Moreover, a band due to the hydroxyl group appears at  $\sim 3300\text{ cm}^{-1}$  in the spectra obtained on the products of alkynol insertion. The IR spectrum in  $CH_2Cl_2$  of complex **2b** is reported in Figure 1: *FT-IR Spectrum ( $CH_2Cl_2$ ) of complex 2b in the carbonyl stretching region.*

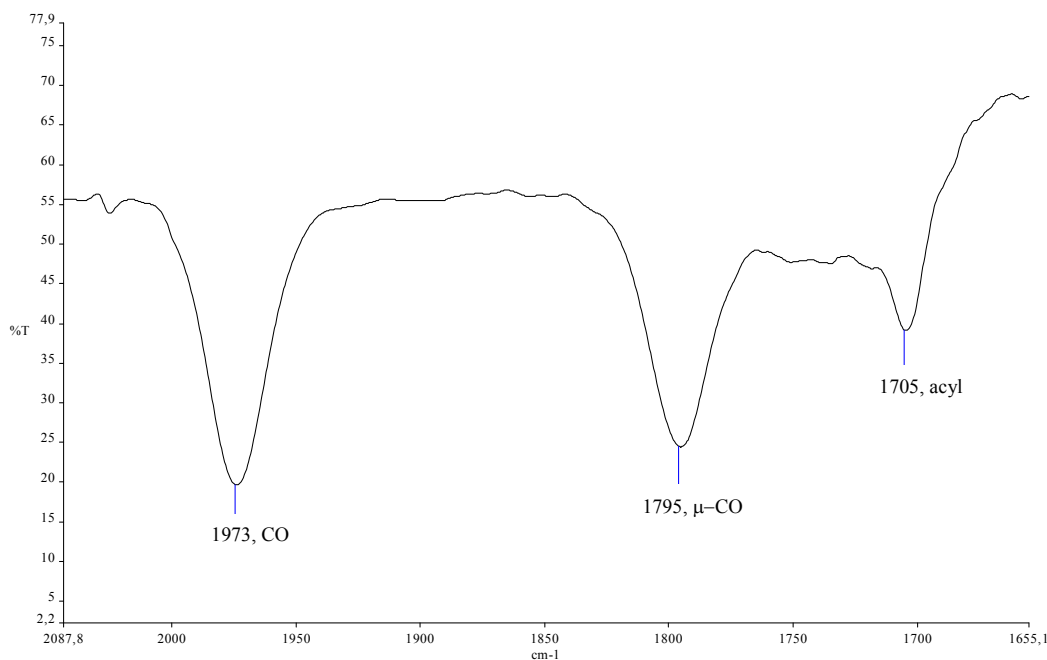


Figure 1: FT-IR Spectrum ( $\text{CH}_2\text{Cl}_2$ ) of complex **2b** in the carbonyl stretching region.

Relevant features regarding both  $^1\text{H}$ -NMR and  $^{13}\text{C}$ -NMR spectra are represented by the resonances of the  $\text{C}_\alpha\text{-H}$  unit, which are typical for a  $\mu$ -carbene ( $^{13}\text{C}$ -NMR:  $\delta = 152\text{-}181$  ppm;  $^1\text{H}$ -NMR:  $\delta = 10\text{-}13$  ppm). On the other hand, the  $\text{C}_\beta\text{-R}$  chemical shifts are characteristic of a coordinated olefinic carbon ( $^{13}\text{C}$ -NMR:  $\delta = 13\text{-}60$  ppm).

In the case of complex **8**, crystals suitable for X-ray analyses were collected from a dichloromethane solution layered with  $\text{Et}_2\text{O}$ , at  $-243\text{K}$ . The structure (see Figure 2) is consistent with that of  $[\text{Ru}_2\text{Cp}_2(\mu\text{-CO})(\text{CO})(\mu\text{-}\eta^1\text{:}\eta^3\text{-C(Ph)C(Ph)C(O)})]$  described by Knox and coworkers<sup>20a</sup>. The two iron atoms are at a distance ( $2.561\text{ \AA}$ ) typical of a single bond and are bridged symmetrically by a carbonyl group. The Fe(1) atom also

carries a terminal carbonyl, and each metal atom has a cyclopentadienyl ligand bound in a  $\eta^5$ -fashion. The coordination at the iron atoms is completed by a  $\text{HC}=\text{C}(\text{Ph})\text{C}(=\text{O})$  species, derived from the coupling of diphenylacetylene and carbon monoxide, bridging the two iron atoms. The  $\text{C}(13)\text{--}\text{C}(14)$  bond length (1.443 Å) is within the range for a coordinated double bond, showing evidence of some  $\pi$  character<sup>57</sup>.

The cyclopentadienyl ligands on the two metal atoms are mutually *cis* with respect to the metal-metal axis.

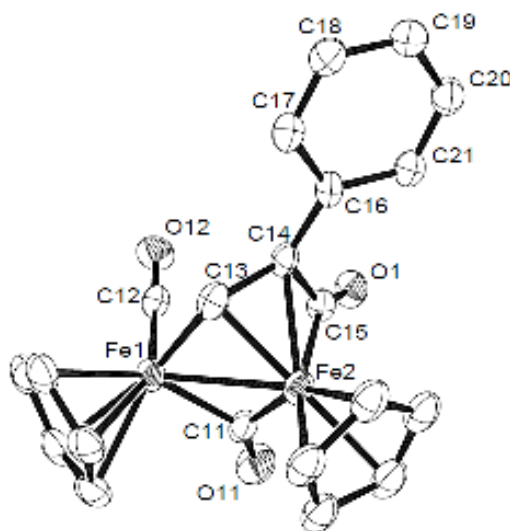
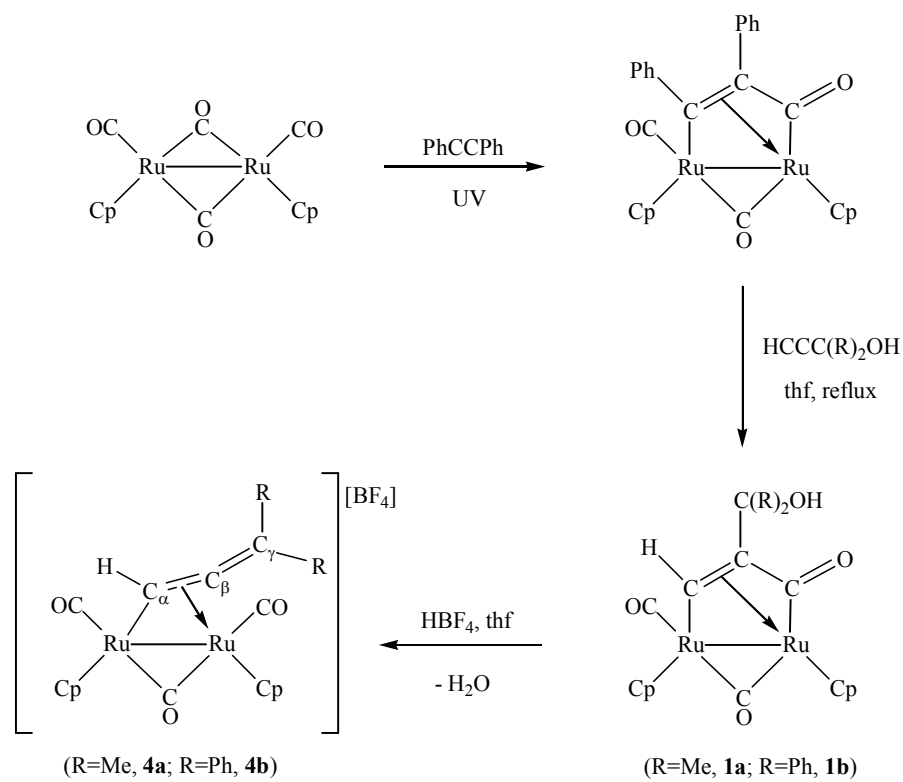


*Figure 2: View of the structure of complex 8. The H-atoms have been omitted for clarity. Thermal ellipsoids are at the 30% probability level. Only the main images of the disordered Cp ligands are drawn.*

### 3.2 Chemistry of the cationic diruthenium $\mu$ -allenyl complexes

#### 3.2.1 Synthesis and characterization

By following the literature procedure (see Introduction), the diruthenium allenyl complex  $[\text{Ru}_2(\text{Cp})_2(\text{CO})_2(\mu\text{-CO})\{\mu\text{-}\eta^1:\eta^2_{\alpha,\beta}\text{-C(H)=C=C(Me)}_2\}][\text{BF}_4]^{22}$  (**4a**) and the unreported  $[\text{Ru}_2(\text{Cp})_2(\text{CO})_2(\mu\text{-CO})\{\mu\text{-}\eta^1:\eta^2_{\alpha,\beta}\text{-C(H)=C=C(Ph)}_2\}][\text{BF}_4]$  (**4b**) have been synthesized. The diruthenium compounds **4** are known in the form of tetrafluoroborate salts, nevertheless no crystallographic description has been reported heretofore and only limited information have appeared on the reactivity<sup>22</sup>. Such diruthenium species can be prepared in good yields by a three-step route, see Scheme 47, starting with photolytic insertion of diphenylacetylene into the Ru–CO bond of  $[\text{Ru}_2\text{Cp}_2(\text{CO})_4]^{20}$ , affording the cyclopentenone  $[\text{Ru}_2\text{Cp}_2(\text{CO})(\mu\text{-CO})\{\mu\text{-}\eta^1:\eta^3\text{-C(Ph)=C(Ph)C(=O)}\}]$ . Successive alkyne-exchange reaction with alkynol, in thf solution at reflux temperature for 4 hours, results in the formation of  $[\text{Ru}_2\text{Cp}_2(\text{CO})_2(\mu\text{-CO})\{\mu\text{-}\eta^1:\eta^3\text{-C(H)=C(C(R)(R'))C(=O)}\}]$  ( $\text{R} = \text{R}' = \text{Me}$ , **1a**;  $\text{R} = \text{Ph}$ ,  $\text{R}' = \text{Me}$ , **1b**). The latter can be isolated by filtration through an alumina column. Further treatment with  $\text{HBF}_4$  in thf yields the final products **4a,b**.



*Scheme 47: Preparation of cationic diruthenium  $\mu$ -allenyl complexes.*

The new complexes **4a,b** have been fully characterized by IR and NMR spectroscopy, and elemental analysis.

The IR spectra (in  $\text{CH}_2\text{Cl}_2$  solution) of **4** display three absorptions ascribable to two terminal carbonyl ligands and one semi-bridging carbonyl (*e.g.* for **4a** at 2039, 2017 and  $1872\text{ cm}^{-1}$ , respectively).



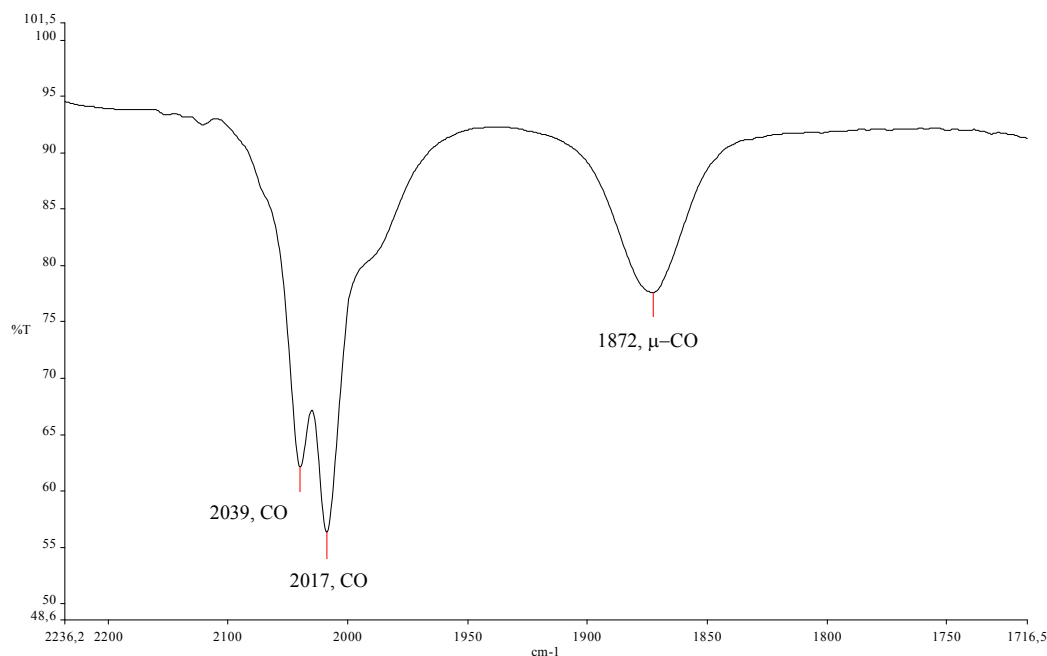
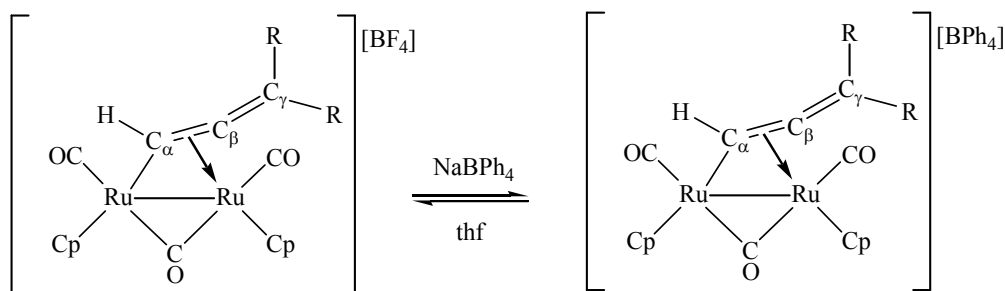


Figure 3: FT-IR solid state spectrum of complex **4a** in the carbonyl region.

The NMR spectra of **4** at room temperature show broad signals, as result of an exchange process. This process probably consists of  $\sigma$ - $\pi$  “windshield wiper” motion of the allenyl moiety, in accord with what observed formerly in analogous bridged-allenyl dinuclear complexes<sup>16b,6e</sup>. Readable  $^1\text{H}$ -NMR spectra could be recorded at 233K in  $\text{CD}_3\text{CN}$  solution. The spectra exhibit a single set of resonances. Relevant feature is represented by the  $\text{C}_\alpha\text{H}$  resonances, falling at typical high-frequency, in accordance with the alkylidene character [*e.g.* in the case of **4b**:  $\delta(^1\text{H}) = 10.96$  ppm;  $\delta(^{13}\text{C}) = 130.9$  ppm]. The allenyl carbons  $\text{C}_\beta$  and  $\text{C}_\gamma$  are found at *ca.* 150 and 125 ppm, respectively

The anion-exchange reactions reported in Scheme 48 were used to obtain the crystalline salts [**4a**][ $\text{BPh}_4$ ] and [**4c**][ $\text{BPh}_4$ ] (see Experimental), and their solid-state structures were solved by X-ray diffraction studies.



Scheme 48: Anion-exchange reaction to obtain the crystalline salts  $[\mathbf{4a}][\text{BPh}_4]$  and  $[\mathbf{4c}][\text{BPh}_4]$ .

The ORTEP representations are shown in Figure 4 and Figure 5. The structures are based on a  $\text{cis-[Ru}_2(\text{Cp})_2(\text{CO})_2(\mu\text{-CO})]$  core, coordinated to the bridging  $\mu\text{-}\eta^1\text{:}\eta^2\text{-C(H)=C=C(R)}_2$  allenyl ligand. The bonding parameters of the latter are as expected for this class of ligands, with bent  $\text{C(14)-C(15)-C(16)}$  bond  $[154.8(10)^\circ]$  for  $[\mathbf{4a}]^+$ ;  $151.7(4)$  and  $151.5(4)^\circ$  for the two independent molecules of  $[\mathbf{4b}]^+$ ; to be compared to the values observed in the  $143\div 157^\circ$  range. The  $\text{C(14)-C(15)}$  [ $1.390(13)$  Å for  $[\mathbf{4a}]^+$ ;  $1.355(6)$  and  $1.360(6)$  Å for the two independent molecules of  $[\mathbf{4b}]^+$ ] and  $\text{C(15)-C(16)}$  [ $1.328(13)$  Å for  $[\mathbf{4a}]^+$ ;  $1.326(6)$  and  $1.329(5)$  Å for the two independent molecules of  $[\mathbf{4b}]^+$ ] bonds display considerable  $\pi$ -character (usual values for reported structures are in the ranges  $1.36\div 1.40$  Å and  $1.31\div 1.35$  Å, respectively). The bridging CO ligand is substantially asymmetric in all structures with  $\text{Ru(1)-C(11)}$  and  $\text{Ru(2)-C(11)}$  distances of  $1.946$  and  $2.186$  Å for  $[\mathbf{4a}]^+$ ,  $1.979$  and  $2.185$  Å,  $1.972$  and  $2.175$  Å for the two independent molecules of  $[\mathbf{4b}]^+$ , being  $\eta^1$ -coordinated to the allenyl ligand.

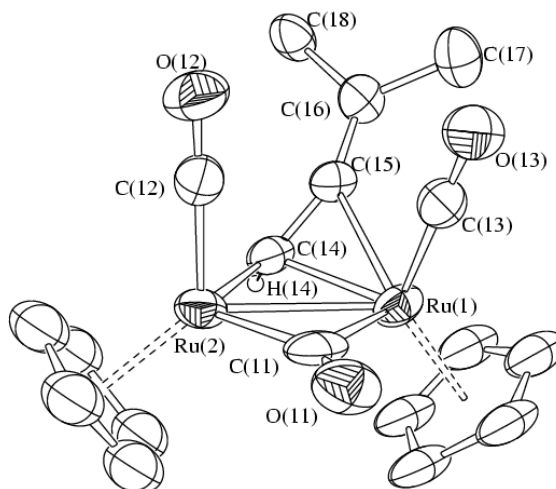


Figure 4: Molecular structure of  $[4a]^+$  in  $[4a]BPh_4$  with key atoms labeled [all H-atoms, except H(14), have been omitted for clarity]. Thermal ellipsoids are at the 30% probability level. Only the main images of the two disordered Cp ligands are drawn.

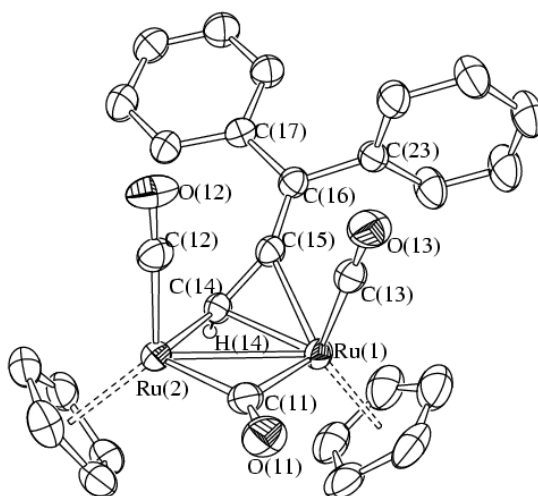
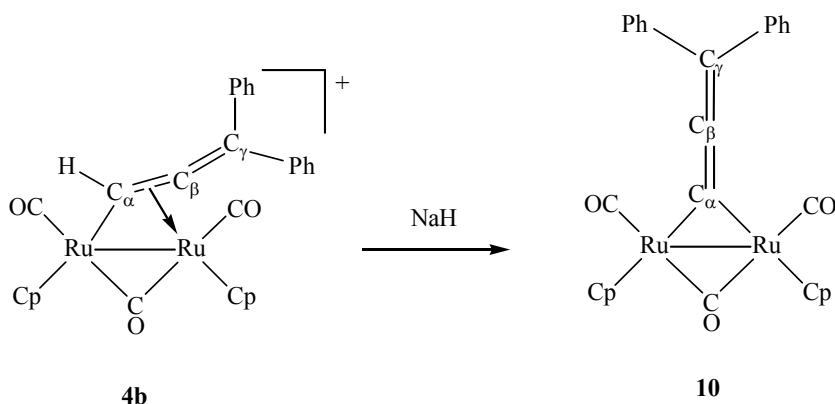


Figure 5: Molecular structure of  $[4b]^+$  in  $[4b]BPh_4$  with key atoms labeled [all H-atoms, except H(14), have been omitted for clarity]. Thermal ellipsoids are at the 30% probability level. Only one of the two independent cations present within the unit cell is represented.

### 3.2.2 Deprotonation Reactions

The chemistry of the cationic species **4** with a variety of compounds (*i.e.* NaH, NaBH<sub>4</sub>, KCN, lithium alkyls, lithium acetylides, alkynes, alkenes, amines, phosphines and isocyanides) was explored. Hence, all the neutral reactants except amines did not react even at high temperature.

Otherwise, ionic reactants and amines acted as Brønsted bases towards **4b** at room temperature, resulting in deprotonation reactions. Thus, the allenylidene dinuclear compound [Ru<sub>2</sub>Cp<sub>2</sub>(CO)<sub>2</sub>(μ-CO){μ-η<sup>1</sup>:η<sup>1</sup>-C<sub>α</sub>=C<sub>β</sub>=C<sub>γ</sub>(Ph)<sub>2</sub>}]<sup>4b,58</sup> (**10**) was obtained by reaction of **4b** with a base<sup>i</sup> (Scheme 49) and identified by spectroscopic methods and elemental analysis.



Scheme 49: Deprotonation of complex **4b**.

The IR spectrum of **10** (in CH<sub>2</sub>Cl<sub>2</sub>) , reported in Figure 6, exhibits the absorptions related to the three CO ligands, at 1991 (vs), 1954 (s) and 1803 (s) cm<sup>-1</sup>.

<sup>i</sup> Sodium hydride resulted to provide best yields (see Experimental).

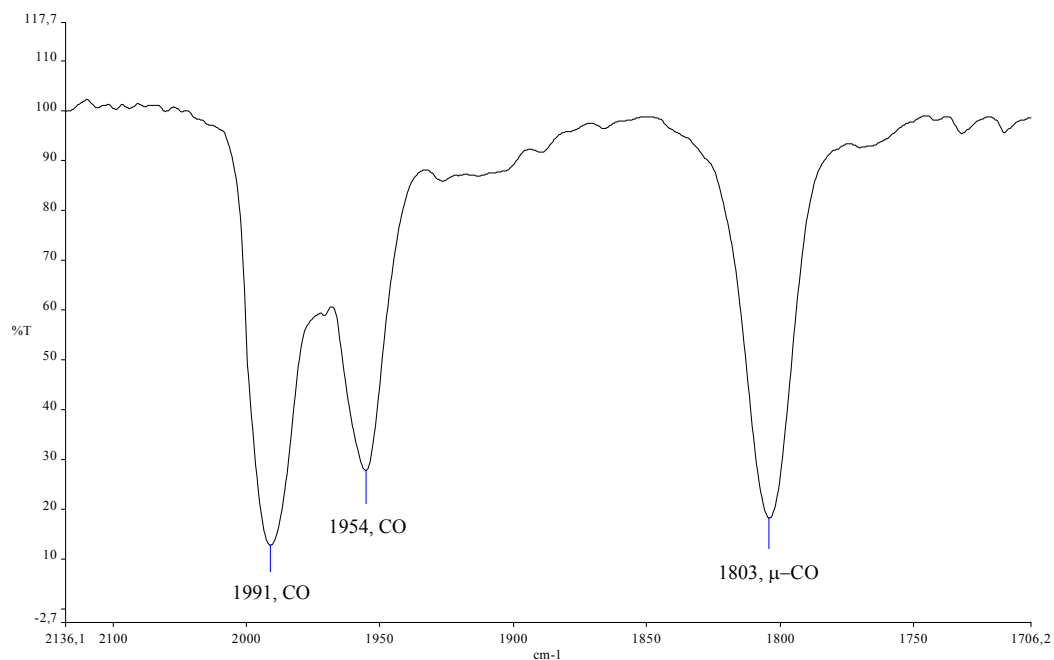


Figure 6: FT-IR spectrum ( $\text{CH}_2\text{Cl}_2$ ) of complex **10**.

The  $^1\text{H}$ - and  $^{13}\text{C}$ -NMR spectra (in  $\text{CDCl}_3$ ) (the  $^1\text{H}$ -NMR spectrum is reported in Figure 7) show a single resonance for the two Cp rings, coherently with the symmetry exhibited by the molecule. The allenylidene-chain carbons resonate at 192.0 ( $\text{C}_\alpha$ ), 201.4 ( $\text{C}_\beta$ ) and 105.8 ppm ( $\text{C}_\gamma$ ), in agreement with what reported previously for similar compounds<sup>59</sup>.

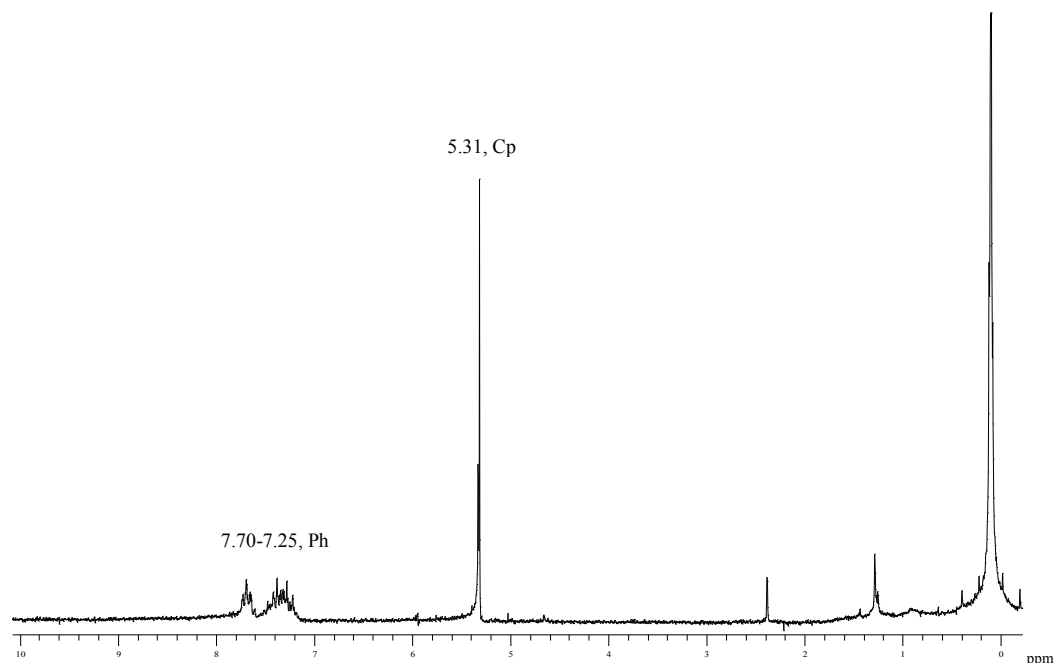


Figure 7:  $^1\text{H}$ -NMR spectrum ( $\text{CDCl}_3$ ) of complex **10**.

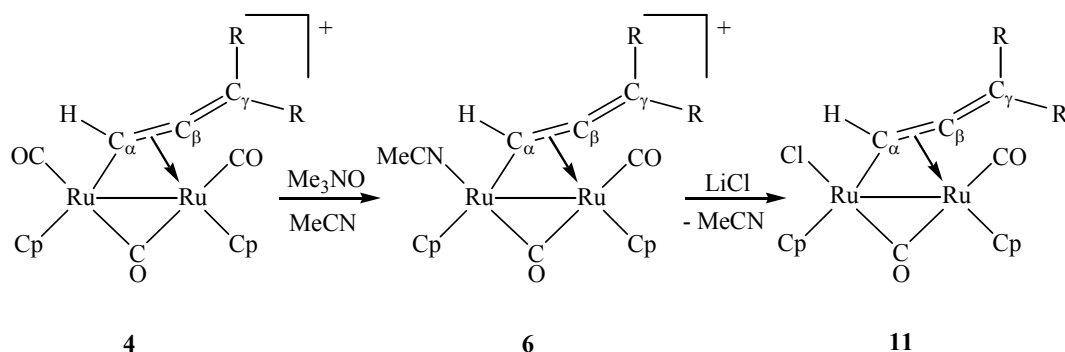
### 3.2.3 Generation of a vacant metal site: synthesis of acetonitrile and chloride derivatives

The reaction leading to **10** evidences the presence of acidic sites within the  $\mu$ -allenyl unit in the cationic complexes **4**. This fact prevents the possibility to address additions of nucleophiles, which are also Brønsted bases, to the allenyl ligand. On the other hand, neutral species (*e.g.* alkynes, alkenes) are almost unreactive towards **4** (see above). In fact, the availability of a vacant metal site in a dinuclear compound is an essential requirement for further intramolecular coupling reactions between the incoming reactant and the bridging hydrocarbyl ligand<sup>2c,d,i,5e,60</sup>. The vacancy may be generated upon replacement of one carbonyl with a labile ligand, and acetonitrile has been often used to the purpose<sup>31</sup>.

Thus, the complexes  $[\text{Ru}_2\text{Cp}_2(\text{CO})(\text{NCMe})(\mu\text{-CO})\{\mu\text{-}\eta^1\text{:}\eta^2\text{-C}_\alpha(\text{H})=\text{C}_\beta=\text{C}_\gamma(\text{R})_2\}][\text{BF}_4]$  (R = Me, **6a**; R = Ph, **6b**) have been prepared by reaction of an acetonitrile solution of **4a,b** with trimethylaminoxide, according to the known procedure<sup>22</sup>, (Scheme 50) and have been used *in situ* for subsequent reactions. Displacement of the nitrile ligand by chloride ion takes place in THF solution to give the neutral  $[\text{Ru}_2\text{Cp}_2(\text{CO})(\text{Cl})(\mu\text{-CO})\{\mu\text{-}\eta^1\text{:}\eta^2\text{-C}_\alpha(\text{H})=\text{C}_\beta=\text{C}_\gamma(\text{R})_2\}]$  (R = Me, **11a**; R = Ph, **11b**), see Scheme 50: Synthesis of the acetonitrile (R=Me, **6a**; R=Ph, **6b**)

and chloride (R=Me, **11a**; R=Ph, **11b**) derivatives.. The X-Ray structure of **11a** was previously determined, showing the chloride bound to the ruthenium  $\sigma$ -connected with  $\text{C}_\alpha$ <sup>22</sup>. The newly synthesized **6b** and **11b** have been characterized spectroscopically. The IR spectrum of **6b** (in  $\text{CH}_2\text{Cl}_2$ ), exhibits only two absorptions related to one terminal and one bridging CO ligands, at 2008 (vs) and 1861 (s)  $\text{cm}^{-1}$  respectively, while the absorption related to the acetonitrile ligand has been found at 2305  $\text{cm}^{-1}$ . The IR spectrum of **11b** (in  $\text{CH}_2\text{Cl}_2$ ) exhibits once again only two absorptions related to one terminal and one bridging CO, at lower frequencies respect to complex **6b** [1992 (vs) and 1883 (s)  $\text{cm}^{-1}$ , respectively], as expected for a neutral compound. The salient  $^1\text{H}$  NMR feature of **11b** is represented by the  $\text{C}_\alpha\text{H}$  resonance, which falls at 10.06 ppm (in  $\text{CDCl}_3$ ).

In principle, both compounds **6-11** may provide a vacant metal site: in **6**, acetonitrile is a labile ligand and may be easily replaced; otherwise, the chloride ligand in **11** could be efficiently removed by silver salts<sup>62</sup>. We have found that the best reactant is  $\text{AgSO}_3\text{CF}_3$ <sup>61</sup>.



*Scheme 50: Synthesis of the acetonitrile ( $R=\text{Me}$ , **6a**;  $R=\text{Ph}$ , **6b**) and chloride ( $R=\text{Me}$ , **11a**;  $R=\text{Ph}$ , **11b**) derivatives.*

### 3.2.4 Reactions of the allenyl unit with ethyldiazoacetate/amine

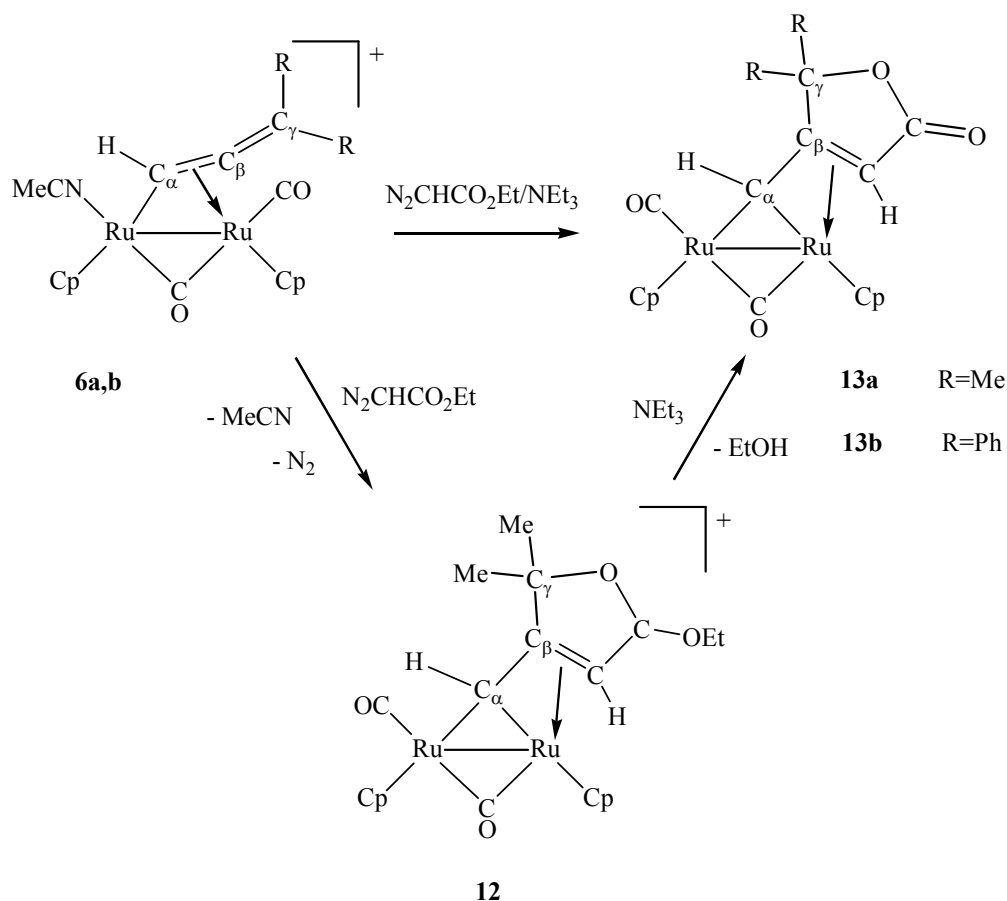
In consideration of the purpose to obtain novel organic fragments by functionalization of the bridging hydrocarbyl ligand, we decided to study the reactivity of the nitrile adduct **6a** with ethyldiazoacetate,  $\text{N}_2\text{CH}(\text{CO}_2\text{Et})$ . The reaction gave the butenolide derivative  $[\text{Ru}_2\text{Cp}_2(\text{CO})(\mu\text{-CO})\{\mu\text{-}\eta^1\text{:}\eta^3\text{-C}_\alpha(\text{H})\overline{\text{C}_\beta\text{C}_\gamma(\text{Me})_2\text{OC}(=\text{O})\text{C}(\text{H})}\}]$  (**13a**), which was isolated as a crystalline solid after work-up; by following analogous procedure, we prepared the bis-phenyl analogues

$[\text{Ru}_2\text{Cp}_2(\text{CO})(\mu\text{-CO})\{\mu\text{-}\eta^1\text{:}\eta^3\text{-C}_\alpha(\text{H})\overline{\text{C}_\beta\text{C}_\gamma(\text{Ph})_2\text{OC}(=\text{O})\text{C}(\text{H})}\}]$  (**13b**), see Scheme 51.

The reaction leading to **13a** proceeds smoothly in dichloromethane solution at room temperature, and it was monitored by IR spectroscopy. Progressive consumption of the starting metal compound was observed, whereas two new carbonylic bands appeared at 1980 and 1812  $\text{cm}^{-1}$ . These were attributed to the cationic adduct



$[\text{Ru}_2\text{Cp}_2(\text{CO})(\mu\text{-CO})\{\mu\text{-}\eta^1\text{:}\eta^3\text{-C}_\alpha(\text{H})\overline{\text{C}_\beta\text{C}_\gamma(\text{Me})_2\text{OC(OEt)}\text{C(H)}}^+\}]^+$  (**12**). After few hours, new IR bands came along at lower wavenumbers (1963, 1792 and 1735  $\text{cm}^{-1}$ ), suggesting the conversion of **12** into **13a** by removal of a  $[\text{Et}]^+$  unit (Scheme 51). Compound **12** could not be isolated in the solid state, however it was further characterized by a  $^1\text{H}$  NMR experiment (see Experimental). We have observed that the addition of a molar excess of  $\text{NEt}_3$ , forcing the abstraction of the  $\text{Et}^+$  fragment, makes the conversion **12**  $\rightarrow$  **13a** quantitative.



*Scheme 51: Reaction steps for the synthesis of heterocycle-substituted carbene ligands via reactions of the allenyl unit with ethyldiazoacetate/amine*

The new complexes **13a,b** have been fully characterized by IR and NMR spectroscopy, elemental analysis and X-Ray diffraction.

*3.2.5 Spectroscopic characterization of the products*

The IR spectra of **13a,b** ( $\text{CH}_2\text{Cl}_2$ ) show two bands due to a terminal carbonyl ligand and a bridging one (*e.g.* for **13b** at 1964 and 1795  $\text{cm}^{-1}$ ), and another absorption related to the acyl group at *ca.* 1740  $\text{cm}^{-1}$  (see Figure 8), in agreement with the presence of an ester unit.

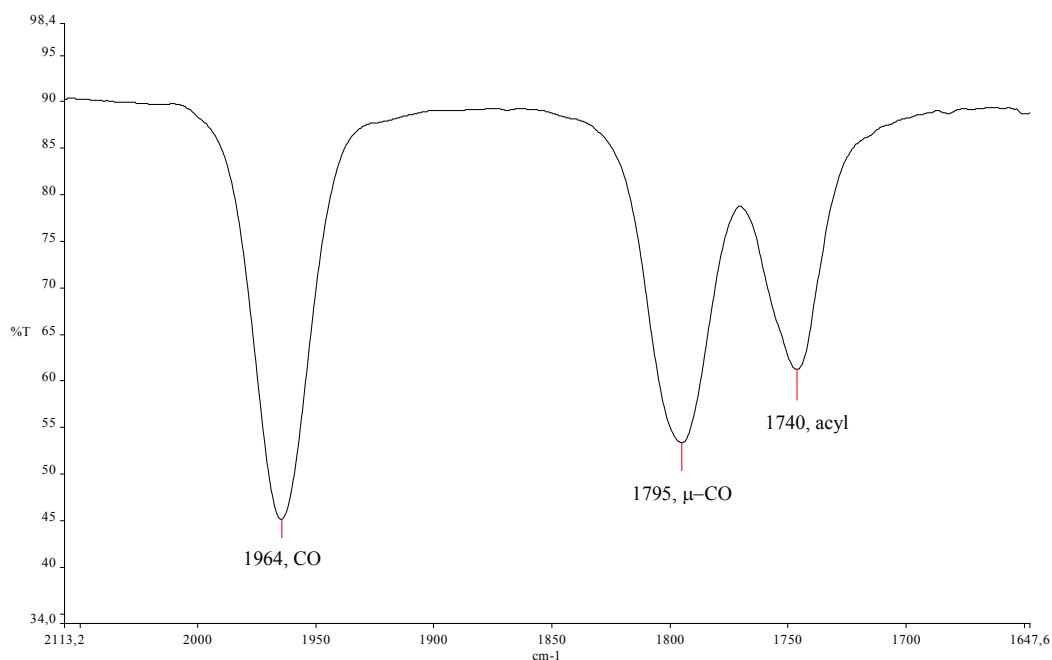


*Figure 8: FT-IR spectrum ( $\text{CH}_2\text{Cl}_2$ ) of complex **13b** in the carbonyl region.*

The salient NMR features are represented by the  $C_\alpha H$  resonances [*e.g.* for **13a**:  $\delta(^1H) = 10.04$  ppm;  $\delta(^{13}C) = 137.9$  ppm]. Coupling along the  $C_\alpha-C-C(O)$  chain is evident in the  $^1H$  NMR spectrum of **13a**, where  $C_\alpha H$  and  $CH(O)$  protons resonate as doublets ( $^4J_{HH} = 1.47$  Hz). Furthermore, the  $^{13}C$  NMR resonances of the  $C_\beta$  and of the  $C_\beta CC(O)$  carbon atoms fall at *ca.* 115 and 40 ppm respectively, while the  $^{13}C$  resonance of the lactone  $C=O$  carbon is seen at *ca.* 180 ppm (See Figure 9 and 10).

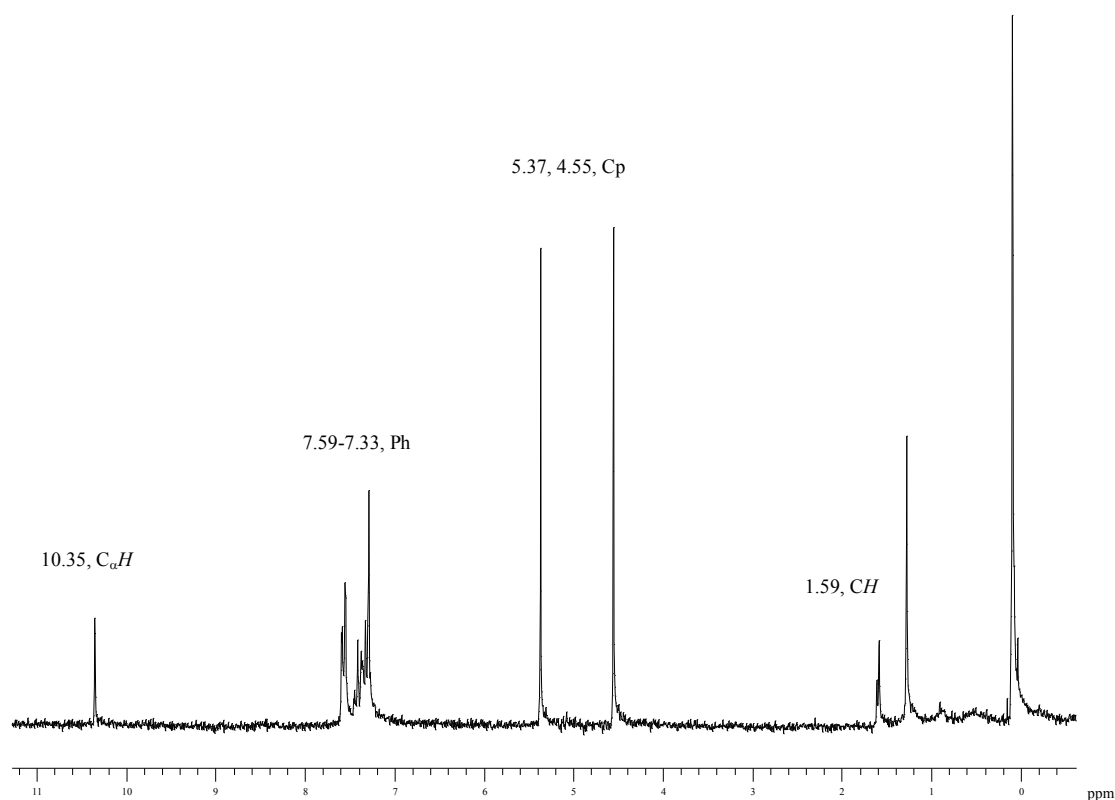


Figure 9:  $^1H$ -NMR ( $CDCl_3$ ) spectrum of complex **13b**.

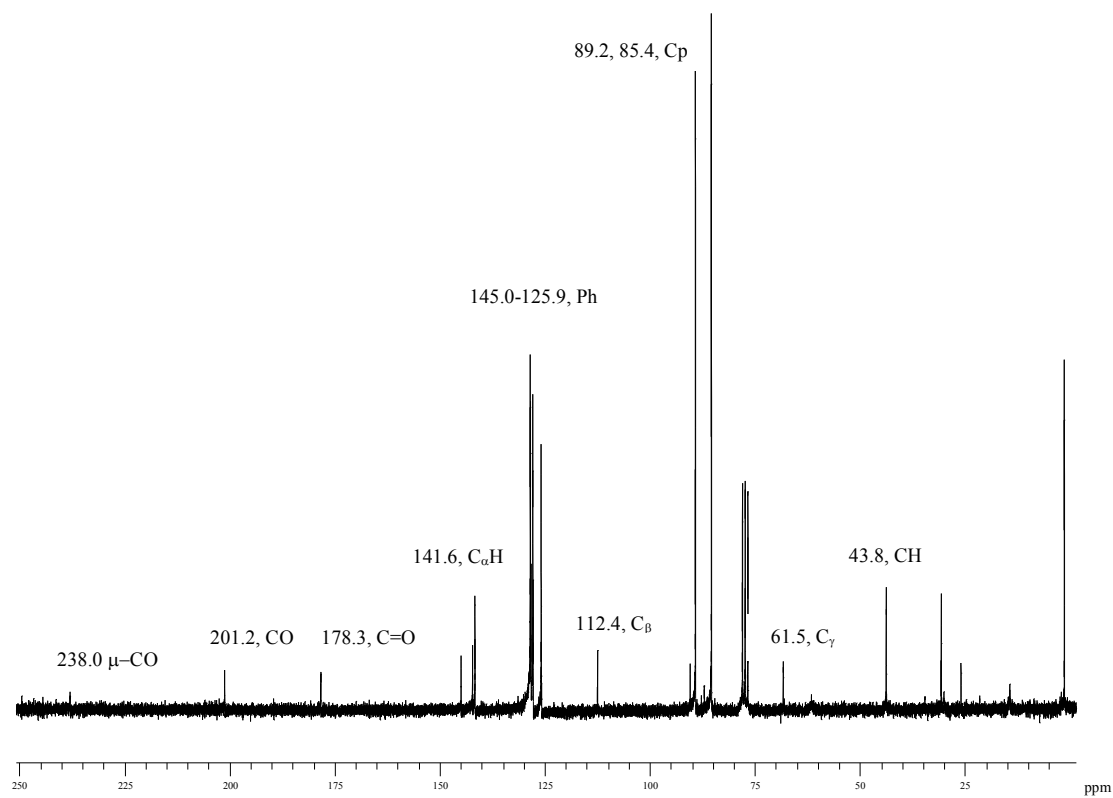


Figure 10:  $^{13}\text{C}$ -NMR ( $\text{CDCl}_3$ ) spectrum of complex **13b**.

### 3.2.6 X-ray Structures

The ORTEP representations of complexes **13a,b** are shown in Figure 11 and Figure 12.

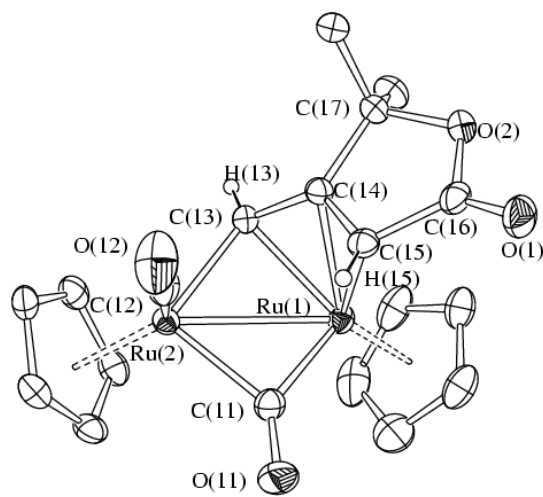


Figure 11: Molecular structure of **13a**. The H-atoms, except H(14) and H(15), have been omitted for clarity. Thermal ellipsoids are at the 30% probability level.

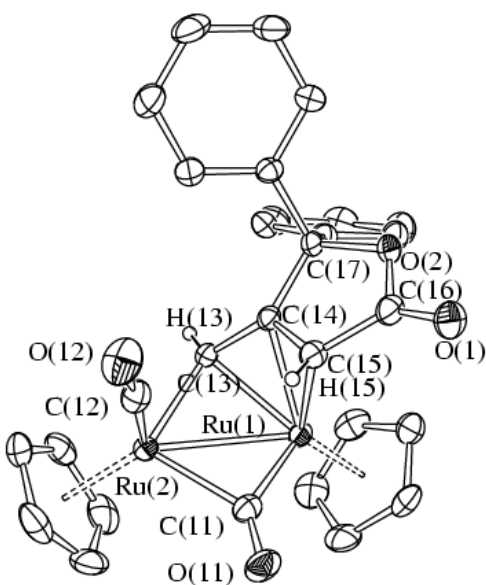
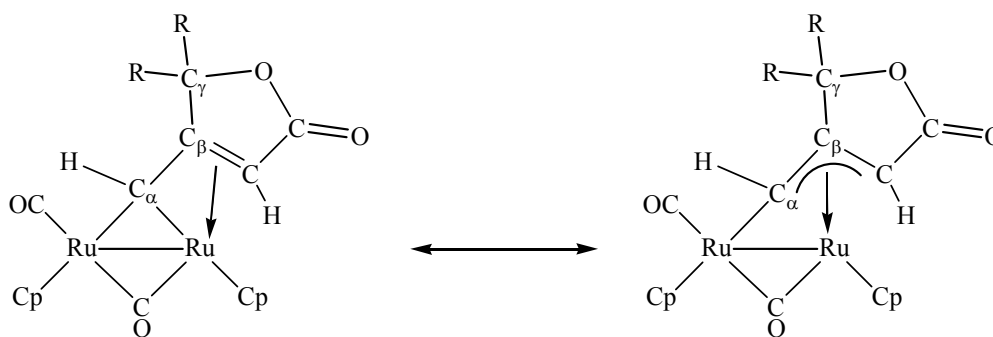


Figure 12: Molecular structure of **13b**. The H-atoms, except H(13) and H(15), have been omitted for clarity. Thermal ellipsoids are a the 30% probability level.

The molecular structures of **13a,b** consist of a bridging 5-dimethyl(diphenyl)-2-furanone-4-carbene ligand  $[\mu\text{-}\eta^1\text{:}\eta^3\text{-C(H)}\overline{\text{CC(R}_2\text{)OC(=O)C(H)}}]$  coordinated to the cis- $[\text{Ru}_2\text{Cp}_2(\text{CO})(\mu\text{-CO})]$  core. The carbene ligand possesses partial bridging allylidene character, hence two main resonance formulas may be traced for its representation (see Scheme 52: *Resonance formulas for compounds 13.*)<sup>62</sup>. Indeed both C(13)–C(14) [1.406(2) Å and 1.404(6) Å for **13a** and **13b**, respectively] and C(14)–C(15) interactions [1.433(2) Å and 1.411(7) Å] show appreciable  $\pi$ -character. Conversely, the C(15)–C(16) [1.461(3) Å and 1.487(7) Å] and C(14)–C(17) [1.533(2) Å and 1.527(6) Å] are characteristic for  $\text{C}_{\text{sp}^2}\text{--C}_{\text{sp}^2}$  and  $\text{C}_{\text{sp}^2}\text{--C}_{\text{sp}^3}$  single bonds. Similarly, C(16)–O(1) [1.205(2) Å and 1.205(6) Å] is a C=O double bond, whereas both C(16)–O(2) [1.376(3) Å and 1.358(6) Å] and C(17)–O(2) [1.461(2) Å and 1.479(6) Å] are in agreement with  $\text{C}_{\text{sp}^2}\text{--O}$  and  $\text{C}_{\text{sp}^3}\text{--O}$  single bonds. The C(14)–C(15)–C(16)–O(2)–C(17) ring is almost planar [mean deviations from the least squares plane are 0.0469 and 0.0494 Å, respectively].



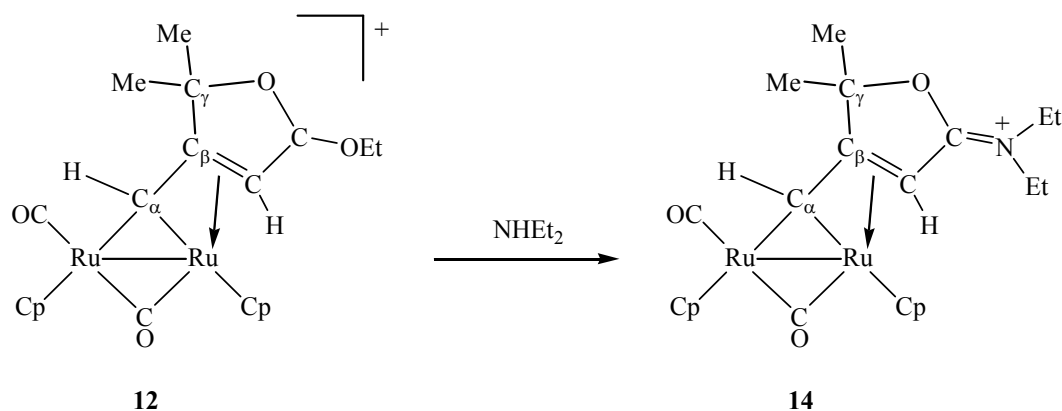
*Scheme 52: Resonance formulas for compounds 13.*

### 3.2.7 Mechanism

The formation of the novel compounds **13a,b** deserves more comments. It has to be remarked that the parent complexes **4a,b** are inert towards  $\text{N}_2\text{CHCO}_2\text{Et}$ . This means that the cyclization reaction involving the diazocompound and the allenyl moiety cannot proceed in the absence of the weakly coordinated NCMe ligand. In other terms, the initial coordination of the  $[\text{:CHCO}_2\text{Et}]$  unit is required in order to have subsequent coupling with the  $\mu$ -allenyl (see above). Unfortunately, we could not collect evidences for the formation of any intermediate species containing the  $[\text{Ru}=\text{CH}(\text{CO}_2\text{Et})]$  frame. The coupling takes place regiospecifically through formation of new  $\text{C}_\beta\text{--C}$  and  $\text{C}_\gamma\text{--O}$  bonds, at room temperature. The final compounds **13a,b** are probably obtained (see Scheme 51) *via*  $[\text{Et}^+]$  abstraction by the tertiary amine  $\text{NEt}_3$  behaving as a Brønsted base, although different pathways (*e.g.* hydrolysis due to adventitious water) should not be excluded in principle. Compounds **13a,b** contain a  $\alpha,\beta$ -butenolide ( $\gamma$ -crotonolactone) substituted carbene. Interestingly, the  $\alpha,\beta$ -butenolide ring represents the substructure of numerous biologically important natural and synthetic products, including terpenoidal lactone pheromones<sup>63</sup>, antileukaemic lignans<sup>64</sup>, and prostacycline analogues<sup>65</sup>: there is still great interest in the development of new synthetic protocols<sup>66</sup>. Examples are not lacking of carbon ligands bearing a  $\alpha,\beta$ -butenolide substituent<sup>67</sup>, however we present here the first case of a crystallographically characterized  $\alpha,\beta$ -butenolide-substituted carbene bridged in a dinuclear complex<sup>68</sup>.

### 3.2.8 Derivatization of the ligand

The presence of the [OEt] moiety, in the supposed intermediate cationic complex **12** (see Scheme 51), gives the opportunity of alternative derivatization of the five-membered cycle. Indeed, the treatment of a dichloromethane solution of **12** with the amine  $\text{NHEt}_2$ , instead of  $\text{NEt}_3$ , yielded the stable  $[\text{Ru}_2\text{Cp}_2(\text{CO})(\mu\text{-CO})\{\mu\text{-}\eta^1\text{:}\eta^3\text{-C}_\alpha(\text{H})\overline{\text{C}_\beta\text{C}_\gamma(\text{Me})_2\text{OC}(\text{NEt}_2)\text{C}(\text{H})}\}^+]$  (**14**), in admixture with minor amounts of **13a** (Scheme 53). The formation of **14** is the result of the nucleophilic attack of the secondary amine  $\text{NHEt}_2$  to replace the alkoxo group ( $-\text{OEt}$ ) in **12**.



Scheme 53: Formation of the 2-furaniminium-carbene **14**.

The cationic complex **14** contains a unprecedented 2-furaniminium substituted carbene ligand. It has to be noted that 2-furaniminium rings are essential constituents of a large number of natural products and pharmaceuticals<sup>69</sup>.

Complex **14** has been characterized by spectroscopic and analytical techniques, and by a X-Ray diffraction study. The structure of **14** (see Figure 13) is closely related to those of



**13a** and **13b**, once the acyl C=O group is replaced by a cationic iminium [C=NEt<sub>2</sub>]<sup>+</sup> fragment. Therefore, the bridging hydrocarbyl ligand in **14** may be alternatively described in terms of allylidene, likewise we have discussed above for **13a,b** (see Scheme 52).

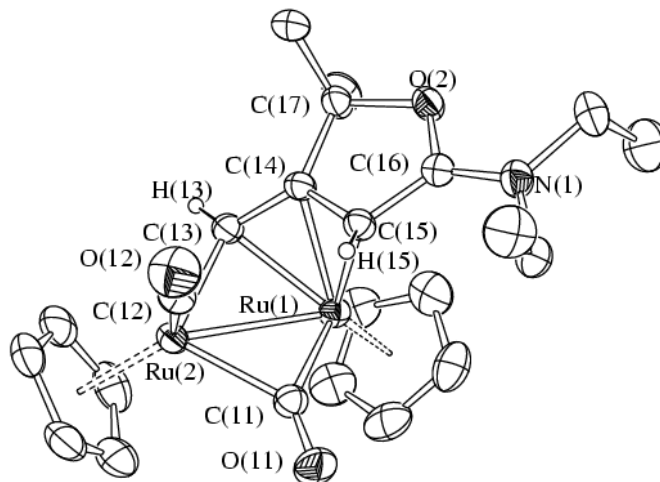
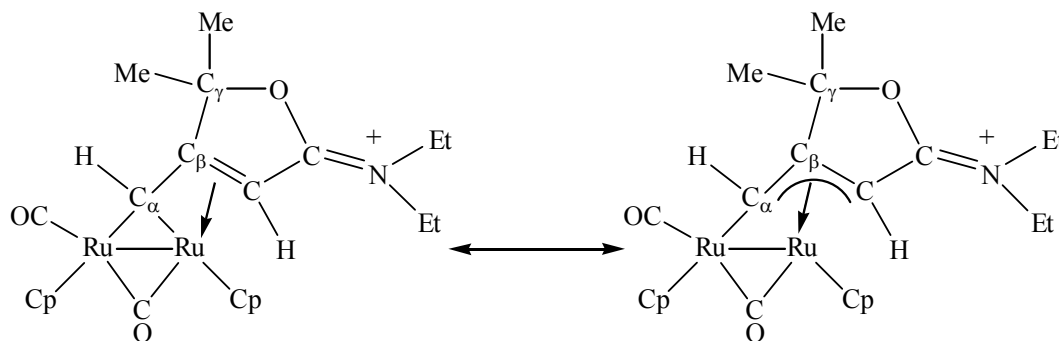


Figure 13: Structure of the cation **14** in [**14**][BF<sub>4</sub>] $\cdot$ CH<sub>2</sub>Cl<sub>2</sub>. The H-atoms, except H(13) and H(15), have been omitted for clarity. Thermal ellipsoids are at the 30% probability level.

The most relevant bonding parameters of **14** are similar to those of **13a,b**. The molecular structure of **14** consists of a bridging 5-dimethyl-2-(N,N-diethylfuraniminium)-4-carbene ligand coordinated to the cis-[Ru<sub>2</sub>Cp<sub>2</sub>(CO)(μ-CO)] core. The carbene ligand possesses partial bridging allylidene character, hence two main resonance formulas may be traced for its representation (see Scheme 52: *Resonance formulas for compounds 13.*)<sup>70</sup>. Indeed both C(13)–C(14) [1.400(6) Å] and C(14)–C(15) interactions [1.429(6) Å] show appreciable  $\pi$ -character. Conversely, the C(15)–C(16) [1.439(7) Å] and C(14)–C(17) [1.520(6) Å] are characteristic for C<sub>sp</sub><sup>2</sup>–C<sub>sp</sub><sup>2</sup> and C<sub>sp</sub><sup>2</sup>–C<sub>sp</sub><sup>3</sup> single bonds. Similarly,

C(16)–N(1) [1.313(6) Å] is a C=N double bond, whereas both C(16)–O(2) [1.330(6) Å] and C(17)–O(2) [1.502(6) Å] are in agreement with C<sub>sp</sub><sup>2</sup>–O and C<sub>sp</sub><sup>3</sup>–O single bonds. The C(14)–C(15)–C(16)–O(2)–C(17) ring is almost planar.



*Scheme 54: Resonance formulas for compound 14.*

The IR spectrum of **14** (CH<sub>2</sub>Cl<sub>2</sub> solution) displays two absorptions at 1975 and 1805 cm<sup>-1</sup>, related to the terminal and the bridging carbonyl groups, respectively. In addition, a medium intensity band at 1644 cm<sup>-1</sup> accounts for the iminium C=NEt<sub>2</sub> fragment (see Figure 14).

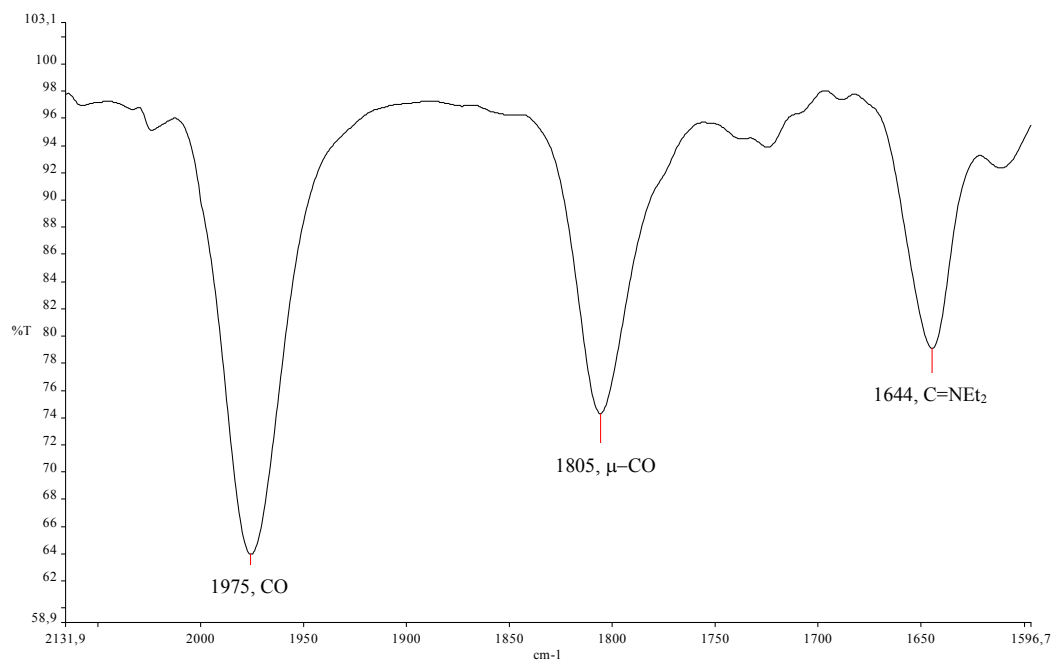


Figure 14: FT-IR ( $\text{CH}_2\text{Cl}_2$ ) spectrum of complex **14** in the carbonyl region.

The iminium carbon is seen (in  $\text{CDCl}_3$ ) at 181.0 ppm in the  $^{13}\text{C}$  NMR spectrum. The resonances of  $\text{C}_\alpha$ ,  $\text{C}_\beta$  and  $\text{C}_\gamma$  fall at 141.3, 114.3 and 97.2 ppm, in the order given, resembling what found for **13a**. The  $\mu$ -alkylidene nature of  $\text{C}_\alpha$  is confirmed by the high-frequency chemical shift ( $\delta$  10.35 ppm) of the related proton in the  $^1\text{H}$  NMR spectrum (see Figure 15).

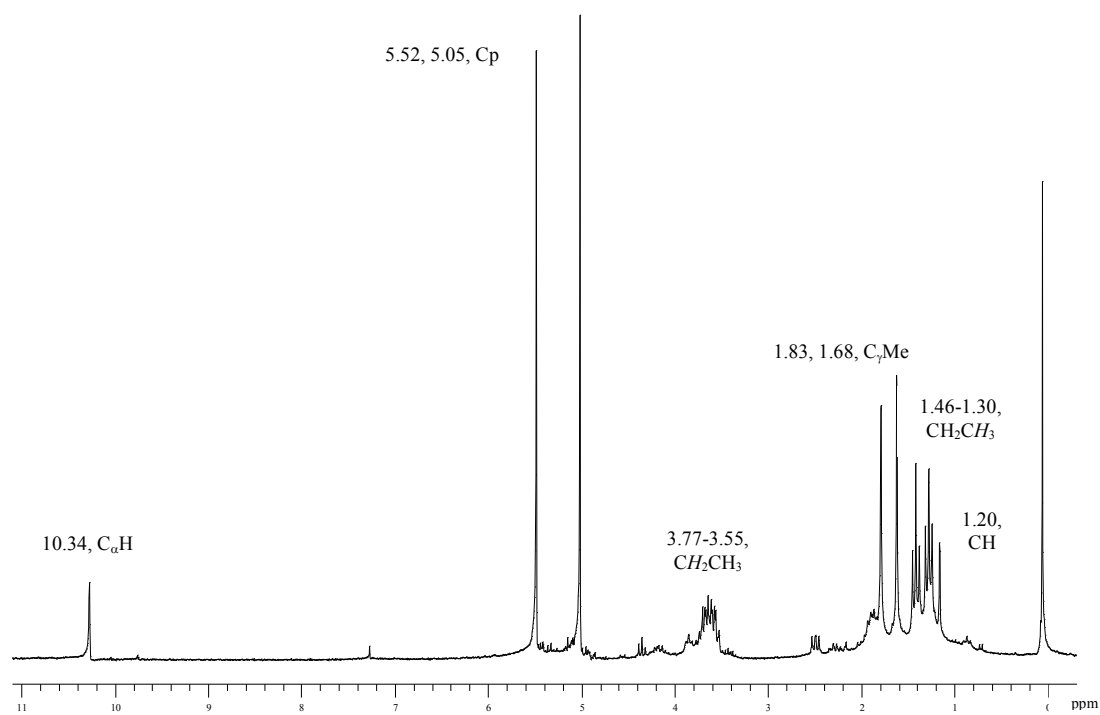


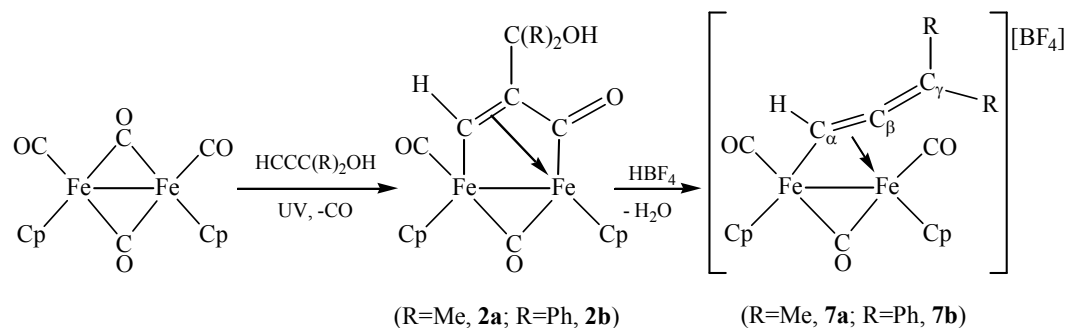
Figure 15:  $^1\text{H}$ -NMR ( $\text{CDCl}_3$ ) spectrum of complex 14.

### 3.3 Chemistry of the cationic diiron $\mu$ -allenyl complexes

In the light of the results obtained in the functionalization of the bridging allenyl ligand in diruthenium complexes **4**, we decided to address our attention to the unreported analogous diiron  $\mu$ -allenyl complexes. In principle, diiron complexes hold the remarkable advantage to be less expensive and less toxic compared to the diruthenium analogous, in the light to obtain organic species which could not be attainable through common organic procedures.

#### 3.3.1 Synthesis

The diiron-allenyl complexes  $[\text{Fe}_2\text{Cp}_2(\text{CO})_2(\mu\text{-CO})\{\mu\text{-}\eta^1\text{:}\eta^2_{\alpha\beta}\text{-C}_\alpha(\text{H})=\text{C}_\beta=\text{C}_\gamma(\text{R})_2\}][\text{BF}_4]$  (R = Me, [**7a**][BF<sub>4</sub>]; R = Ph, [**7b**][BF<sub>4</sub>]) could be prepared by a two-step procedure, consisting of photolytic CO displacement and insertion of the alkynol  $\text{HC}\equiv\text{CCR}_2\text{OH}$  into a Fe–CO bond, followed by protonation of the –OH group and H<sub>2</sub>O removal. Compared to the synthesis of the analogous diruthenium complexes **4**, the alkynol can be inserted directly into the Fe–CO bond (see Scheme 55).



Scheme 55: Preparation of the cationic diiron  $\mu$ -allenyl complexes ( $R = \text{Me}$ , **7a**;  $R = \text{Ph}$ , **7b**).

The intermediate dimetallacyclopentenone species  $[\text{Fe}_2\text{Cp}_2(\text{CO})_2(\mu\text{-CO})\{\mu\text{-}\eta^1\text{:}\eta^3\text{-C(H)C(CR}_2\text{OH)C(=O)\}}]$  ( $R = \text{Me}$ , **2a**;  $R = \text{Ph}$ , **2b**) have been isolated and fully characterized by analytical and spectroscopic techniques (see Experimental). The successive generation of the allenyl moiety is accompanied by the cleavage of a C–C bond and the conversion of the acyl group into a terminal carbonyl ligand (see Scheme 55). Compounds **7** have been isolated in good yields after filtration on alumina.

The crystalline triflate salt  $[\mathbf{7a}][\text{SO}_3\text{CF}_3]$  was obtained from **7a** via anion-exchange reaction (see Experimental), and the solid-state structure could be ascertained by X-ray diffraction studies. The ORTEP representation is shown in Figure 16.

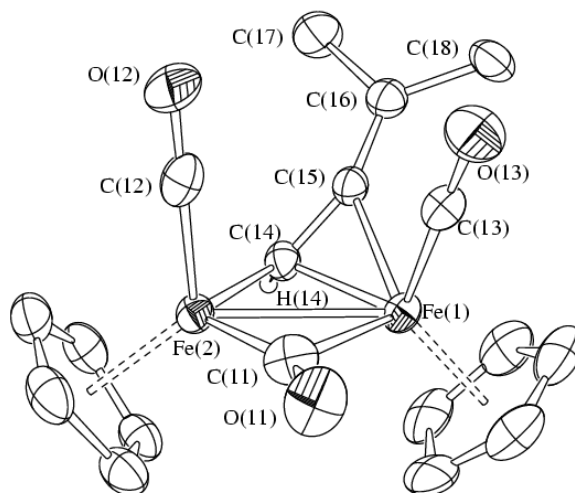


Figure 16: Structure of the cation  $[7a]^+$  in  $[7a][SO_3CF_3]$ . The H-atoms, except H(14), have been omitted for clarity. Thermal ellipsoids are at the 30% probability level.

Complex **7a** consists of a  $cis$ - $[M_2(Cp)_2(CO)_2(\mu-CO)]$  core, to which is coordinated the bridging  $\mu$ - $\eta^1:\eta^2$ -C(H)=C=C(Me)<sub>2</sub> allenyl ligand. The bonding parameters of the latter are comparable to those obtained for the diruthenium analogous **4a** and as expected for this class of ligands, with C(14)–C(15)–C(16) considerably bent [ $152.0(8)^\circ$ ;  $154.8(10)^\circ$  for **4a**] and both C(14)–C(15) [ $1.332(11)$  Å;  $1.390(13)$  Å for **4a**] and C(15)–C(16) [ $1.339(11)$  Å;  $1.328(13)$  Å for **4a**] displaying considerable  $\pi$ -character. The bridging CO ligand is again substantially asymmetric in all structures, showing the shorter contact toward M(2), that is  $\eta^1$ -coordinated to the allenyl ligand.

Both IR and NMR spectroscopic features of complexes **7** are comparable with those of the diruthenium analogous **4**. The IR spectra (in CH<sub>2</sub>Cl<sub>2</sub> solution, see Figure 17) of **7** display three absorptions ascribable to two terminal carbonyl ligands and one semi-

bridging carbonyl (*e.g.* for **7a** at 2036, 2011 and 1864  $\text{cm}^{-1}$ , respectively), coherently with the solid state features.

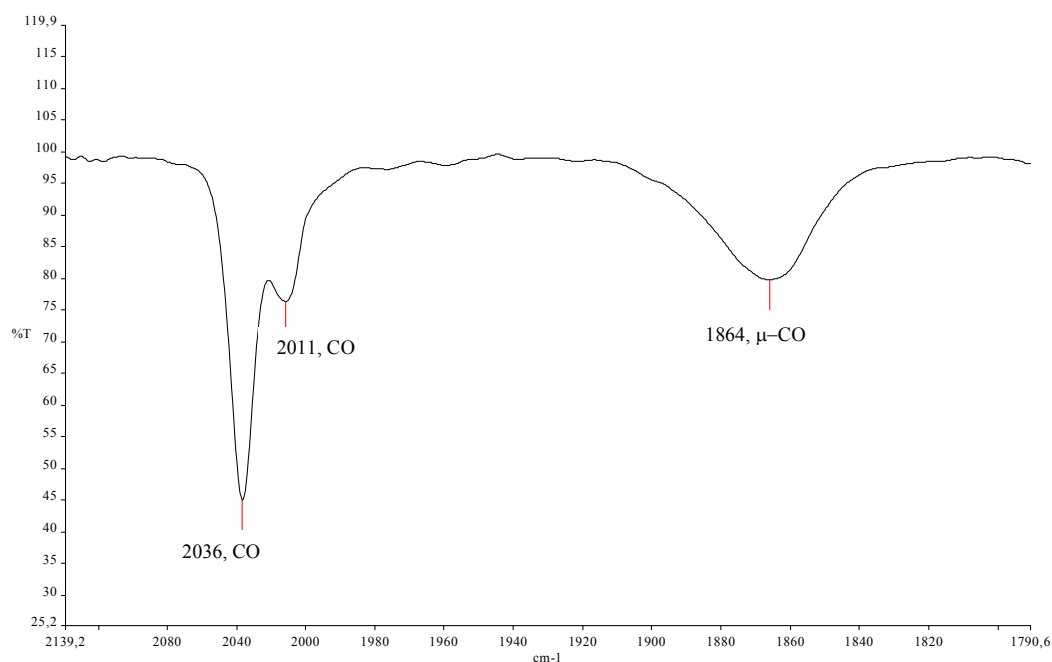


Figure 17: FT-IR ( $\text{CH}_2\text{Cl}_2$ ) spectrum of complex **7a** in the carbonyl region.

Analogously to what reported above for complexes **4**, a  $\sigma$ - $\pi$  “windshield wiper” motion of the allenyl moiety is probably responsible for the broad signals observed in the NMR spectra of **7** at room temperature. Readable  $^1\text{H}$ -NMR spectra (single sets of resonances) could be recorded at 233K. in  $\text{CD}_3\text{CN}$  (see Figure 18); thus typical high-frequency  $\text{C}_\alpha\text{H}$  resonances could be detected, in accordance with the  $\mu$ -alkylidene character [*e.g.* in the case of **4a**:  $\delta(^1\text{H}) = 11.77$  ppm;  $\delta(^{13}\text{C}) = 147.2$  ppm].



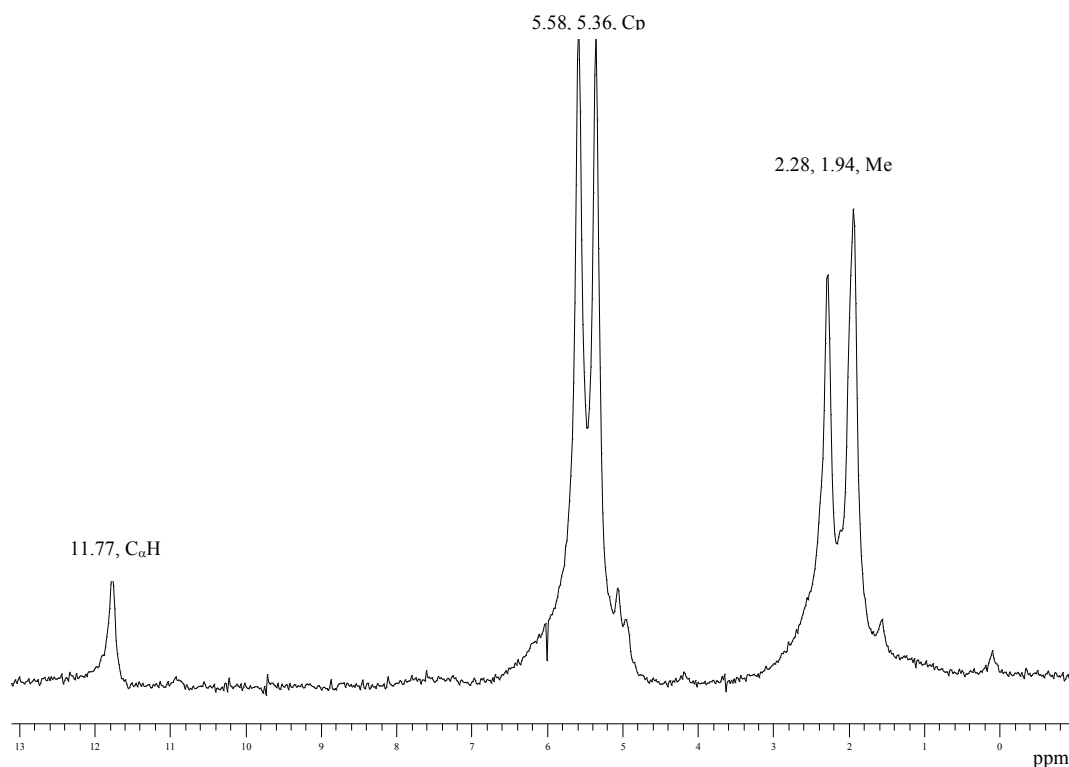
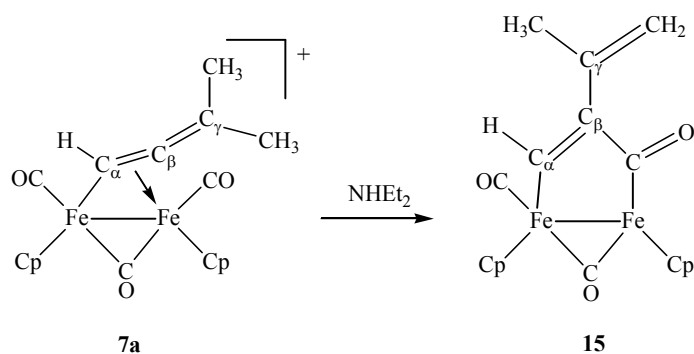


Figure 18:  $^1\text{H}$ -NMR ( $\text{CD}_3\text{CN}$ , 238K) spectrum of complex **7a**.

### 3.3.2 Deprotonation Reactions

In order to explore the chemistry of the cationic species **7**, reactions with a variety of compounds (*i.e.*  $\text{NaH}$ ,  $\text{NaBH}_4$ ,  $\text{KCN}$ , lithium alkyls, lithium acetylides, alkynes, alkenes, amines, phosphines and isocyanides) were performed. Hence, in accordance with what obtained for the diruthenium complexes **4**, all the neutral reactants except amines did not give any reaction even at high temperature. Otherwise, ionic reactants and amines acted as Brönsted bases towards **7a** at room temperature, resulting in deprotonation reaction. However, while the deprotonation of  $\text{C}_\alpha\text{-H}$  in compound **4b** afforded the allenylidene compound **10**, treatment of complex **7a** with bases resulted in formation of the

dimetallacyclopentenone  $[\text{Fe}_2\text{Cp}_2(\text{CO})(\mu\text{-CO})\{\mu\text{-}\eta^1:\eta^3\text{-C}_\alpha(\text{H})=\text{C}_\beta(\text{C}_\gamma(\text{Me})\text{CH}_2)\text{C}(=\text{O})\}]$  (**15**) (see Scheme 56). Compound **15** results from single deprotonation of one  $\text{C}_\gamma$ -bound methyl group in **7a**, and successive cyclization consisting of carbon-carbon bond formation between the  $\text{C}_\beta$  and one carbonyl ligand. Best yields were reached by using  $\text{NHEt}_2$  (see Experimental)<sup>ii</sup>. The product was obtained and identified by spectroscopy and elemental analysis.



Scheme 56: Deprotonation reactions of the allenyl complex **4a**.

The spectroscopic features of **15** agree with the structure shown in Scheme 56: the IR spectrum (in  $\text{CH}_2\text{Cl}_2$ , see Figure 19) shows four bands at 1975, 1796, 1748 and  $1611\text{ cm}^{-1}$ , attributed respectively to the terminal carbonyl ligand, the bridging carbonyl, the acyl group and the  $\text{C}=\text{C}$  fragment.

<sup>ii</sup> The reaction of **7b** with diethylamine gave complicated mixtures of products, with clear identification of relevant amounts of  $[\text{Fe}_2\text{Cp}_2(\text{CO})_4]$ .

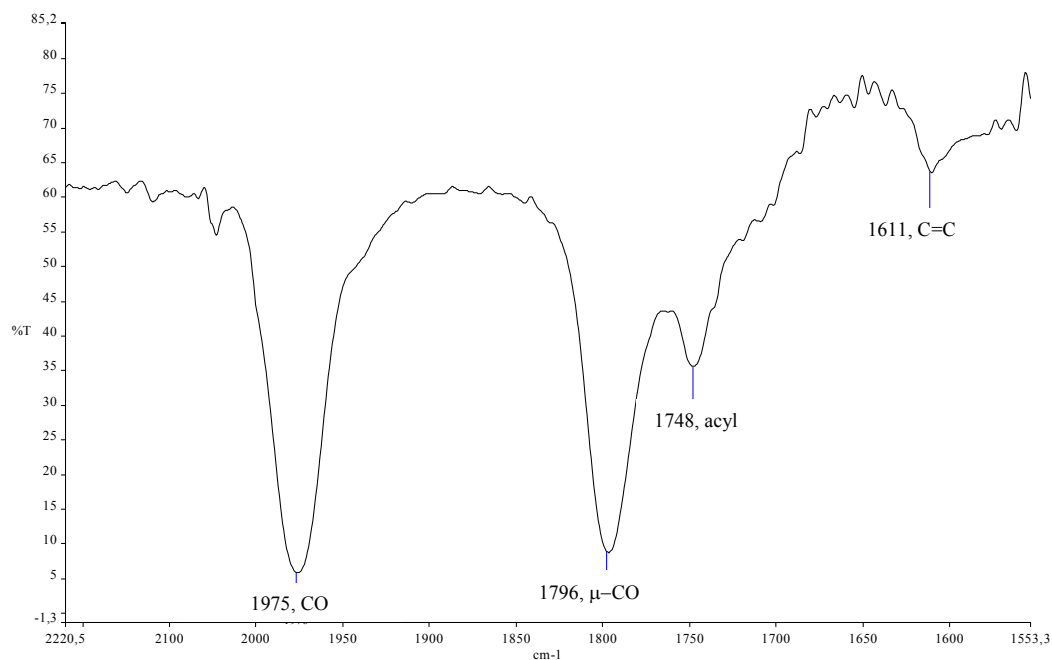


Figure 19: FT-IR ( $\text{CH}_2\text{Cl}_2$ ) spectrum of complex **15**.

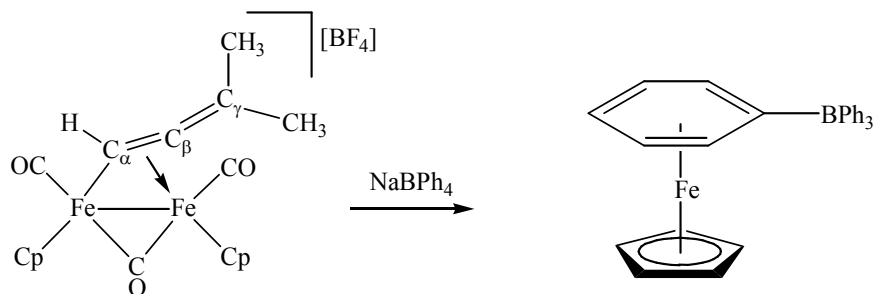
The  $^1\text{H}$  NMR spectrum displays the singlet related to the  $\text{C}_\alpha\text{-H}$  proton at typical high frequency ( $\delta$  12.29 ppm), whereas the resonances due to  $\text{CH}_3$  and  $\text{C}_{sp^2}\text{-H}_2$  are observed at 2.09 and 5.40-5.23 ppm respectively, as expected for a propenyl fragment  $[-\text{C}(\text{CH}_3)=\text{CH}_2]$ <sup>71</sup>. Furthermore, the  $^{13}\text{C}$  NMR resonances for  $\text{C}_\alpha$ ,  $\text{C}_\beta$  and *acyl*-CO at 173.2, 31.2 and 232.7 ppm respectively, are in accordance with those reported for similar diiron-cyclopentenone compounds<sup>20a</sup>.

### 3.3.3 Reactivity of **7** with $\text{MeCN}/\text{Me}_3\text{NO}$ .

The reaction leading to **15** evidences the presence of acidic site within the  $\mu$ -allenyl unit in the cationic complex **7a**, as previously found for complexes **4**. This fact prevents

the possibility to address additions of nucleophiles, which are also Brønsted bases, to the allenyl ligand. On the other hand, neutral species (*e.g.* alkynes, alkenes) are almost unreactive towards **7**. In order to favour the possible coupling between the allenyl ligand and unsaturated reactants, we tried the substitution of one carbonyl with acetonitrile in **7**; unfortunately, all of the attempts failed. These reactions resulted in fragmentation to give non identified mononuclear iron species, together with minor amounts of  $[\text{Fe}_2\text{Cp}_2(\text{CO})_4]$ . Similar results were obtained allowing complex **7** to react with  $\text{Me}_3\text{NO}$  in the presence of an unsaturated species, *i.e.* alkenes and alkynes.

The easy cleavage of the Fe–Fe bond in **7** is confirmed by the room temperature formation of  $[\text{FeCp}(\eta^6\text{-PhBPh}_3)]^{72}$ , identified by X-Ray diffraction analysis, in an attempt to prepare  $[\mathbf{7a}][\text{BPh}_4]$  by addition of  $\text{NaBPh}_4$  to an acetonitrile solution of  $[\mathbf{7a}][\text{BF}_4]$  (Scheme 57).



*Scheme 57: formation of  $[\text{FeCp}(\eta^6\text{-PhBPh}_3)]$  and other products by reaction of **7a** with  $\text{NaBPh}_4$ .*

The weakness of the Fe–Fe bond with respect to the Ru–Ru one is in agreement with the observation that, in general, the heavier transition elements are more prone to form

stronger M–M bonds than their congeners in the first transition series<sup>73</sup>. The combination of the acidic properties of **7** with the instability of the dinuclear system makes unattainable the idea of building functionalized organic fragments stabilized by coordination to the  $[\text{Fe}_2\text{Cp}_2(\text{CO})_2]$  framework (see Introduction), starting from **7**.

### 3.4 Chemistry of the cationic diiron $\mu$ -vinyl complexes

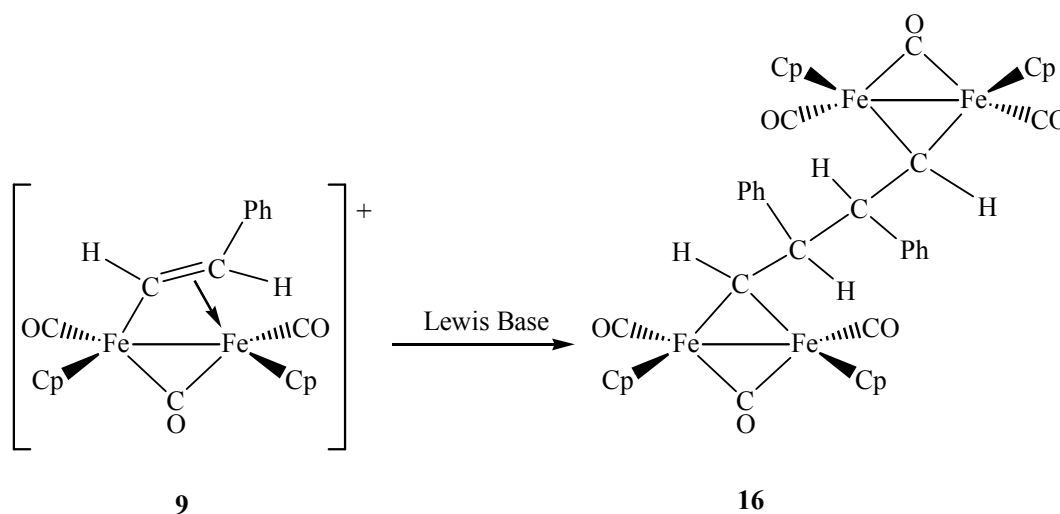
Due to the difficulties encountered with the study of the reactivity of the diiron  $\mu$ -allenyl complexes **7**, I decided to address my attention to a different unsaturated ligand. Hence I moved to investigate the chemistry of the diiron  $\mu$ -vinyl complex  $[\text{Fe}_2\text{Cp}_2(\text{CO})_2(\mu\text{-CO})(\mu\text{-CH}=\text{C}(\text{H})(\text{Ph}))][\text{BF}_4]$  (**9**), which can be obtained by protonation of the dimetallacyclopentenone species  $[\text{Fe}_2\text{Cp}_2(\text{CO})_2(\mu\text{-CO})(\mu\text{-}\eta^1\text{:}\eta^3\text{-CR}=\text{C}(\text{R})\text{C}(\text{O}))]^{48}$  (see Scheme 39).

First I tried the addition of a variety of unsaturated neutral species (*e.g.* alkynes, alkenes) to **9**, nevertheless these attempts came unsuccessful. Otherwise, the substitution of one carbonyl with acetonitrile in **9** by using the trimethylamineoxide /  $\text{CH}_3\text{CN}$  method (see Scheme 50) gave non identified mononuclear iron species and minor amounts of  $[\text{Fe}_2\text{Cp}_2(\text{CO})_4]$ . In other terms, the easy cleavage of the Fe–Fe bond makes unattainable the idea of introducing one labile ligand in order to facilitate the coupling of the bridging hydrocarbyl ligand with neutral organic species.

#### 3.4.1 Reductive Coupling of compound **9**

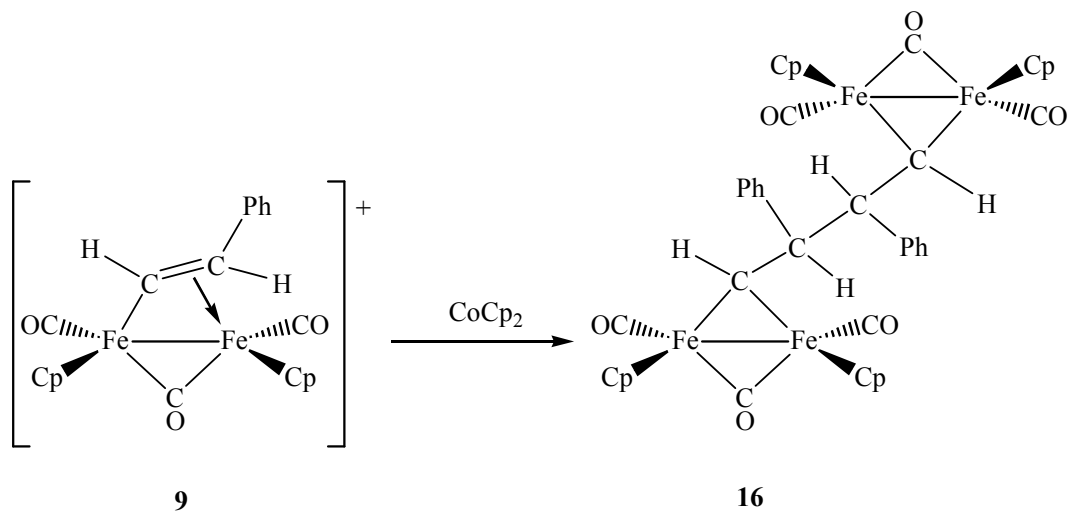
The nucleophilic additions of a restricted series of anionic nucleophiles (*e.g.*  $\text{H}^-$ ,  $\text{CN}^-$ ) to **9** were reported to occur at the phenyl-substituted carbon, to afford alkylidene derivatives<sup>48a</sup>. All my attempts to extend this chemistry to various Lewis bases (*e.g.*  $\text{PhLi}$ ,  $\text{LiC}\equiv\text{CPh}$ ,  $\text{NEt}_3$ ) resulted in the formation of a unique product which was

identified as the tetrairon complex  $[\text{Fe}_2\text{Cp}_2(\text{CO})_2(\mu\text{-CO})\{\mu\text{-}\eta^2\text{-CHCH(Ph)}\}]_2$ , **16** (see Scheme 58).



Scheme 58: Reaction of **9** with various Lewis bases ( $B = \text{PhLi}$ ,  $\text{LiC}\equiv\text{CPh}$ ,  $\text{NaOMe}$ ,  $\text{NEt}_3$ ).

The reaction reported in Scheme 58 is substantially a reduction, so I reckoned that the best conditions for the formation of **16** could be found by using a reducing agent. On consideration that cobaltocene,  $\text{CoCp}_2$ , has been widely employed for monoelectronic reductions in non aqueous medium<sup>74</sup>, best conditions for the synthesis of **16** were found by using  $\text{CoCp}_2$  as reactant (see Scheme 59). Immediate reaction accompanied by color change from brown to red was observed. Then chromatography on an alumina column gave compound **16** in high yields after work-up.



*Scheme 59: Reductive dimerization of complex **9** through reaction with cobaltocene.*

The formation of **16** is clearly the result of the C–C homocoupling of a diiron complex derived from the monoelectron reduction of **9**. This outcome resembles the previous finding that  $[\text{Fe}_2\text{Cp}_2(\text{CO})_2(\mu\text{-CO})\{\mu\text{-}\eta^1\text{-}\eta^2\text{-CH=CH}(\text{CO}_2\text{Me})\}]^+$  may dimerize to  $[\text{Fe}_2\text{Cp}_2(\text{CO})_2(\mu\text{-CO})\{\mu\text{-}\eta^2\text{-CHCH}(\text{CO}_2\text{Me})\}]_2$  upon reaction with  $\text{NaHCO}_3$ .<sup>75</sup>

The new complex **16** has been fully characterized by IR and NMR spectroscopy, elemental analysis and X-Ray diffraction.

The IR spectrum of **16** (in  $\text{CH}_2\text{Cl}_2$ ) clearly shows two bands due to two terminal carbonyl ligand and a bridging one at 1973, 1936, and 1774  $\text{cm}^{-1}$ , respectively (see Figure 20).



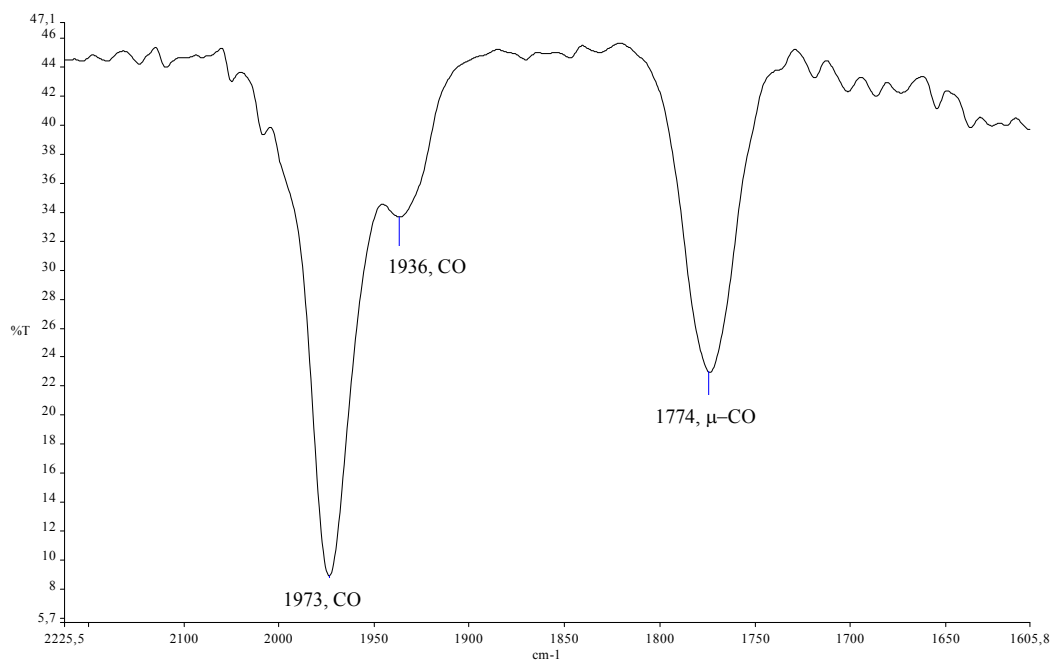


Figure 20: FT-IR ( $\text{CH}_2\text{Cl}_2$ ) spectrum of complex **16** in the carbonyl region.

The NMR spectra exhibit single set of resonances corresponding to two equivalent  $[\text{Fe}_2]$  units linked by the newly formed C–C bond. Salient NMR features are represented by the high frequency resonances at 12.10 ppm ( $^1\text{H}$ ) and 178.7 ppm ( $^{13}\text{C}$ ), ascribable to the carbene moiety. The  $sp^3$  Ph-substituted carbons fall at 77.5 ppm. Coupling along the  $\text{C}_\alpha\text{--C}_\beta$  chain is evident in the  $^1\text{H}$  NMR spectrum, where  $\text{C}_\alpha\text{H}$  and  $\text{C}_\beta\text{H}$  protons resonate as doublets ( $^4J_{\text{HH}} = 8.07$  Hz) (see Figure 21:  $^1\text{H}$ -NMR ( $\text{CDCl}_3$ ) spectrum of complex **16**).

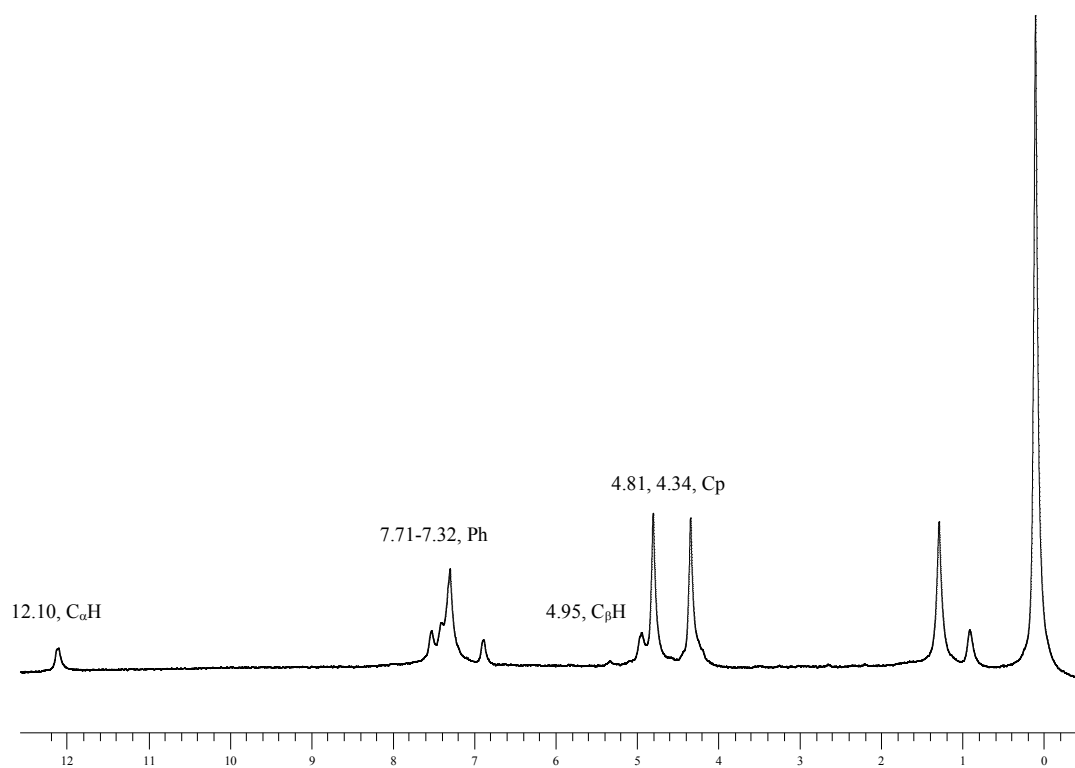


Figure 21:  $^1\text{H}$ -NMR ( $\text{CDCl}_3$ ) spectrum of complex **16**.

The ORTEP representation of complexes **16** is shown in Figure 22.

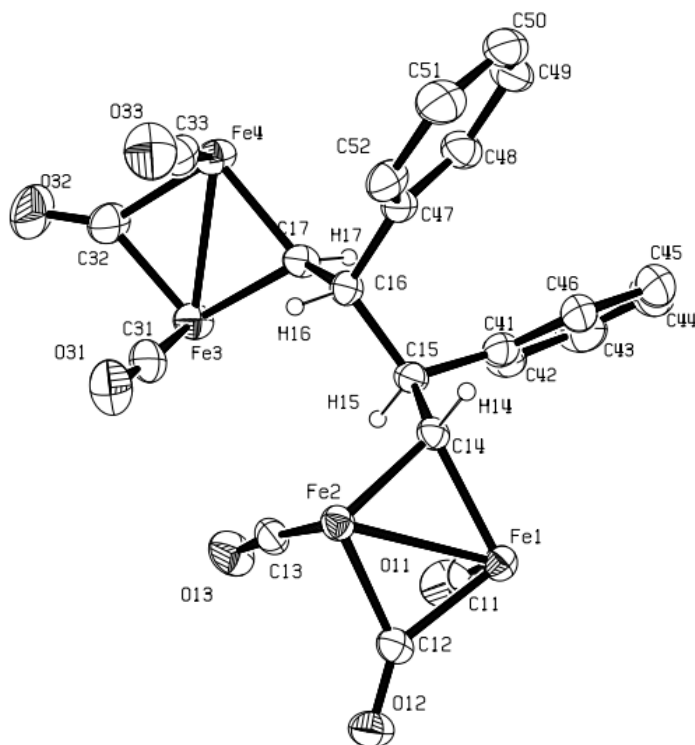
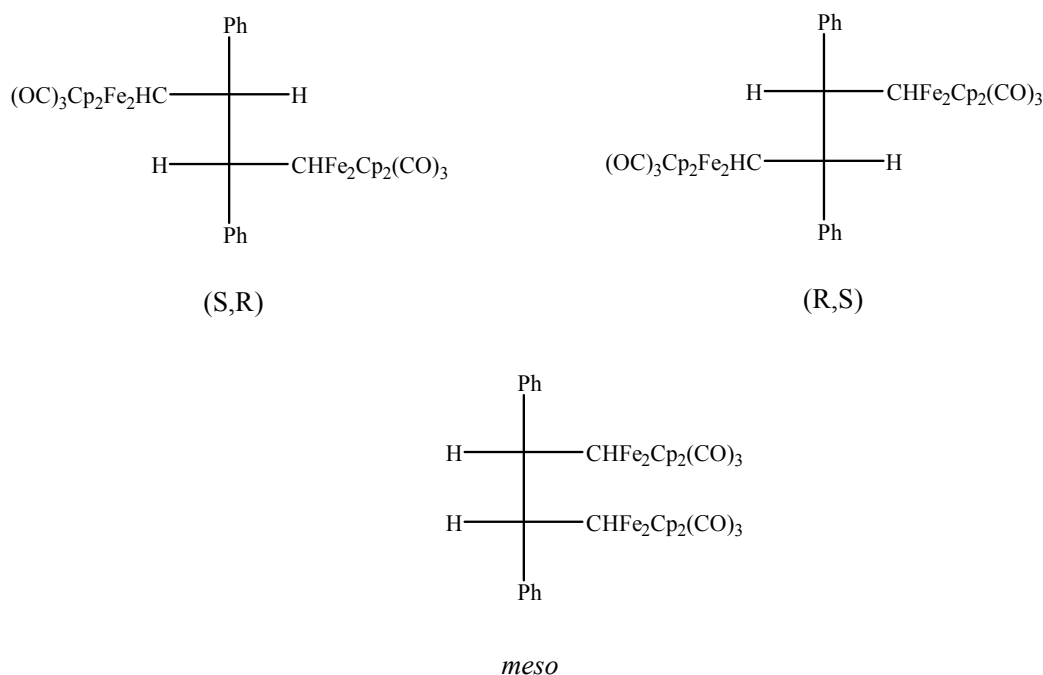


Figure 22: Molecular structure of **16** with key atoms labeled [the cyclopentadienyl rings and all H-atoms, except H(14), H(15), H(16), and H(17), have been omitted for clarity]. Thermal ellipsoids are at the 30% probability level.

The features related to the two diiron units which constitute complex **16** are very similar to each other and are in accordance with a good number of crystallographically-characterized diiron  $\mu$ -carbene complexes<sup>76</sup>. The connected iron atoms in **16** are within bond length (2.513÷2.515 Å) and are bridged symmetrically by a carbonyl and a carbene ligand. The C(14)–C(15), C(15)–C(16) and C(16)–C(17) bond distances (1.538, 1.582, 1.542 Å respectively) are as expected for single C–C bonds. The bridging carbene moiety is substantially symmetric, being Fe(1)–C(14) and Fe(2)–C(14) distances respectively 2.022 and 1.992 Å.

It has to be noted that, due to the presence of two chiral carbons [C(15) and C(16)], complex **16** may exist in principle in the form of three stereoisomeric forms, i.e. a couple of enantiomers and a *meso* species (see Scheme 60). The X-Ray molecular structure of **16** corresponds to the former situation. The  $^1\text{H}$  NMR spectrum of the mixture of reaction leading to **16** shows a single set of resonances, which is reasonably attributable to the enantiomers (*S,R*) and (*R,S*). In other words, the C–C coupling generating **16** seems to proceed in stereoselective way with no formation of the *meso* isomer.



Scheme 60: Fischer representation of the stereoisomers of complex **16**.

### 3.4.2 Reversibility of the reduction of **9** to **16**

The electrochemical properties of **9** and **16** have been preliminarily studied by cyclic voltammetry and the formal electrode potentials for the observed electron-transfers are

compiled in Table 1. In  $\text{CH}_2\text{Cl}_2/[\text{N}^n\text{Bu}_4][\text{PF}_6]$  solutions, compound **9** undergoes two reduction processes at  $-0.92$  and  $-1.73$  V, respectively, and one irreversible oxidation, presumably multielectronic, at  $+1.17$  V. Analysis of the cyclic voltammetric response of the reductions with scan rates varying between  $0.02$  and  $1.00$   $\text{V s}^{-1}$  confirms that the first reduction is an electrochemically reversible, diffusion-controlled process (the peak-to-peak separation,  $\Delta E_p$ , approaches the theoretical value of  $59$  mV and the  $(i_p)_{\text{red}}/\nu^{1/2}$  remains almost constant<sup>77</sup>) complicated by a subsequent chemical reaction ( $i_{pc}/i_{pa} = 0.7$  at  $0.10$   $\text{V s}^{-1}$ ). The chemical complications are testified by the appearance of oxidation processes in the back scan towards positive potentials, which have been attributed to the product deriving from the coupling of two radicals.

As suggested by the shape of the peaks and by the peak-to-peak separation, the reduction process occurring at the more negative potential ( $-1.73$  V) appears as a quasireversible process (Figure 23).

The cyclic voltammetric profile exhibited by **16** in  $\text{CH}_2\text{Cl}_2/[\text{N}^n\text{Bu}_4][\text{PF}_6]$  solution shows, in addition to the two irreversible reductions at rather negative potentials ( $-2.14$  and  $-2.38$  V), several not-well resolved, irreversible oxidation processes at potential higher than  $+0.20$  V (Figure 24). The peaks at  $+0.21$ ,  $+0.28$ , and  $+0.52$  V appear irreversible also when the scans are reversed at lower potentials. We have been observed the appearance of a reduction at  $-0.92$  V when cycling the potential several times between positive and negative values.

Compound	oxidation processes				reduction processes			
	$E^{\circ\circ}$	$E^{\circ\circ}$	$E^{\circ\circ}$	$E^{\circ\circ}$	$E^{\circ\circ}$	$\Delta E_p^{[a]}$	$E^{\circ\circ}$	$\Delta E_p^{[a]}$
<b>9</b>	+1.17 <sup>[c]</sup>				-0.92 <sup>[b]</sup>	70	-1.73 <sup>[c,a]</sup>	255
<b>16</b>	+1.19 <sup>[c]</sup>	+0.52 <sup>[c]</sup>	+0.28 <sup>[c]</sup>	+0.21 <sup>[c]</sup>	-2.14 <sup>[c]</sup>		-2.38 <sup>[c]</sup>	

Table 1: Formal electrode potentials ( $V$ , vs  $\text{FeCp}_2$ ) and peak-to-peak separations ( $mV$ ) for the redox changes exhibited by **9** and **16** in  $0.2\text{ M } [N^i\text{Bu}_4][\text{PF}_6]/\text{CH}_2\text{Cl}_2$  solution.

[a] Measured at  $0.1\text{ V s}^{-1}$ ; [b] coupled to relatively fast chemical reactions;

[c] peak potential value for irreversible or quasireversible processes.

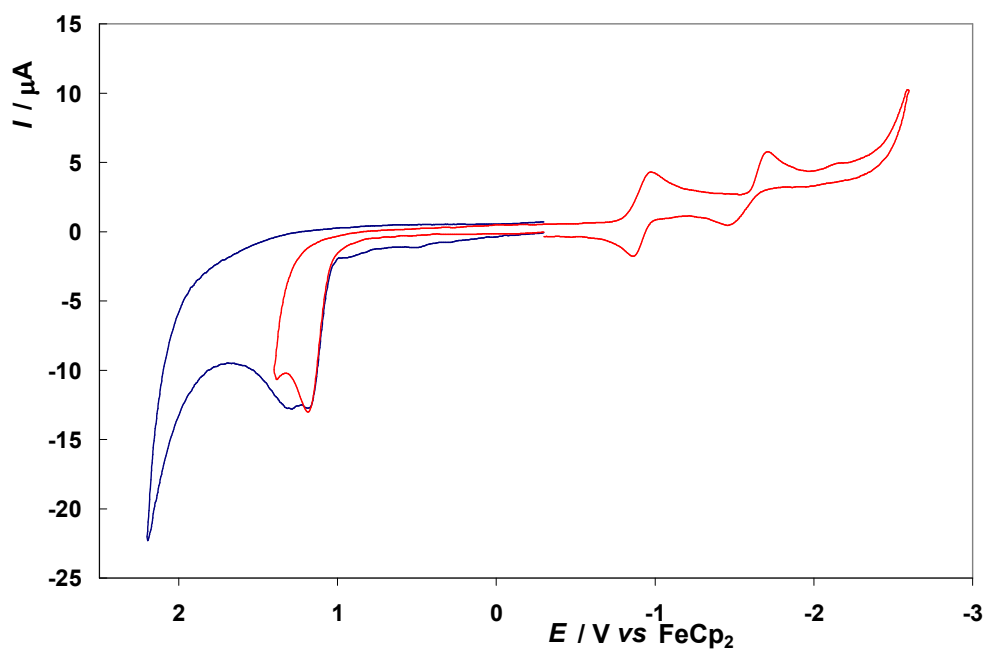


Figure 23: Cyclic voltammograms of **9** ( $10^{-3}\text{ M}$ ) recorded at a platinum electrode in  $\text{CH}_2\text{Cl}_2$  solution containing  $[N^i\text{Bu}_4][\text{PF}_6]$   $0.2\text{ M}$ . Scan rate =  $0.1\text{ V s}^{-1}$ .

The red line is obtained starting the scan towards positive potentials;  
the blue line is obtained after one scan at negative potentials.

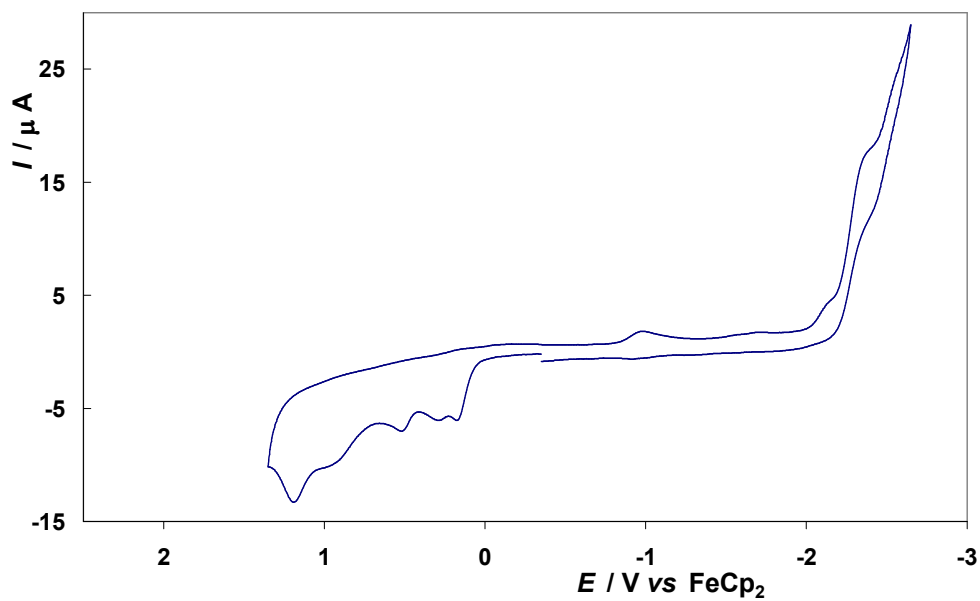


Figure 24: Cyclic voltammograms of **16** ( $10^{-3}$  M) recorded at a platinum electrode in  $\text{CH}_2\text{Cl}_2$  solution containing  $[\text{N}^n\text{Bu}_4][\text{PF}_6]$  0.2 M. Scan rate =  $0.1 \text{ V s}^{-1}$ .

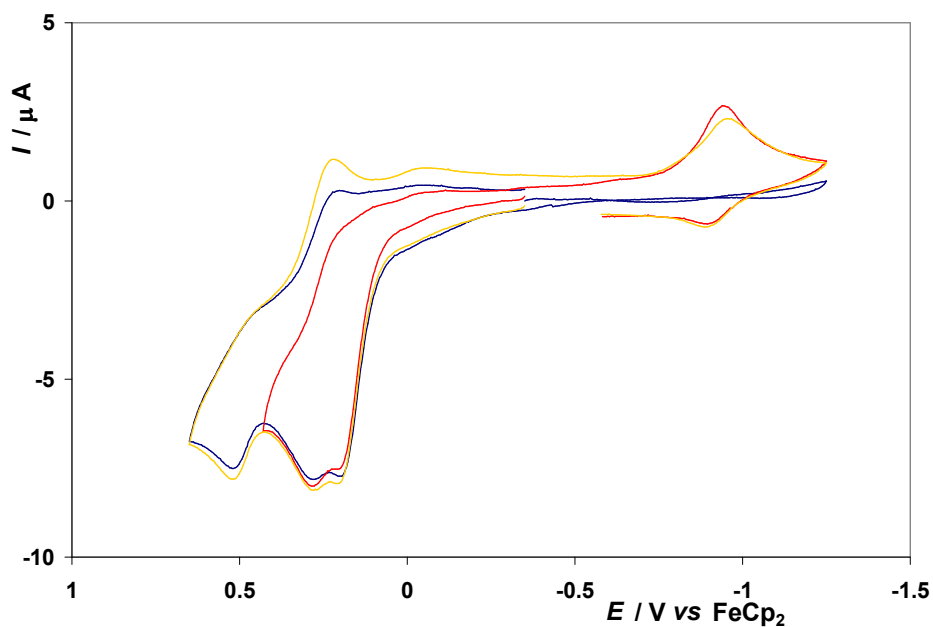
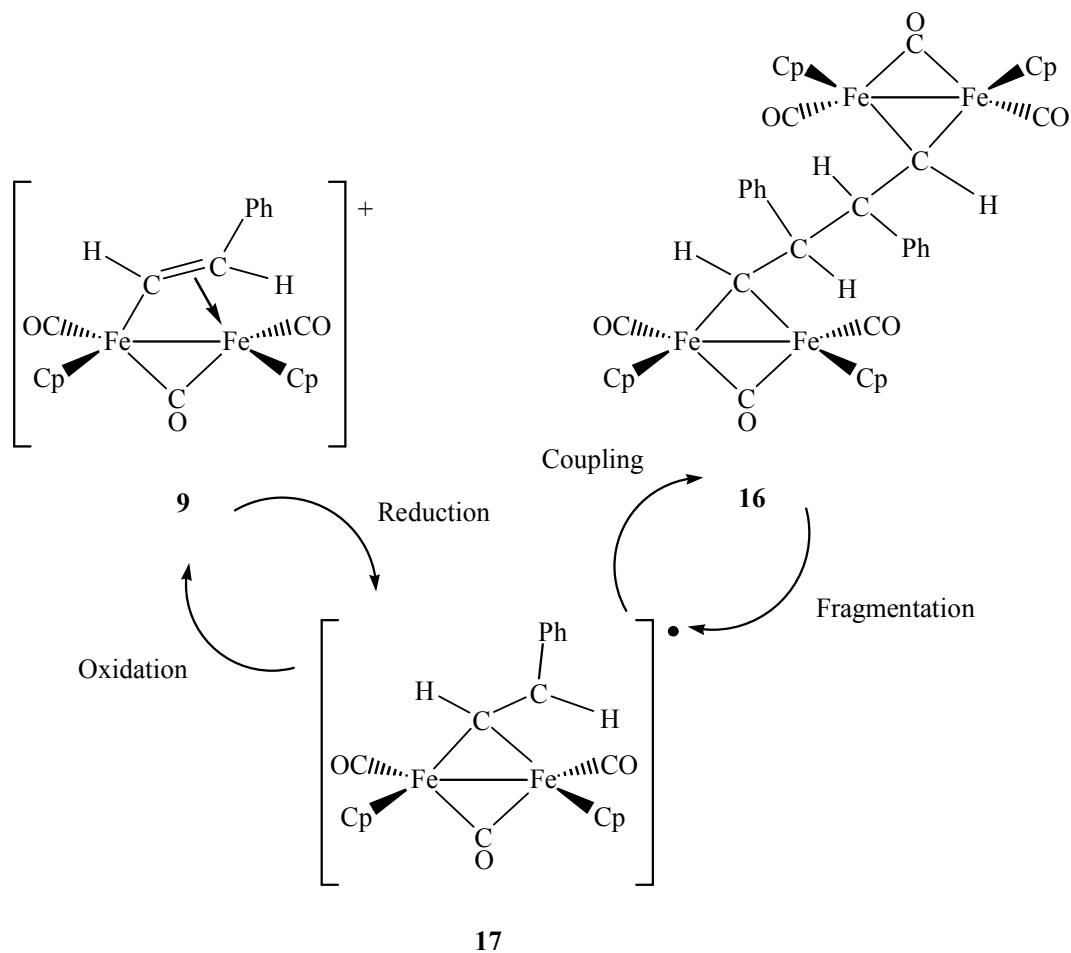


Figure 25: Cyclic voltammograms of **16** ( $10^{-3}$  M) recorded at a platinum electrode in  $\text{CH}_2\text{Cl}_2$  solution containing  $[\text{N}^t\text{Bu}_4][\text{PF}_6]$  0.2 M. Scan rate =  $0.1 \text{ V s}^{-1}$ . The red and the yellow lines are obtained starting the scan towards positive potentials; the blue line is obtained starting the scan towards negative potentials.

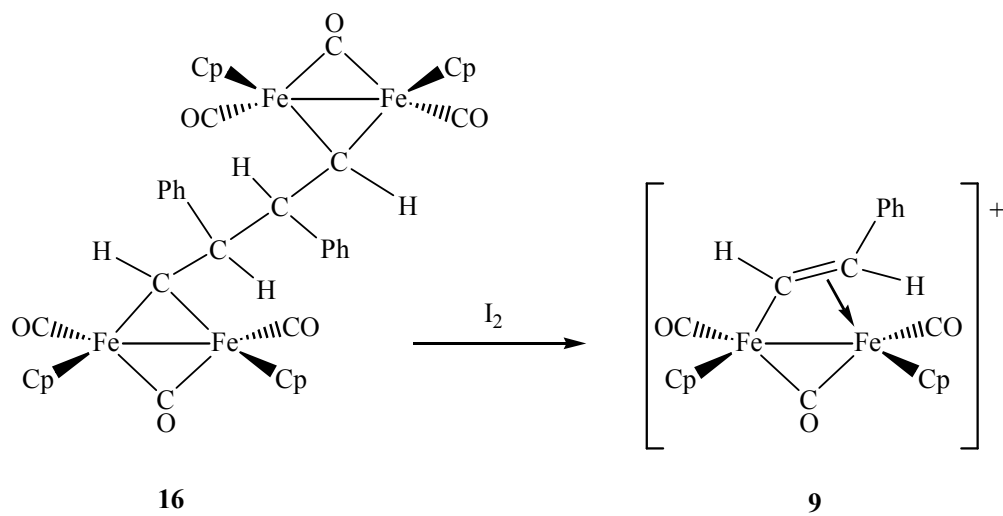
Due to the fact that the reduction at  $-0.92 \text{ V}$  suggests the formation of compound **9** (Figure 25), it can be deduced that the electrochemical oxidation of **16** generates an instable radical cation, **17**, that quickly undergoes a fragmentation process to the cationic complex **9** (Scheme 61: Mechanism for the reversible transformation of **9** into **16**). The electrochemical reversibility of the reduction process at  $-0.92 \text{ V}$  of compound **9** foreshadows a quite similar geometry for compounds **9** and **17**<sup>77</sup>.





*Scheme 61: Mechanism for the reversible transformation of **9** into **16** through the radical intermediate species **17**.*

According to the electrochemical results, the reductive dimerization leading to **16** holds some reversible character; indeed the treatment of a tetrahydrofuran solution of **16** with elemental iodine resulted in clean recovery of the vinyl complex **[9]<sup>+</sup>** (see Experimental). The reaction is rather slow, and the conversion completes in 48 hours at room temperature.



*Scheme 62: Oxidation of 16.*

The propensity of **9** to dimerize upon reduction to **16** with the formation of an additional C–C bond and its re-oxidation to **9** by cleavage of this C–C bond, constitutes a very promising redox cycle. This system approaches the concept of a “molecular battery” proposed by Floriani<sup>78</sup>, *i.e.* a molecular device capable of storing and releasing electrons through the formation and cleavage of chemical bonds. This reservoir of electrons controlled by the reversible formation of C–C bonds may represent an interesting device for electrical energy storage<sup>79</sup>.

The reversible character of the reduction of **9** to **16** suggested the possibility that the allenyl complexes **7** could display a similar behaviour. A preliminary electrochemical investigation has shown that the allenyl complex **7a** in  $\text{CH}_2\text{Cl}_2/[\text{N}^n\text{Bu}_4][\text{PF}_6]$  solution undergoes two consecutive reduction processes at  $-1.03$  and  $-2.04$  V, respectively, and one irreversible oxidation at  $+1.09$  V. Analysis of the cyclic voltammetric response of the reductions, with scan rates varying between  $0.02$  and  $1.00 \text{ V s}^{-1}$ , confirms that the

first reduction is an electrochemically reversible, diffusion controlled process (the peak-to-peak separation,  $\Delta E_p$ , approaches the theoretical value of 59 mV and the  $(i_p)_{red}/v^{1/2}$  remains almost constant<sup>77</sup>). However, differently from what found for complex **9**, complications arise by a subsequent chemical reaction ( $i_{pc}/i_{pa} = 0.73$  at  $0.10 \text{ V s}^{-1}$ ). The coupled chemical complications are testified by the appearance of oxidation processes in the back scan towards positive potentials, and by deposition, after several cycles, of insoluble by-products onto the electrode surface.

As suggested by the shape of the peaks and by the peak-to-peak separation, the reduction process occurring at the more negative potential ( $-2.04 \text{ V}$ ) appears as a quasireversible process (Figure 26).

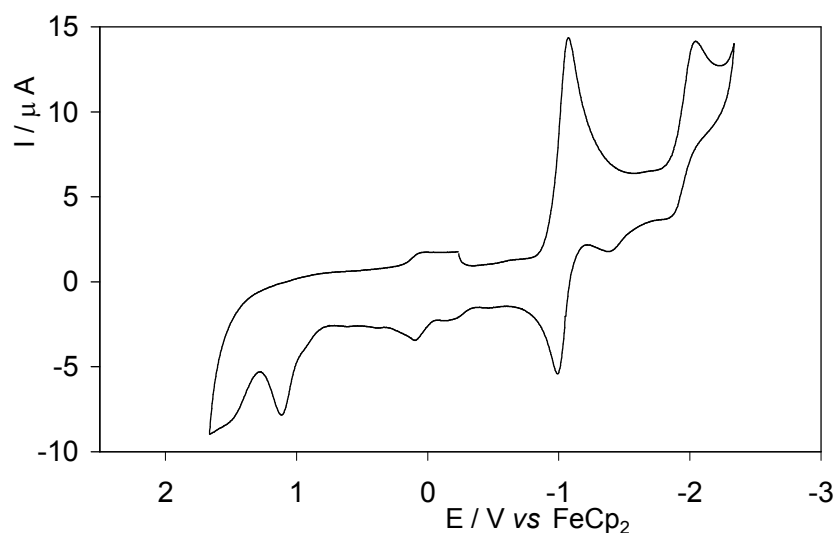
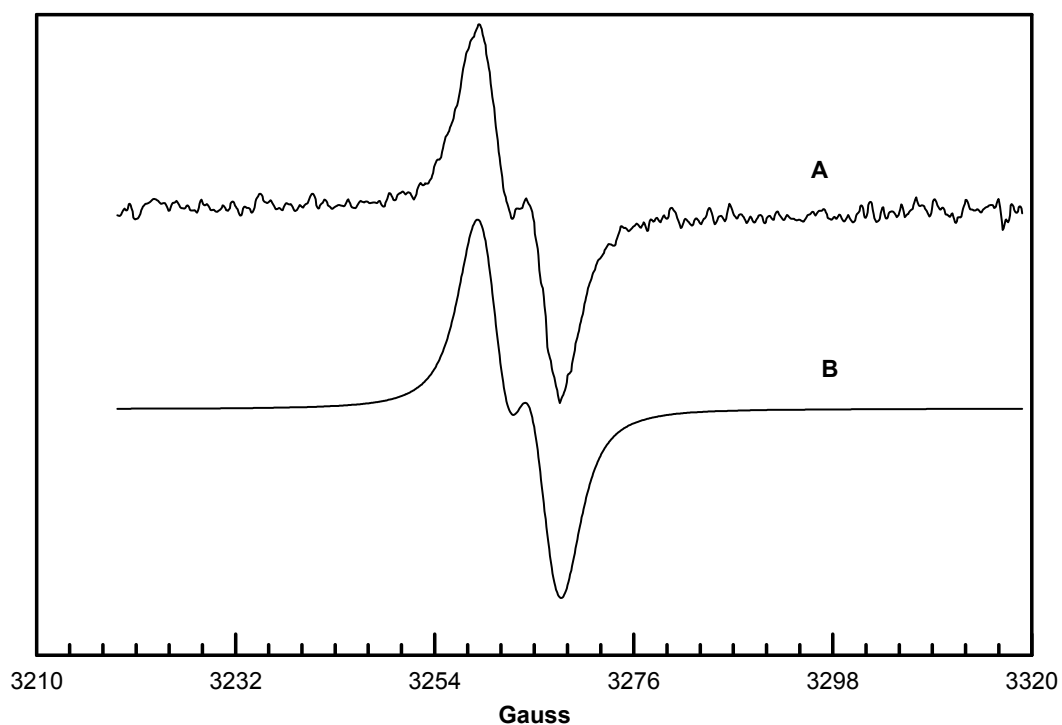


Figure 26: Cyclic voltammograms of **7a** ( $2.0 \cdot 10^{-3} \text{ M}$ ) recorded at a platinum electrode in  $\text{CH}_2\text{Cl}_2$  solution containing  $[\text{N}^n\text{Bu}_4][\text{PF}_6]$   $0.2 \text{ M}$ . Scan rate =  $0.1 \text{ V s}^{-1}$ .

In accord with what hypothesized previously for the dimerization of the vinyl species  $[\text{Fe}_2\text{Cp}_2(\text{CO})_2(\mu\text{-CO})\{\mu\text{-}\eta^1\text{:}\eta^2\text{-CH=CH(CO}_2\text{Me)}\}]^+$ , the synthesis of **16** may proceed with formation of an intermediate radical species. Therefore, combined electrochemical/EPR analysis aimed to intercept a possible intermediate radical species was carried out.

The experiment was performed on a  $2.5 \cdot 10^{-3}$  M solution of **9** in  $\text{CH}_2\text{Cl}_2/[\text{N}^n\text{Bu}_4][\text{PF}_6]$ , which was introduced into the EPR spectroelectrochemical cell under argon atmosphere; the solution was electrolyzed at constant potential ( $E_w = -1.0$  V, vs  $\text{FeCp}_2$ ). Indeed the analysis suggested the room-temperature formation of the radical compound  $[\text{Fe}_2\text{Cp}_2(\text{CO})_2(\mu\text{-CO})\{\mu\text{-CHCH(Ph)}\}]$ , **17**. The EPR spectrum of **17** is shown in (Figure 27, A). The EPR spectrum shows evidence for hyperfine interaction, with  $g_{\text{iso}} = 2.0067$ , due to the coupling of the unpaired electron with H(20). Moreover the remarkable line width (3.5 G) suggests a fast relaxation process, while the lorentzian shape (91%) indicates that the unpaired electron interacts with few nuclei.



*Figure 27: (A) Experimental and (B) Calculated EPR Spectrum of 16.*

The experimental EPR spectrum matches very well with the computer one, related to the DFT-calculated structure of **17** (gas-phase). The calculated structure and the calculated spin-density distribution of **17** are shown in FiguresFigure 28, Figure 29 andFigure 30.

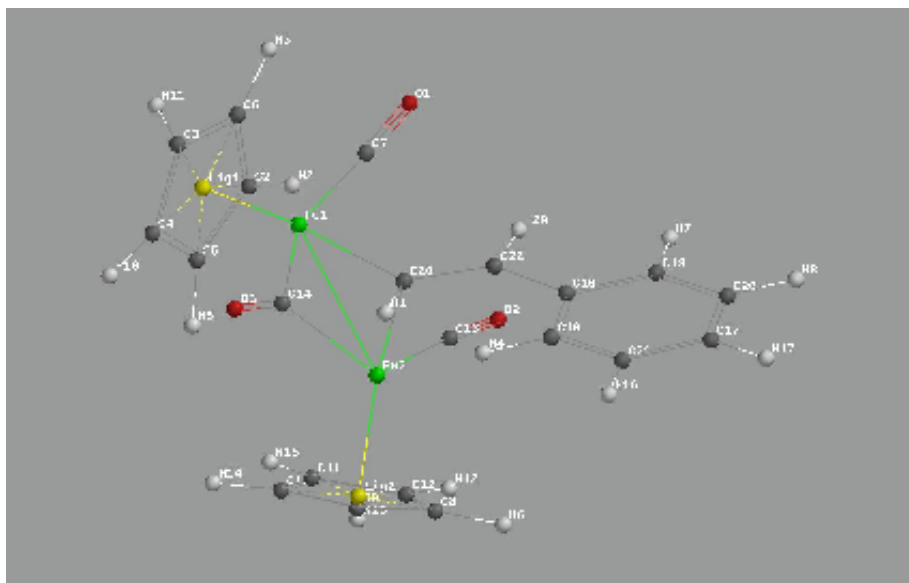


Figure 28: DFT calculated geometry of the radical species  $[\text{Fe}_2\text{Cp}_2(\text{CO})_3(\text{C}_2\text{H}_2\text{Ph})]$ .

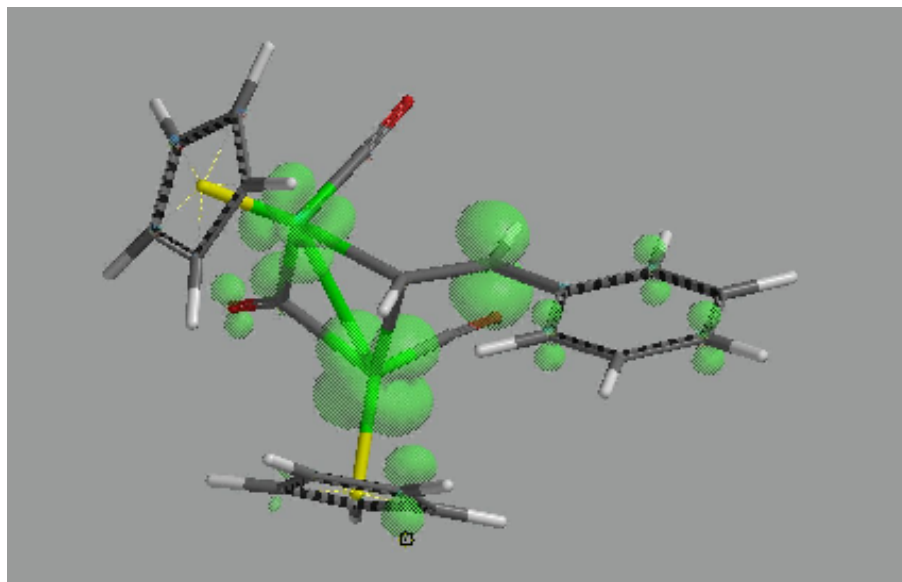


Figure 29: DFT calculated Spin density surface of  $[\text{Fe}_2\text{Cp}_2(\text{CO})_3(\text{C}_2\text{H}_2\text{Ph})]$ .  
Positive spin density (0.004 electron/ $\text{au}^3$ ).

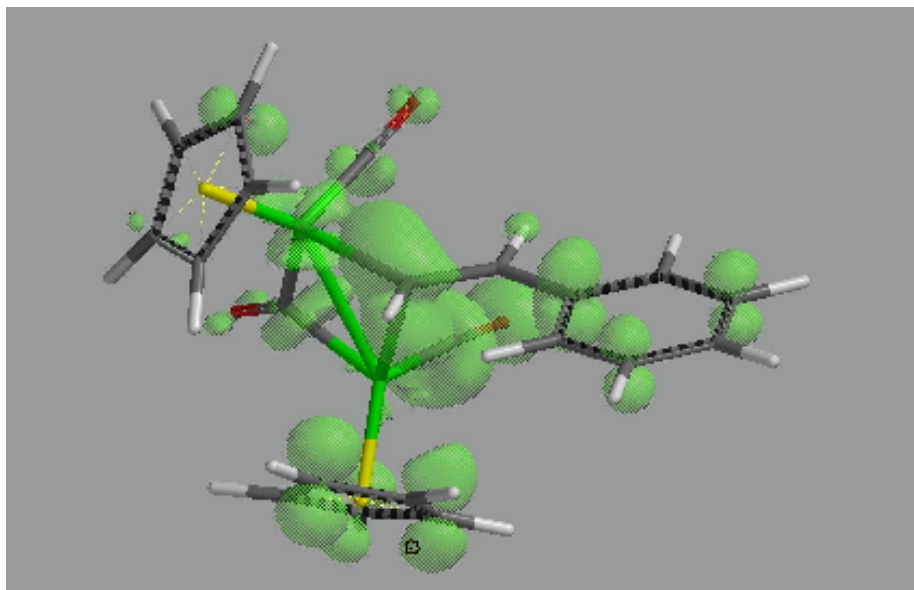
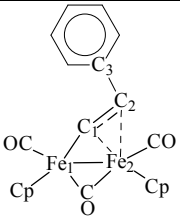


Figure 30: DFT calculated Spin density surface of  $[\text{Fe}_2\text{Cp}_2(\text{CO})_3(\text{C}_2\text{H}_2\text{Ph})]$ .  
Negative spin density (0.001 electron/ $\text{au}^3$ ).

The calculated spin-density distribution of **17** indicates that the radical is mainly localized at the iron center Fe(2) (0.7646 electron/ $\text{au}^3$ ), however significant density is found both at Fe(1) (0.1678 electron/ $\text{au}^3$ ) and at the bridging, C(22),  $sp^3$  carbon atom (0.1848 electron/ $\text{au}^3$ ). The latter is actually a substituted benzyl carbon,  $[\text{RCHPh}]$ ; probably the delocalization of the unpaired electron to the benzyl moiety is responsible for the additional stability of **17** with respect to the possible analogues  $[\text{Fe}_2\text{Cp}_2(\text{CO})_2(\mu\text{-CO})\{\mu\text{-CHCH}(\text{CO}_2\text{Me})\}]$ , which could not be observed in the course of the non-reversible dimerization of the vinyl complex  $[\text{Fe}_2\text{Cp}_2(\text{CO})_2(\mu\text{-CO})\{\mu\text{-}\eta^1\text{:}\eta^2\text{-CH=CH}(\text{CO}_2\text{Me})\}]^+$ . Thus the contribution of the phenyl group to the stability of **17** may be considered crucial for the detection of the radical intermediate at room temperature, and in order to give reversible character to the  $\mathbf{9} \rightleftharpoons \mathbf{16}$  transformation.

With the aim to understand better the structural modifications of the bridging hydrocarbyl ligand in the course of the reductive reaction **9**  $\rightarrow$  **17**  $\rightarrow$  **16**, we moved to optimize the gas-phase molecular structures of **9** and **16**. Thus salient bond distances and angles are reported in Table 2, together with the experimental values available for **16**.

	<b>9</b> <sup>a</sup>	<b>17</b> <sup>a</sup>	<b>16</b> <sup>b</sup>	<b>16</b> <sup>a</sup>
Fe1–Fe2	2.632	2.643	2.632	2.513(12) 2.515(12)
C1–C2	1.392	1.375	1.547	1.539(7) 1.541(6)
C1–Fe1	1.933	1.984	1.988	2.021(5) 1.999(5)
C1–Fe2	2.052	2.141	1.984	1.992(5) 2.008(5)
C2–Fe2	2.349	2.785	3.156	3.135 3.092
C2–C3	1.474	1.466	1.532	1.520(8) 1.514(7)
C1–C2–C3	127.75	127.80	113.21	110.2(4) 112.1(4)
Fe1–C1–C2	129.24	130.94	125.45	120.6(3) 124.9(3)

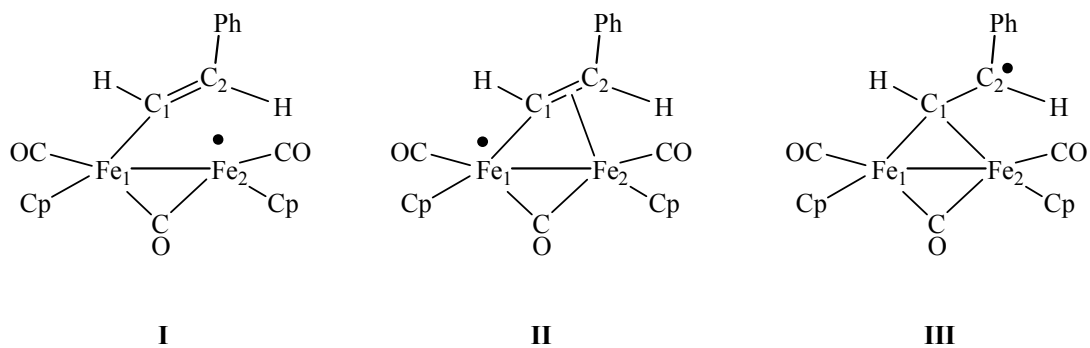
<sup>a</sup> Gas-phase (DFT). <sup>b</sup> Solid state (X-Ray).

Table 2: bond distances ( $\text{\AA}$ ) and angles (deg) related to the molecular structures of **9-16**.



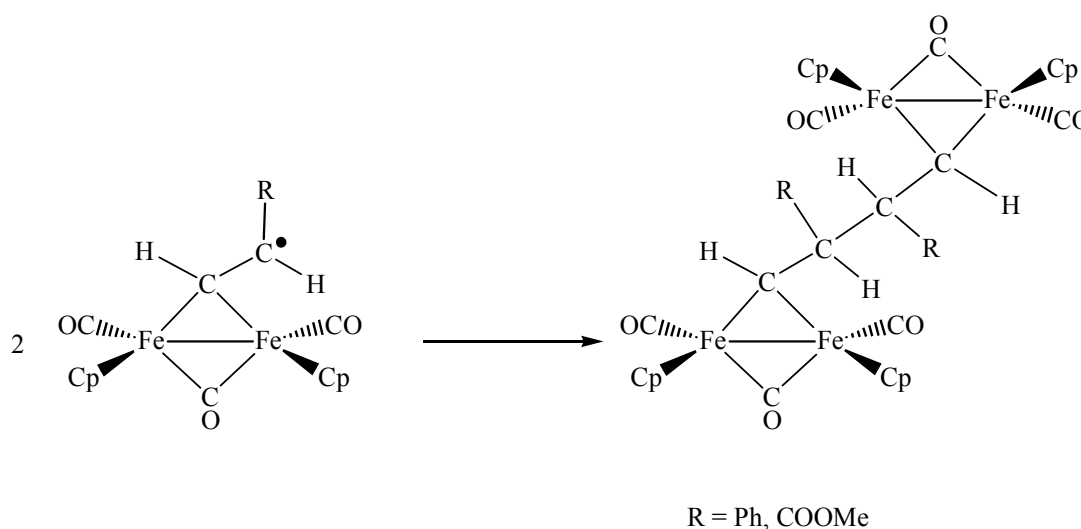
The data reported in Table 2 evidence substantial agreement between the values obtained for **16** by calculations (gas-phase) and by X-Ray analysis (solid-state), respectively.

Elongation of the C1–C2 and C2–C3 distances is observed on going through **9** to **16**, as consequence of the change in the hybridization of the C2 carbon ( $sp^2$  in **9**,  $sp^3$  in **16**). Furthermore the C2 and Fe2 atoms, being at bond-distance in **1** (2.349 Å), become non interacting in **9** (3.156 Å). Intermediate situation is observed in the radical species **17** (2.785 Å); otherwise, the C1–C2 and C2–C3 distances in **17** approximate the corresponding ones in the vinyl complex **9**. These features suggest that the bridging hydrocarbyl ligand in **17** may be conveniently described in terms of three resonance formulas (see Scheme 63), with prevalence of the form **I**, coherently with the observation that the unpaired electron is mainly located at the iron center Fe2 (see above).



*Scheme 63: Resonance formulas of **17**.*

With the aim to find some explanation for the different stability of the radical intermediates  $[17]^{\bullet}$  and  $[\text{Fe}_2\text{Cp}_2(\text{CO})_2(\mu\text{-CO})\{\mu\text{-}\eta^1:\eta^2\text{-CH=CH(CO}_2\text{Et)}\}]^{\bullet}$ , the latter supposed to form during the reductive dimerization of  $[\text{Fe}_2\text{Cp}_2(\text{CO})_2(\mu\text{-CO})\{\mu\text{-}\eta^1:\eta^2\text{-CH=CH(CO}_2\text{Me)}\}]^+$ <sup>75</sup>, we calculated the enthalpy variations of the dimerization reactions for the gas phase (see Scheme 64).



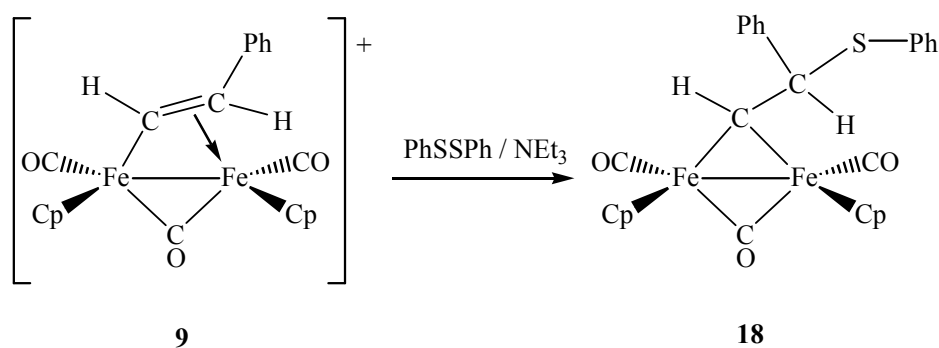
*Scheme 64: Coupling of vinyl complexes.*

According to the computer results,  $\Delta H^\circ = -62.82$  kJ/mol for  $\text{R} = \text{CO}_2\text{Et}$  and  $\Delta H^\circ = -12.25$  KJ/mol for  $\text{R} = \text{Ph}$ . These data are in accord with the fact that the radical intermediate  $[17]^{\bullet}$  may be observed in the course of the reductive dimerization of the parent vinyl complex, whereas the analogous carboxylato-containing radical could not be detected<sup>75</sup>.

### 3.4.3 Reduction of **9** in the presence of diphenyl disulfide

On considering that the reduction process leading to **16** occurs with intermediate formation of the reactive species **17**, in principle the same reaction may be exploited in order to functionalize the bridging hydrocarbyl ligand. Indeed trapping of highly-reactive organic fragments coordinated to the diiron frame  $[\text{Fe}_2\text{Cp}_2(\text{CO})_2]^{80}$  has previously allowed the synthesis of unusual and interesting species. More in detail, the vinyliminium complexes  $[\text{Fe}_2\{\mu\text{-}\eta^1\text{:}\eta^3\text{-C(R)=CHC=N(Me)(R')}\}(\mu\text{-CO})(\text{CO})(\text{Cp})_2]^+$  ( $\text{R} = \text{Me}, \text{CO}_2\text{Me}, \text{Tol}, \text{SiMe}_3$ ;  $\text{R}' = \text{Me}, 2,6\text{-Me}_2\text{C}_6\text{H}_4$ ) were reported to react with sodium hydride in the presence of chalcogens,  $\text{PhSSPh}$ , isocyanides or diazocompounds affording selectively the corresponding functionalized derivatives<sup>5</sup>.

Thus, the reductive reaction of **9**, carried out in the presence of excess  $\text{PhSSPh}$ , led to selective formation of the thioether-alkylidene compound  $[\text{Fe}_2\text{Cp}_2(\text{CO})_2(\mu\text{-CO})\{\mu\text{-}\eta^2\text{-CHCH(Ph)(SPh)}\}]$ , **18** (see Scheme 65). Best yield (*ca.* 80%) was achieved by using  $\text{NEt}_3$  as a reductant agent.



Scheme 65: Reduction of **9** in the presence of  $\text{PhSSPh}$ .

The new complex **9** has been fully characterized by IR and NMR spectroscopy, elemental analysis and X-Ray diffraction.

The IR spectrum of **18** (in CH<sub>2</sub>Cl<sub>2</sub>) shows two bands due to two terminal carbonyl ligand and a bridging one at 1972, 1934, and 1774 cm<sup>-1</sup>, respectively.

The NMR spectra (in CDCl<sub>3</sub>) contain single sets of resonances and resemble those of the analogous complex **16**. In particular, the carbene moiety gives rise to resonances at 11.28 ppm (<sup>1</sup>H) and 180.3 ppm (<sup>13</sup>C), respectively; moreover, the quaternary carbons bearing the -Ph and -SPh substituents resonate at 66.9 ppm. Coupling along the C<sub>α</sub>-C<sub>β</sub> chain is evident in the <sup>1</sup>H NMR spectrum, where C<sub>α</sub>H and C<sub>β</sub>H protons resonate as doublets (<sup>4</sup>J<sub>HH</sub> = 12.5 Hz).

The ORTEP representation of complexes **18** is shown in Figure 31.

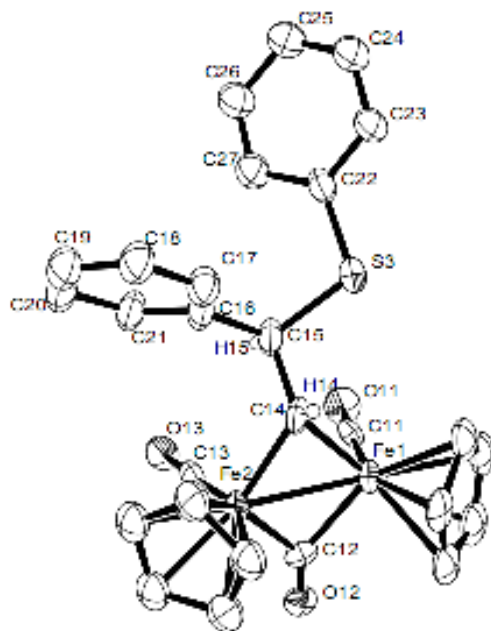


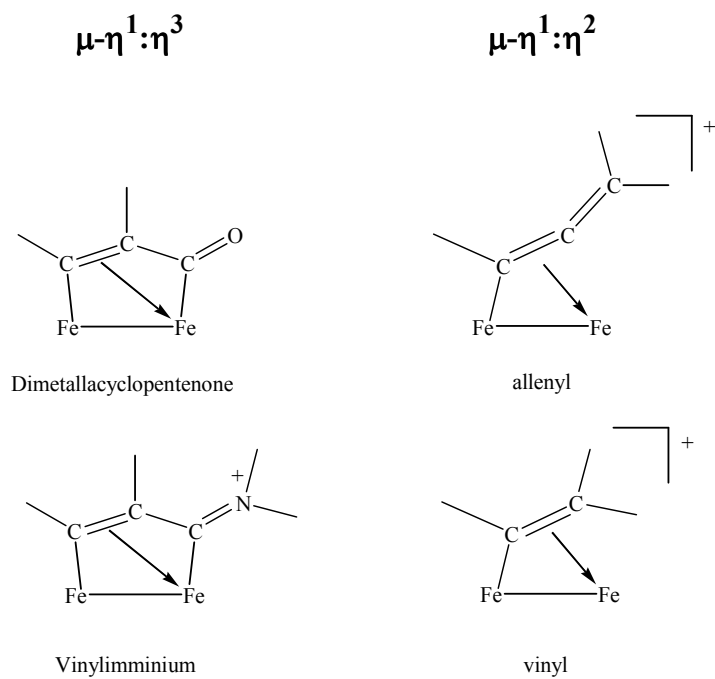
Figure 31: Molecular structure of **18** with key atoms labeled [the cyclopentadienyl rings and all *H*-atoms, except *H*(14) and *H*(15), have been omitted for clarity]. Thermal ellipsoids are at the 30% probability level.

The structure of complex **18** presents similar features to the one reported above for complex **16**, and it is in accordance with a wide range of structurally established  $\mu$ -carbene complexes<sup>81</sup>. The iron atoms are at a single bond distance (2.498 Å) and are bridged symmetrically by a carbonyl and a carbene ligand. The C(14)–C(15) bond distance (1.542 Å) is as expected for single C–C bonds. Both the C(15)–S(3) and C(22)–S(3) bond distances (1.810(17) and 1.72(2), respectively) are within the range of single C–S bonds in thioethers<sup>82</sup>.

#### 4. Conclusions

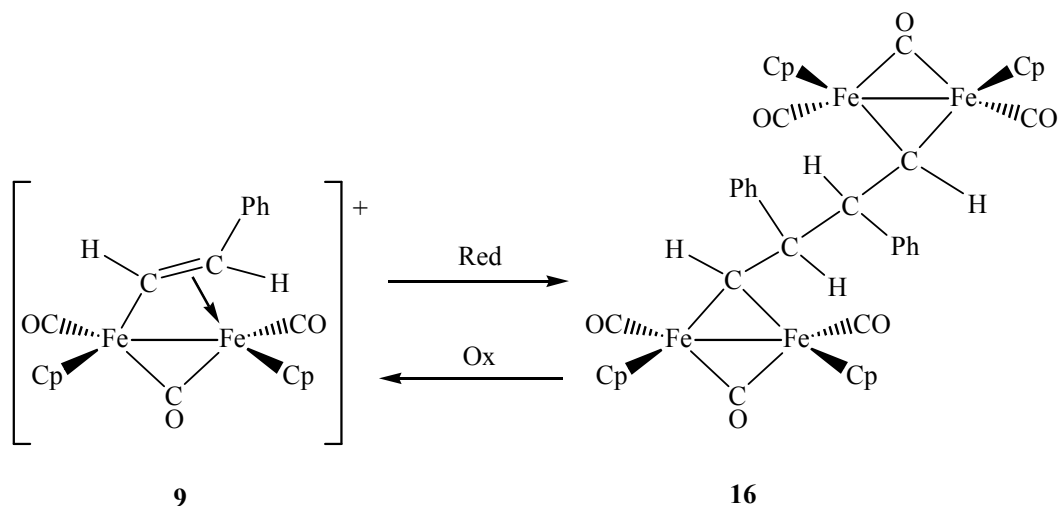
Novel cationic  $\mu$ -allenyl diiron complexes have been prepared by a two-step procedure from the commercially available  $[\text{Fe}_2\text{Cp}_2(\text{CO})_4]$ . In analogy to previously reported vinyl species, the reactivity of the new allenyl complexes is limited by the fact that the iron-iron bond is easily cleaved in the attempt to generate a coordination vacancy at one metal center, upon substitution of one CO with a labile ligand (NCMe). It has to be noted that this strategy is necessary in order to favour the coupling of the bridging unsaturated ligand with a variety of compounds.

The possibility to use this approach to develop the chemistry of dinuclear systems bearing the  $[\text{Fe}_2\text{Cp}_2(\text{CO})_2]$  frame and a bridging hydrocarbyl ligand seems to be related to the coordination mode adopted by the latter. Thus the previously reported dimetallacyclopentenone and vinyliminium complexes, which tolerate CO removal without affecting the dinuclear frame, exhibit  $\mu\text{-}\eta^1\text{:}\eta^3$  coordination of the ligand; conversely, both allenyl and vinyl adopt  $\mu\text{-}\eta^1\text{:}\eta^2$  coordination (see Scheme 66).



*Scheme 66: bridging ligands coordinated in diiron complexes.*

Despite the considerations above, cationic diiron complex with a Ph-substituted bridging vinyl ligand is susceptible of reductive dimerization to  $[\text{Fe}]_4$  derivative occurring *via* C-C bond coupling. The process may be reversed by C-C cleavage oxidation, providing a possible model of device for electric energy storage (Scheme 67).



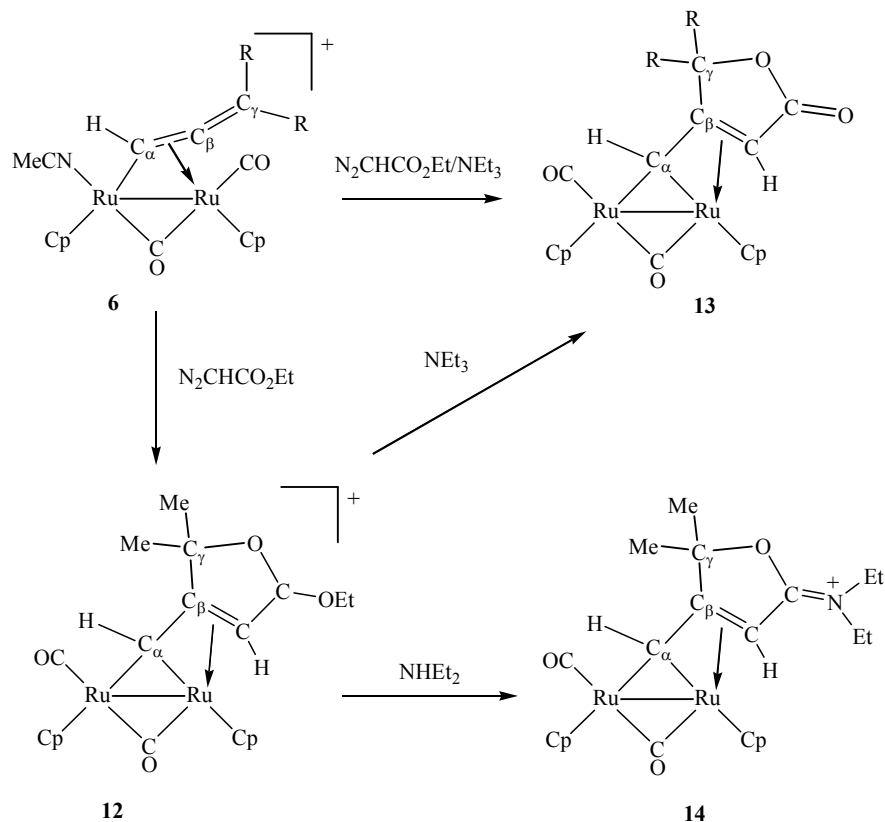
*Scheme 67: Redox cycle of the  $\mu$ -vinyl diiron complex.*

Spectroscopic, electrochemical and DFT studies agree in that the reductive dimerization reaction proceeds with formation of a radical intermediate; the contribution of the phenyl group to the stability of this radical species is crucial in order to observe reversibility. Moreover, we have found that it is possible to exploit the reductive reaction in order to obtain functionalized organic fragments, by trapping the reactive intermediate with a radical scavenger as is diphenyl disulfide. Work is in progress in order to use this approach for extending the chemistry of diiron  $\mu$ -vinyl complexes.

Analogous electrochemical studies on the diiron allenyl complexes have not provided results worthy of notice. The drawback to the construction of “molecular architectures” by stepwise functionalization of the bridging allenyl ligand, represented by the fragmentation observed easily in the attempt to generate a coordination vacancy, has been overcome by moving to analogous diruthenium systems (see Scheme 68).



Thus, unprecedented carbene ligands bearing heterocyclic substituents, that represent the skeleton of several natural products and/or pharmaceuticals, have been obtained by straightforward reaction of the acetonitrile derivatives of the cationic diruthenium  $\mu$ -allenyl complexes with ethyldiazoacetate/amine.



*Scheme 68: Reactivity of the diruthenium allenyl complexes*

The reaction proceeds with regiospecific [3+2] cyclization, assisted by the  $[\text{Ru}_2\text{Cp}_2(\text{CO})_2]$  framework, involving the diazocompound and the allenyl unit. The remarkable results obtained show that diruthenium  $\mu$ -allenyl complexes are valuable materials for obtaining unusual organic fragments stabilized by the bridging coordination to the two metal centers.

## 5. Experimental

### 5.1 General

All reactions were carried out under nitrogen atmosphere, using standard Schlenk techniques. Solvents were distilled immediately before use under nitrogen from appropriate drying agents. Photolysis reactions were carried out in silica glass tubes by using a 150 W mercury lamp. Chromatography separations were carried out on columns of alumina (Fluka, Brockmann Activity I) for neutral compounds and deactivated alumina (6% w/w water) for ionic compounds, respectively. Glassware was oven-dried before use. Infrared spectra were recorded at 298 K on a FT-IR Perkin–Elmer Spectrometer equipped with a UATR sampling accessory (solid samples). NMR measurements were performed on a Varian Mercury Plus 400 instrument. The chemical shifts for  $^1\text{H}$  and  $^{13}\text{C}$  were referenced to the non-deuterated aliquot of the solvent. The spectra were fully assigned *via* DEPT experiments and  $^1\text{H}$ ,  $^{13}\text{C}$  correlation measured through gs-HSQC and gs-HMBC experiments.<sup>83</sup> Unless otherwise stated, NMR spectra were recorded at 298 K.

Cyclic voltammograms were performed with a Princeton Applied Research (PAR) 273A Potentiostat/Galvanostat, interfaced to a personal computer, employing PAR M270 Electrochemical Software. All measurements were carried out in a three-electrode home built cell at room temperature ( $293 \pm 5\text{K}$ ). The working and the counterelectrode consisted of a platinum disk electrode and a platinum wire spiral, respectively, both sealed in a glass tube. A quasi-reference electrode of platinum was employed as reference. The Schlenk-type construction of the cell maintained anhydrous

and anaerobic conditions. The cell was predried by heating under vacuum and filled with argon. A 0.2 M  $\text{CH}_2\text{Cl}_2$  solution of tetrabutylammonium hexafluorophosphate prepared under an atmosphere of argon was then introduced into the cell and the working electrode was cycled several times between the anodic and the cathodic limits of interest until there was no change in the charging current. The substrate was then introduced to obtain a 1 mM solution, and voltammograms were recorded at a sweep rate of 100 mV/sec. After several voltammograms were obtained on the substrate solution, a small amounts of ferrocene was added, and the voltammogram was repeated. The  $E^\circ$  values of the compounds were then determined placing the  $E_{1/2}$  of the ferrocene couple at 0.0 V.

EPR analyses were recorded at 298 K by Varian (Palo Alto, CA, USA) E112 spectrometer operating at X band, equipped with Varian E257 temperature control unit and interfaced to IPC 610/P566C industrial grade Advantech computer, using acquisition board<sup>84</sup> and software package especially designed for EPR experiments.<sup>85</sup> Experimental EPR spectra were simulated by the WINSIM 32 program.<sup>86</sup> DFT geometry optimization, UV-VIS and calculation of the electron spin density distribution of compounds **9-16-17** were performed by the parallel Linux version of the Spartan '08 software.<sup>87</sup> We adopted the B3LYP (Becke, three-parameter, Lee-Yang-Parr)<sup>88,89</sup> exchange-correlation functional formulated with the Becke 88 exchange functional,<sup>90</sup> the correlation functional of Lee, Yang and Parr,<sup>91</sup> and the 6-31G\*\* base functions set, which is appropriate for calculations of split-valence plus-polarization quality.

Cathodic reduction of **9** was carried out directly in the spectrometer cavity on a platinum foil placed in the flat region of a quartz solution rectangular cell (Wilma

Glass WG-808-Q). A platinum quasi-reference electrode and a platinum wire counter electrode, placed in the upper part of the cell, near to the working electrode, was used. The connecting wires from the three electrodes were sheathed in PTFE tape so that contact was avoided in the narrow 3mm-i.d. tube and electrolysis only occurred in the flat portion of the cell. The quartz cell was customised in house by supplying its upper part with a Schlenk-type constructed head with ground-glass joints as inlet for the three platinum electrodes. A  $2.5 \times 10^{-3}$  M **9** solution in  $\text{CH}_2\text{Cl}_2/[\text{N}^n\text{Bu}_4][\text{PF}_6]$  was used for EPR studies. The solution was transferred by syringe into the cell previously deoxygenated thoroughly by evacuation and filling with argon gas. EPR spectra were taken at room temperature during an electrolysis experiment at constant potential ( $E_w = -1.0$  V, vs  $\text{FeCp}_2$ ) using a BAS CV-27 electrochemical analyzer as polarizing unit.

Electrochemical measurements were performed in 0.2 M dichloromethane solutions of  $[\text{N}^n\text{Bu}_4][\text{PF}_6]$  as supporting electrolyte. HPLC grade dichloromethane (Sigma-Aldrich) was stored under argon over 3Å molecular sieves.  $[\text{N}^n\text{Bu}_4][\text{PF}_6]$  (Fluka, puriss. electrochemical grade), was used as purchased. Ferrocene ( $\text{Fe}(\text{C}_5\text{H}_5)_2$ ,  $\text{FeCp}_2$ ) was prepared according to literature<sup>92</sup> and purified by sublimation.

All organic reactants, including  $\text{HC}\equiv\text{CCR}_2\text{OH}$  ( $\text{R} = \text{Me}, \text{Ph}$ ),  $\text{HBF}_4$  (54% w/w in  $\text{Et}_2\text{O}$ ),  $\text{NHEt}_2$ ,  $\text{NEt}_3$ ,  $\text{LiCl}$  and  $\text{N}_2\text{CHCO}_2\text{Et}$ , were commercial products (Aldrich) of the highest purity available and used as received.  $[\text{Fe}_2\text{Cp}_2(\text{CO})_4]$  was purchased from Strem and used as received;  $[\text{Ru}_2\text{Cp}_2(\text{CO})_4]$  was prepared by published procedure from  $\text{Ru}_3(\text{CO})_{12}$ ,<sup>93</sup> which was generously gifted by Prof. Giuseppe Fachinetti, University of Pisa.

## 5.2 Synthesis of $[\text{Ru}_2\text{Cp}_2(\text{CO})(\mu\text{-CO})\{\mu\text{-}\eta^1\text{:}\eta^3\text{-C(H)=C(CPh}_2\text{OH)C(=O)}\}]]$ (**1b**)

A thf (25 mL) solution of  $[\text{Ru}_2\text{Cp}_2(\text{CO})(\mu\text{-CO})\{\mu\text{-}\eta^1\text{:}\eta^3\text{-C(Ph)=C(Ph)C(=O)}\}]]$  (1.25 g, 2.10 mmol), was treated with  $\text{HC}\equiv\text{CCPh}_2\text{OH}$  (2.20 g, 10.6 mmol). The mixture was stirred at the boiling temperature for 4 hours, then it was allowed to cool to room temperature and filtered through an alumina column. The product  $[\text{Ru}_2\text{Cp}_2(\text{CO})(\mu\text{-CO})\{\mu\text{-}\eta^1\text{:}\eta^3\text{-C(H)=C(CPh}_2\text{OH)C(=O)}\}]]$  (**1b**) was obtained as an orange microcrystalline solid upon removal of the solvent under vacuo. Yield: 1.15 g, 88%. Anal. Calcd. for  $\text{C}_{28}\text{H}_{22}\text{O}_4\text{Ru}_2$ : C, 53.84; H, 3.55. Found: C, 53.68; H, 3.39. IR ( $\text{CH}_2\text{Cl}_2$ ):  $\nu(\text{CO})$  1976 (vs), 1804 (s), 1738 (m)  $\text{cm}^{-1}$ .  $^1\text{H}$  NMR ( $\text{CDCl}_3$ )  $\delta$  10.51 (s, 1 H, CH); 7.42–7.20 (10 H, Ph); 5.37, 4.98 (s, 10 H, Cp).  $^{13}\text{C}$  NMR  $\{^1\text{H}\}$  ( $\text{CDCl}_3$ )  $\delta$  223.0 ( $\mu\text{-CO}$ ); 221.3 ( $\text{C=O}$ ); 198.9 ( $\text{CO}$ ); 153.2 (CH); 145.4, 144.7 (*ipso*-Ph); 127.8, 127.7, 127.6, 127.5, 127.3 (Ph); 89.3, 87.7 (Cp); 79.1 ( $\text{CPh}_2\text{OH}$ ); 58.6 ( $\text{C-CPh}_2\text{OH}$ ).

## 5.3 Synthesis of $[\text{Ru}_2\text{Cp}_2(\text{CO})_2(\mu\text{-CO})\{\mu\text{-}\eta^1\text{:}\eta^2_{\alpha,\beta}\text{-C}_\alpha(\text{H)=C}_\beta\text{=C}_\gamma(\text{Ph})_2\}]][\text{BF}_4]$ (**[4b][BF<sub>4</sub>]**) and characterization of $[\text{Ru}_2\text{Cp}_2(\text{CO})_2(\mu\text{-CO})\{\mu\text{-}\eta^1\text{:}\eta^2_{\alpha,\beta}\text{-C}_\alpha(\text{H)=C}_\beta\text{=C}_\gamma(\text{Me})_2\}]][\text{BPh}_4]$ (**[4a][BPh<sub>4</sub>]**)

A solution of  $\text{HBF}_4$  in  $\text{Et}_2\text{O}$  (3.53 mL, 14.0 mmol) was added dropwise to a solution of **1b** (0.880 g, 1.48 mmol) in thf (20 mL). The resulting mixture was stirred for 2 h at room temperature. The solvent was removed under vacuo and the residue was dissolved in  $\text{CH}_2\text{Cl}_2$  (10 mL). Subsequent addition of diethyl ether (60 mL) caused precipitation

of **[4b][BF<sub>4</sub>]**, as air-stable orange microcrystalline solid. Yield: 0.862 g, 84%. Anal. Calcd. for C<sub>27</sub>H<sub>21</sub>BF<sub>4</sub>O<sub>3</sub>Ru<sub>2</sub>: C, 48.43; H, 3.05. Found: C, 47.86; H, 3.21. IR (CH<sub>2</sub>Cl<sub>2</sub>)  $\nu$ (CO) 2048 (vs), 2026 (m), 1881 (m) cm<sup>-1</sup>. <sup>1</sup>H NMR(CD<sub>3</sub>CN, 238K)  $\delta$  11.00 (s, 1 H, C <sub>$\alpha$</sub> H); 7.49÷7.20 (10 H, Ph); 6.04, 5.72 (s, 10 H, Cp). <sup>13</sup>C{<sup>1</sup>H} NMR (CD<sub>3</sub>CN, 238K)  $\delta$  216.7 ( $\mu$ -CO); 195.5, 193.6 (CO); 155.0 (C <sub>$\beta$</sub> ); 139.8 (*ipso*-Ph); 130.9 (C <sub>$\alpha$</sub> ); 130.1, 129.0, 128.4 (Ph); 127.6 (C <sub>$\gamma$</sub> ); 94.2, 92.0 (Cp). Crystals suitable for X ray analysis were obtained as follows: a large excess of NaBPh<sub>4</sub> (0.500 g, 1.46 mmol) was added to a stirred acetonitrile solution of **[4b][BF<sub>4</sub>]** (0.145 mmol in 20 mL). The mixture was stirred overnight, and then filtered on a Celite pad in order to remove insoluble salts. The resulting solution was dried under vacuo, affording a yellow microcrystalline solid. X-Ray quality crystals of **[4b][BPh<sub>4</sub>]** were collected from CH<sub>2</sub>Cl<sub>2</sub>/Et<sub>2</sub>O at 243K. Crystals of **[4a][BPh<sub>4</sub>]**, suitable for X-Ray analysis, were obtained from **[4a][BF<sub>4</sub>]** by the same procedure described above.

#### 5.4 Synthesis of **[Ru<sub>2</sub>Cp<sub>2</sub>(CO)<sub>2</sub>( $\mu$ -CO){ $\mu$ - $\eta^1$ : $\eta^1$ -C <sub>$\alpha$</sub> =C <sub>$\beta$</sub> =C <sub>$\gamma$</sub> (Ph)<sub>2</sub>}]** (**10**)

Sodium hydride (0.052 g, 2.17 mmol) was added to a solution of complex **[4b][BF<sub>4</sub>]** (0.420 g, 0.615 mmol) in thf (15 mL). The mixture was stirred for 4 hours, then it was filtered on a Celite pad in order to remove insoluble salts. The solvent was eliminated under vacuo, the residue was dissolved in CH<sub>2</sub>Cl<sub>2</sub> (5 mL) and chromatographed on alumina. A red band was collected by using neat CH<sub>2</sub>Cl<sub>2</sub> as eluent, hence microcrystalline **10** was obtained upon removal of the solvent. Yield: 0.302 g, 81%.

Anal. Calcd. for  $C_{28}H_{20}O_3Ru_2$ : C, 55.44; H, 3.32. Found: C, 55.21; H, 3.50. IR ( $CH_2Cl_2$ )  $\nu(CO)$ , 1954 (vs), 1803 (s)  $cm^{-1}$ .  $^1H$  NMR ( $CDCl_3$ )  $\delta$  7.70–7.25 (10 H, Ph); 5.31 (s, 10 H, Cp).  $^{13}C$  NMR  $\{^1H\}$  ( $CDCl_3$ )  $\delta$  242.9 ( $\mu-CO$ ); 201.4 ( $C_\beta$ ); 198.4, 197.9 (CO); 192.0 ( $C_\alpha$ ); 141.0 (*ipso*-Ph); 128.9, 128.6, 127.5, 126.3 (Ph); 105.8 ( $C_\gamma$ ); 89.9 (Cp).

### 5.5 Synthesis of $[Ru_2Cp_2(CO)(NCMe)(\mu-CO)\{\mu-\eta^1:\eta^2-C_\alpha(H)=C_\beta=C_\gamma(Ph)_2\}][BF_4]$ (**6b**).

A solution of [**4b**][ $BF_4$ ] (0.280 g, 0.410 mmol) in  $CH_2Cl_2$  (15 mL) was treated with  $Me_3NO$  (0.040 g, 0.533 mmol) in solution of MeCN (5.3 mL). The resulting mixture was stirred at room temperature for 1 hour. Hence the mixture was filtered through a Celite pad and the volatile materials were removed under vacuo. Compound [**6b**][ $BF_4$ ] was obtained as a red microcrystalline solid. Yield: 0.258 g, 89%. Anal. Calcd. for  $C_{29}H_{24}BF_4NO_2Ru_2$ : C, 49.23; H, 3.42; N, 1.98. Found: C, 49.76; H, 3.38; N, 2.05. IR ( $CH_2Cl_2$ )  $\nu(CO)$  2008 (vs), 1861 (s)  $cm^{-1}$ .

### 5.6 Synthesis of $[Ru_2Cp_2(CO)(Cl)(\mu-CO)\{\mu-\eta^1:\eta^2-C_\alpha(H)=C_\beta=C_\gamma(Ph)_2\}]$ (**11b**)

A dichloromethane solution (20 mL) of [**6b**][ $BF_4$ ], freshly prepared from **4b** (0.239 g, 0.350 mmol) and  $Me_3NO/MeCN$  (0.380 mmol in 3.80 mL), was treated with LiCl (0.140 g, 3.30 mmol). The resulting mixture was stirred at room temperature for 3 hours. Then, the mixture was charged on an alumina column. An orange band was

collected by using a mixture of CH<sub>2</sub>Cl<sub>2</sub> and thf (1:1 v/v) as eluent. Compound **11b** was obtained as a microcrystalline solid upon removal of the solvent under vacuo. Yield: 0.185 g, 86%. Anal. Calcd. for C<sub>27</sub>H<sub>21</sub>ClO<sub>2</sub>Ru<sub>2</sub>: C, 52.73; H, 3.44; Cl, 5.76. Found: C, 52.50; H, 3.58; Cl, 5.56. IR (CH<sub>2</sub>Cl<sub>2</sub>)  $\nu$ (CO) 1992 (vs), 1883 (s) cm<sup>-1</sup>. <sup>1</sup>H NMR (CDCl<sub>3</sub>)  $\delta$  10.06 (s, 1 H, C <sub>$\alpha$</sub> H); 7.66–7.23 (10 H, Ph); 5.19, 5.02 (s, 10 H, Cp).

**5.7 Synthesis of [Ru<sub>2</sub>Cp<sub>2</sub>(CO)( $\mu$ -CO){ $\mu$ - $\eta^1$ : $\eta^3$ -C <sub>$\alpha$</sub> (H) $\overline{\text{C}_\beta\text{C}_\gamma(\text{R})_2\text{OC}(=\text{O})\text{C}(\text{H})$ }, (R = Me, **13a**; R = Ph, **13b**)**

A dichloromethane solution of [**6a**][BF<sub>4</sub>], freshly prepared from [**4a**][BF<sub>4</sub>] (0.189 g, 0.331 mmol) and Me<sub>3</sub>NO/MeCN (0.350 mmol in 3.50 mL), was treated with N<sub>2</sub>CHCO<sub>2</sub>Et (0.18 mL, 1.67 mmol). The mixture was stirred for 4 h, during which progressive colour turning from orange to red was observed. IR spectrum (CH<sub>2</sub>Cl<sub>2</sub>) indicated the disappearance of the starting ruthenium compound and the clean formation of [Ru<sub>2</sub>Cp<sub>2</sub>(CO)( $\mu$ -CO){ $\mu$ - $\eta^1$ : $\eta^3$ -C <sub>$\alpha$</sub> (H) $\overline{\text{C}_\beta\text{C}_\gamma(\text{Me})_2\text{OC}(\text{OEt})\text{C}(\text{H})$ ][BF<sub>4</sub>](**12**) [ $\nu$ (CO) 1980, 1812 cm<sup>-1</sup>]. Hence NEt<sub>3</sub> (0.14 mL, 1.00 mmol) was added to the solution, resulting in immediate turning to orange. The mixture was charged on a alumina column and chromatographed. Elution with CH<sub>2</sub>Cl<sub>2</sub>/thf (1:1 v/v) gave an orange fraction: compound **13a** was obtained as an orange microcrystalline solid upon removal of the solvent under vacuo. Yield: 0.134 g, 79 %. Anal. Calcd. for C<sub>19</sub>H<sub>18</sub>O<sub>4</sub>Ru<sub>2</sub>: C, 44.53; H, 3.54. Found: C, 44.36; H, 3.63. IR (CH<sub>2</sub>Cl<sub>2</sub>)  $\nu$ (CO) 1963 (vs), 1792 (s), 1735 (m) cm<sup>-1</sup>. <sup>1</sup>H NMR



(CDCl<sub>3</sub>)  $\delta$  10.04 (d, 1 H,  $^4J_{HH} = 1.47$  Hz, C <sub>$\alpha$</sub> H); 5.31, 4.94 (s, 10 H, Cp); 1.66, 1.35 (s, 6 H, Me); 1.50 (d, 1 H,  $^4J_{HH} = 1.47$  Hz, CH). <sup>13</sup>C NMR {<sup>1</sup>H} (CDCl<sub>3</sub>)  $\delta$  238.2 ( $\mu$ -CO); 200.8 (CO); 179.3 (C=O); 137.9 (C <sub>$\alpha$</sub> ); 116.9 (C <sub>$\beta$</sub> ); 91.3 (C <sub>$\gamma$</sub> ); 89.1, 85.4 (Cp); 41.9 (CH); 32.2, 25.0 (Me).

Compound **13b** was prepared by the same procedure described for **13a**, by reacting [**6b**][BF<sub>4</sub>], freshly prepared from [**4b**][BF<sub>4</sub>] (0.310 mmol) and Me<sub>3</sub>NO/MeCN, with N<sub>2</sub>CHCO<sub>2</sub>Et/NEt<sub>3</sub>. Chromatography: CH<sub>2</sub>Cl<sub>2</sub> 100%. Colour: yellow. Yield: 0.162 g, 82%. Anal. Calcd. for C<sub>29</sub>H<sub>22</sub>O<sub>4</sub>Ru<sub>2</sub>: C, 54.71; H, 3.48. Found: C, 54.34; H, 3.61. IR (CH<sub>2</sub>Cl<sub>2</sub>)  $\nu$ (CO) 1965 (vs), 1795 (s), 1746 (m) cm<sup>-1</sup>. <sup>1</sup>H NMR (CDCl<sub>3</sub>)  $\delta$  10.35 (s, 1 H, C <sub>$\alpha$</sub> H); 7.59–7.33 (10 H, Ph); 5.37, 4.55 (s, 10 H, Cp); 1.59 (s, 1 H, CH). <sup>13</sup>C NMR {<sup>1</sup>H} (CDCl<sub>3</sub>)  $\delta$  238.0 ( $\mu$ -CO); 201.2 (CO); 178.3 (C=O); 145.0, 142.2 (*ipso*-Ph); 141.6 (C <sub>$\alpha$</sub> ); 128.4, 127.9, 125.9 (Ph); 112.4 (C <sub>$\beta$</sub> ); 89.2, 85.4 (Cp); 61.5 (C <sub>$\gamma$</sub> ); 43.8 (CH).

Crystals of **13a** and **13b** suitable for X-ray analyses were collected from dichloromethane solutions layered with pentane, at 243K.

In a different experiment, compound [**6a**][BF<sub>4</sub>] (0.250 mmol) was dissolved in CDCl<sub>3</sub> (0.65 mL) and treated with N<sub>2</sub>CHCO<sub>2</sub>Et in a NMR tube. Then the tube was sealed and after 2 hours <sup>1</sup>H NMR spectroscopy indicated the prevalent formation of [**12**][BF<sub>4</sub>]. <sup>1</sup>H NMR (CDCl<sub>3</sub>)  $\delta$  10.50 (d, 1 H,  $^4J_{HH} = 1.2$  Hz, C <sub>$\alpha$</sub> H); 5.59, 5.35 (s, 10 H, Cp); 4.27 (q, 2 H,  $^3J_{HH} = 7.0$  Hz, OCH<sub>2</sub>); 2.27 (t, 3 H,  $^3J_{HH} = 7.0$  Hz, OCH<sub>2</sub>CH<sub>3</sub>); 1.96, 1.82 (s, 6 H, Me); 1.67 (d, 1 H,  $^4J_{HH} = 1.2$  Hz, CH).

## 5.8 Synthesis of $[\text{Ru}_2\text{Cp}_2(\text{CO})(\mu\text{-CO})\{\mu\text{-}\eta^1\text{:}\eta^3\text{-C}_\alpha(\text{H})\overline{\text{C}_\beta\text{C}_\gamma(\text{Me})_2\text{OC}(\text{NEt}_2)\text{C}(\text{H})}\}][\text{BF}_4]$ (**14**)[**BF**<sub>4</sub>])

The treatment of **12**, prepared from **4a** (0.350 mmol) in  $\text{CH}_2\text{Cl}_2$  (20 mL), with  $\text{NHET}_2$  (1.80 mmol) gave an orange mixture which was chromatographed on alumina. Compound **13a** was recovered in 33% yield by using  $\text{CH}_2\text{Cl}_2/\text{thf}$  (1:1 v/v) as eluent. Then, elution with acetonitrile gave a second yellow band which afforded [**14**][**BF**<sub>4</sub>] in the form of yellow microcrystalline solid after removal of the solvent. Yield: 0.110 g, 48%. Anal. Calcd. for  $\text{C}_{23}\text{H}_{28}\text{BF}_4\text{NO}_3\text{Ru}_2$ : C, 42.15; H, 4.31; N, 2.14. Found: C, 42.63; H, 4.26; N, 2.27. IR ( $\text{CH}_2\text{Cl}_2$ )  $\nu(\text{CO})$  1975 (s), 1806 (m),  $\nu(\text{C}=\text{N})$  1644 (m)  $\text{cm}^{-1}$ .  $^1\text{H}$  NMR ( $\text{CDCl}_3$ )  $\delta$  10.35 (s, H,  $\text{C}_\alpha\text{H}$ ); 5.52, 5.05 (s, 10 H, Cp); 3.77÷3.55 (m, 4 H,  $\text{CH}_2\text{CH}_3$ ); 1.83, 1.68 (s, 6 H,  $\text{C}_\gamma\text{Me}$ ); 1.46, 1.30 (m, 6 H,  $\text{CH}_2\text{CH}_3$ ); 1.20 (s, 1 H, CH).  $^{13}\text{C}\{^1\text{H}\}$  NMR ( $\text{CDCl}_3$ )  $\delta$  238.1 ( $\mu\text{-CO}$ ); 200.8 (CO); 181.0 (C=N); 141.3 ( $\text{C}_\alpha$ ); 114.3 ( $\text{C}_\beta$ ); 97.2 ( $\text{C}_\gamma$ ); 90.2, 85.3 (Cp); 47.7, 44.8 ( $\text{CH}_2\text{CH}_3$ ); 38.4 (CH); 31.2, 25.3 ( $\text{C}_\gamma\text{Me}$ ); 13.3, 13.2 ( $\text{CH}_2\text{CH}_3$ ). Crystals suitable for X-Ray analyses were obtained from a dichloromethane solution layered with diethyl ether, at 243K.

## 5.9 Synthesis of $[\text{Fe}_2\text{Cp}_2(\text{CO})(\mu\text{-CO})\{\mu\text{-}\eta^1\text{:}\eta^3\text{-C}(\text{H})=\text{C}(\text{CR}_2\text{OH})\text{C}(=\text{O})\}][\text{R}=\text{Me}, \text{2a}; \text{R}=\text{Ph}, \text{2b})]$

A solution of  $\text{HC}\equiv\text{CCMe}_2\text{OH}$  (8.00 mL, 82.6 mmol) and  $[\text{Fe}_2\text{Cp}_2(\text{CO})_4]$  (15.0 g, 42.4 mmol), in thf (160 mL), was irradiated with UV light for 180 h. Then the volatile

materials were removed under vacuo, and the brown residue was dissolved in CH<sub>2</sub>Cl<sub>2</sub> and charged on an alumina column. Elution with neat acetone afforded a brown-green band corresponding to **2a**. The product was obtained as a brown microcrystalline solid upon removal of the solvent. Yield: 10.8 g, 62%. Anal. Calcd. for C<sub>18</sub>H<sub>18</sub>Fe<sub>2</sub>O<sub>4</sub>: C, 52.73; H, 4.42. Found: C, 52.31; H, 4.57. IR (solid state):  $\nu(\text{OH})$  3307 (m-br),  $\nu(\text{CO})$  1961 (vs), 1766 (s), 1740 (m) cm<sup>-1</sup>. <sup>1</sup>H NMR (CDCl<sub>3</sub>)  $\delta$  12.58 (s, 1 H, CH); 5.03, 4.75 (s, 10 H, Cp); 3.34, 1.50 (s, 6 H, Me); 1.99 (br, 1 H, OH).

Compound **2b** was prepared by the same procedure described for **2a**, by irradiating a solution of HC≡CCPh<sub>2</sub>OH (8.20 g, 39.4 mmol) and [Fe<sub>2</sub>Cp<sub>2</sub>(CO)<sub>4</sub>] (6.40 g, 18.1 mmol) in thf (180 mL) for 215 h. Yield: 6.28 g, 65%. Anal. Calcd. for C<sub>28</sub>H<sub>22</sub>Fe<sub>2</sub>O<sub>4</sub>: C, 62.96; H, 4.15. Found: C, 62.29; H, 4.19. IR (CH<sub>2</sub>Cl<sub>2</sub>):  $\nu(\text{OH})$  3298 (m-br),  $\nu(\text{CO})$  1973 (vs), 1752 (s), 1705 (m) cm<sup>-1</sup>. <sup>1</sup>H NMR (CDCl<sub>3</sub>)  $\delta$  12.26 (s, 1 H, CH); 7.40÷7.20 (10 H, Ph); 5.01, 4.62 (s, 10 H, Cp); 1.60 (br, 1 H, OH).

#### 5.10 Synthesis of [Fe<sub>2</sub>Cp<sub>2</sub>(CO)<sub>2</sub>( $\mu$ -CO){ $\mu$ - $\eta^1$ : $\eta^2_{\alpha,\beta}$ -C <sub>$\alpha$</sub> (H)=C <sub>$\beta$</sub> =C <sub>$\gamma$</sub> (R)<sub>2</sub>}][BF<sub>4</sub>] (R=Me, [7a][BF<sub>4</sub>]; R=Ph, [7b][BF<sub>4</sub>])

Compound **2a** (2.50 g, 6.10 mmol), prepared according to the procedure described above, was dissolved in thf (50 mL). The solution was cooled to 223K, and then treated with a solution of HBF<sub>4</sub> in Et<sub>2</sub>O (1.74 mL, 6.90 mmol). The resulting mixture was allowed to warm to room temperature, and stirred overnight. Subsequent removal of the volatile materials and chromatography of the residue on alumina gave a red fraction

which was collected by using neat acetonitrile. Thus compound **[7a][BF<sub>4</sub>]** was obtained as a red microcrystalline solid upon removal of the solvent under vacuo. Yield: 2.58 g, 88%. Anal. Calcd. for C<sub>18</sub>H<sub>17</sub>BF<sub>4</sub>Fe<sub>2</sub>O<sub>3</sub>: C, 45.06; H, 3.57. Found: C, 44.52; H, 3.68. IR (CH<sub>2</sub>Cl<sub>2</sub>):  $\nu(\text{CO})$  2036 (vs), 2011 (s), 1864 (m) cm<sup>-1</sup>. <sup>1</sup>H NMR (CD<sub>3</sub>CN, 238K)  $\delta$  11.77 (s, 1 H, C <sub>$\alpha$</sub> H); 5.58, 5.36 (s, 10 H, Cp); 2.28, 1.94 (s, 6 H, Me). <sup>13</sup>C NMR {<sup>1</sup>H} (CD<sub>3</sub>CN, 238K)  $\delta$  242.0 ( $\mu$ -CO); 210.6, 206.3 (CO); 149.1 (C <sub>$\beta$</sub> ); 147.2 (C <sub>$\alpha$</sub> ); 121.4 (C <sub>$\gamma$</sub> ); 92.3, 89.1 (Cp); 27.7, 23.2 (Me). Crystals suitable for X-Ray analysis were obtained as follows: to a solution of **[7a][BF<sub>4</sub>]** (0.25 mmol) in thf (20 mL), CF<sub>3</sub>SO<sub>3</sub>Na (2.30 mmol) was added. The mixture was stirred overnight, then it was filtered through a Celite pad. The resulting solution was layered with diethyl ether, in a Schlenk tube. Crystals of **[7a][SO<sub>3</sub>CF<sub>3</sub>]** were collected after 48 hours at 243K.

Complex **[7b][BF<sub>4</sub>]** was prepared by a procedure analogous to that described for **[7a][BF<sub>4</sub>]**, by treating **2b** (2.40 g, 4.49 mmol) with HBF<sub>4</sub>/Et<sub>2</sub>O (1.24 mL, 4.90 mmol). Yield: 2.23 g, 82%. Anal. Calcd. for C<sub>28</sub>H<sub>21</sub>BF<sub>4</sub>Fe<sub>2</sub>O<sub>3</sub>: C, 55.68; H, 3.50. Found: C, 55.33; H, 3.46. IR (CH<sub>2</sub>Cl<sub>2</sub>):  $\nu(\text{CO})$  2042 (vs), 2017 (s), 1870 (m) cm<sup>-1</sup>. <sup>1</sup>H NMR (CD<sub>3</sub>CN, 238K)  $\delta$  12.30 (s, 1 H, C <sub>$\alpha$</sub> ); 7.78÷7.02 (10 H, Ph); 5.74, 5.38 (s, 10 H, Cp).

### 5.11 Synthesis of **[Fe<sub>2</sub>Cp<sub>2</sub>(CO)( $\mu$ -CO){ $\mu$ - $\eta^1$ : $\eta^3$ -C <sub>$\alpha$</sub> (H)=C <sub>$\beta$</sub> (C <sub>$\gamma$</sub> (Me)CH<sub>2</sub>)C(=O)}]** (**15**)

A solution of complex **[7a][BF<sub>4</sub>]** (1.40 g, 2.92 mmol), in CH<sub>2</sub>Cl<sub>2</sub> (15 mL), was treated with NHET<sub>2</sub> (0.36 mL, 3.5 mmol). The mixture was stirred overnight at room

temperature. Then the final mixture was charged on an alumina column. A brown fraction was collected by using a mixture of CH<sub>2</sub>Cl<sub>2</sub> and thf (1:1 v/v) as eluent. Yield: 0.940 g, 82%. Anal. Calcd. for C<sub>18</sub>H<sub>16</sub>Fe<sub>2</sub>O<sub>3</sub>: C, 55.15; H, 4.11. Found: C, 54.70; H, 4.31. IR (CH<sub>2</sub>Cl<sub>2</sub>)  $\nu$ (CO) 1975 (vs), 1796 (s), 1748 (m),  $\nu$ (C=C) 1611 (m) cm<sup>-1</sup>. <sup>1</sup>H NMR (CDCl<sub>3</sub>)  $\delta$  12.29 (s, 1 H, C <sub>$\alpha$</sub> H); 5.40, 5.23 (m, 2 H, CH<sub>2</sub>); 5.06, 4.62 (s, 10 H, Cp); 2.09 (s, 3 H, Me). <sup>13</sup>C NMR {<sup>1</sup>H} (CDCl<sub>3</sub>)  $\delta$  261.9 ( $\mu$ -CO); 232.7 (C=O); 210.5 (CO); 173.2 (C <sub>$\alpha$</sub> ); 139.8 (C <sub>$\gamma$</sub> ); 116.9 (CH<sub>2</sub>); 87.9, 87.3 (Cp); 31.2 (C <sub>$\beta$</sub> ); 20.8 (Me).

### 5.12 Synthesis of [Fe<sub>2</sub>Cp<sub>2</sub>(CO)<sub>2</sub>( $\mu$ -CO){ $\mu$ - $\eta^1$ : $\eta^2$ <sub>$\alpha,\beta$</sub> -C <sub>$\alpha$</sub> (H)=C <sub>$\beta$</sub> (H)(Ph)}][BF<sub>4</sub>] (9)

Compound **8** (3.0 g, 7.00 mmol), prepared according to the procedure described above, was dissolved in THF (50 mL). The solution was cooled to 223K, and then treated with a solution of HBF<sub>4</sub> in Et<sub>2</sub>O (2.00 mL, 7.93 mmol). The resulting mixture was allowed to warm to room temperature, and stirred overnight. The solvent was removed under vacuo, thus the residue was washed with Et<sub>2</sub>O (3x50 mL) and dissolved in CH<sub>2</sub>Cl<sub>2</sub> (10 mL). Filtration on a celite pad and subsequent removal of the solvent gave a black powder corresponding to compound **9**. Yield: 3.00 g, 82%. Anal. Calcd. for C<sub>22</sub>H<sub>17</sub>BF<sub>4</sub>Fe<sub>2</sub>O<sub>3</sub>: C, 50.06; H, 3.25. Found: C, 49.52; H, 3.30. IR (solid state):  $\nu$ (CO) 2018 (vs), 1995 (m-s), 1854 (m) cm<sup>-1</sup>. <sup>1</sup>H NMR (CDCl<sub>3</sub>)  $\delta$  13.00 (d, 1 H, <sup>4</sup>J<sub>HH</sub> = 9.8 Hz, C <sub>$\alpha$</sub> H); 7.87, 7.47, 7.29 (m, 5H, Ph); 5.37 (s, 10 H, Cp); 4.63 (d, 1 H, <sup>4</sup>J<sub>HH</sub> = 9.8 Hz, C <sub>$\beta$</sub> H). <sup>13</sup>C NMR {<sup>1</sup>H} (CDCl<sub>3</sub>)  $\delta$  301.0 ( $\mu$ -CO); 220.1, 210.8 (CO); 170.4 (C <sub>$\beta$</sub> ); 138.2, 130.4, 130.1, 128.0 (Ph); 94.0 (C <sub>$\alpha$</sub> ); 91.2 (Cp).

### 5.13 Synthesis of $\text{Fe}_2\text{Cp}_2(\text{CO})_2(\mu\text{-CO})\{\mu\text{-}\eta^1\text{-}\eta^2\text{-CHCH(Ph)}\}_2$ (**16**)

Compound  $[\text{Fe}_2\text{Cp}_2(\text{CO})_2(\mu\text{-CO})\{\mu\text{-}\eta^1\text{-}\eta^2\text{-CH=CH(Ph)}\}][\text{BF}_4]$  (**9**; 0.350 g, 0.678 mmol) was dissolved in  $\text{CH}_2\text{Cl}_2$  (15 mL) and then treated with  $\text{CoCp}_2$  (0.150 g, 0.793 mmol). The mixture was stirred for 1 hour at room temperature. Thus the volatile materials were removed under vacuo; the resulting red residue was dissolved in  $\text{Et}_2\text{O}$  (20 mL) and charged on an alumina column. A red fraction corresponding to **16** was collected by using neat  $\text{CH}_2\text{Cl}_2$  as eluent. Compound **16** was obtained as a powder upon removal of the solvent. Yield: 0.239 g, 82%. Crystals suitable for X-Ray analysis were obtained from a  $\text{CH}_2\text{Cl}_2$  solution layered with pentane, at  $-30^\circ\text{C}$ . Anal. Calcd. for  $\text{C}_{42}\text{H}_{34}\text{Fe}_4\text{O}_6$ : C, 58.79; H, 3.99. Found: C, 58.34; H, 4.11. IR ( $\text{CH}_2\text{Cl}_2$ ):  $\nu(\text{CO})$  1973 vs, 1936 m, 1774 m  $\text{cm}^{-1}$ .  $^1\text{H}$  NMR ( $\text{CDCl}_3$ ):  $\delta$  12.10 (d, 1 H,  $^3J_{\text{HH}} = 12.5$  Hz,  $\mu\text{-CH}$ ); 7.67–6.87 (5 H, Ph); 4.91 (d, 1 H,  $^3J_{\text{HH}} = 12.5$  Hz,  $\text{CHPh}$ ); 4.77, 4.30 (s, 10 H, Cp).  $^{13}\text{C}$  NMR  $\{^1\text{H}\}$  ( $\text{CDCl}_3$ ):  $\delta$  274.2 ( $\mu\text{-CO}$ ); 213.4, 212.9 (CO); 178.7 ( $\mu\text{-C}$ ); 146.6 (*ipso*-Ph); 134.3, 131.2, 128.3, 126.6, 125.4 (Ph); 88.2 (Cp); 77.5 (CPh).

### 5.14 The reaction of $[\text{Fe}_2\text{Cp}_2(\text{CO})_2(\mu\text{-CO})\{\mu\text{-}\eta^2\text{-CHCH(Ph)}\}_2$ (**16**) with $\text{I}_2$ : formation of $[\text{Fe}_2\text{Cp}_2(\text{CO})_2(\mu\text{-CO})\{\mu\text{-}\eta^1\text{-}\eta^2\text{-CH=CH(Ph)}\}]^+$ (**9**)

The treatment of a solution of compound  $[\text{Fe}_2\text{Cp}_2(\text{CO})_2(\mu\text{-CO})\{\mu\text{-}\eta^2\text{-CHCH(Ph)}\}_2$  (**16**; 0.100 g, 0.117 mmol) in tetrahydrofuran (15 mL) with  $\text{I}_2$  (0.075 g, 0.295 mmol) resulted in slight colour change.  $^1\text{H}$  NMR spectrum (in  $\text{CDCl}_3$ ), performed after 8 hours

on an aliquot of the mixture priorly dried under vacuo, indicated the clean formation of the complex  $[\text{Fe}_2\text{Cp}_2(\text{CO})_2(\mu\text{-CO})\{\mu\text{-}\eta^1\text{:}\eta^2\text{-CH=CH(Ph)}\}]^+$ ,  $[\mathbf{9}]^+$ .

### 5.15 Synthesis of $[[\text{Fe}_2\text{Cp}_2(\text{CO})_2(\mu\text{-CO})\{\mu\text{-}\eta^2\text{-CHCH(Ph)(SPh)}\}]]$ (**18**)

To a solution of compound  $[\text{Fe}_2\text{Cp}_2(\text{CO})_2(\mu\text{-CO})\{\mu\text{-}\eta^1\text{:}\eta^2\text{-CH=CH(Ph)}\}][\text{BF}_4]$  (**9**; 0.200 g, 0.388 mmol) in  $\text{CH}_2\text{Cl}_2$  (15 mL), PhSSPh (0.840 g, 3.85 mmol) and  $\text{NEt}_3$  (0.17 mL, 1.2 mmol) were added in the order given. The mixture was stirred for 1 hour at room temperature. Then the volatile materials were removed under vacuo; the resulting red residue was washed with pentane (3 x 10 mL), dissolved in  $\text{Et}_2\text{O}$  (15 mL) and chromatographed on alumina. Compound **18** was collected as an orange band by using a mixture of  $\text{CH}_2\text{Cl}_2$  and THF (5:1 v/v) as eluent, and obtained as a powder upon removal of the solvent. Yield: 0.163 g, 78%. Crystals suitable for X-Ray analysis were obtained from a  $\text{CH}_2\text{Cl}_2$  solution layered with pentane, at  $-30^\circ\text{C}$ . Anal. Calcd. for  $\text{C}_{27}\text{H}_{22}\text{Fe}_2\text{O}_3\text{S}$ : C, 60.25; H, 4.12. Found: C, 60.02; H, 4.26. IR ( $\text{CH}_2\text{Cl}_2$ ):  $\nu(\text{CO})$  1972 vs, 1934 m, 1774  $\text{m cm}^{-1}$ .  $^1\text{H}$  NMR ( $\text{CDCl}_3$ ):  $\delta$  11.28 (d, 1 H,  $^4J_{\text{HH}} = 12.5$  Hz,  $\text{C}_\alpha\text{H}$ ); 7.73-7.11 (10 H, Ph); 5.12 (d, 1 H,  $^4J_{\text{HH}} = 12.5$  Hz,  $\text{C}_\beta\text{H}$ ) 4.94, 4.93 (s, 10 H, Cp).  $^{13}\text{C}$  NMR  $\{^1\text{H}\}$  ( $\text{CDCl}_3$ ):  $\delta$  266.7 ( $\mu\text{-CO}$ ); 218.0, 212.4 (CO); 180.3 ( $\text{C}_\alpha$ ); 139.6-124.7 (Ph); 88.0, 87.4 (Cp); 66.9 ( $\text{C}_\beta$ ).

## 6. Crystallography Appendix

Single crystal X-ray structures were solved by Prof. Stefano Zacchini (University of Bologna) on crystal specimens prepared in Pisa.

<i>Complex</i>	<b>[4a][BPh<sub>4</sub>]·CH<sub>2</sub>Cl<sub>2</sub></b>	<b>[4c][BPh<sub>4</sub>]·0.5thf</b>	<b>[7a][CF<sub>3</sub>SO<sub>3</sub>]</b>
Formula	C <sub>43</sub> H <sub>39</sub> BCl <sub>2</sub> O <sub>3</sub> Ru <sub>2</sub>	C <sub>54</sub> H <sub>45</sub> BO <sub>3.5</sub> Ru <sub>2</sub>	C <sub>19</sub> H <sub>17</sub> F <sub>3</sub> Fe <sub>2</sub> O <sub>6</sub> S
<i>F</i> <sub>w</sub>	887.59	962.85	542.09
T, K	294(2)	294(2)	294(2)
$\lambda$ , Å	0.71073	0.71073	0.71073
Crystal system	Orthorhombic	Monoclinic	Orthorhombic
Space group	<i>P</i> 2 <sub>1</sub> 2 <sub>1</sub> 2 <sub>1</sub>	<i>C</i> 2/ <i>c</i>	<i>P</i> 2 <sub>1</sub> 2 <sub>1</sub> 2 <sub>1</sub>
<i>a</i> , Å	9.9707(18)	56.255(6)	10.6193(15)
<i>b</i> , Å	14.798(3)	9.6487(10)	21.194(3)
<i>c</i> , Å	27.089(5)	36.085(4)	9.5464(14)
$\beta$ , °	90	114.9470(10)	90
Cell Volume, Å <sup>3</sup>	3996.9(12)	17759(3)	2148.5(5)
<i>Z</i>	4	16	4
<i>D</i> <sub>c</sub> , g cm <sup>-3</sup>	1.475	1.441	1.676
$\mu$ , mm <sup>-1</sup>	0.927	0.725	1.506
<i>F</i> (000)	1792	7840	1096
Crystal size, mm	0.19×0.16×0.12	0.18×0.12×0.11	0.18×0.15×0.11
$\theta$ limits, °	1.50–25.03	1.24–26.00	1.92–25.99
Reflections collected	28799	89261	16383
Independent reflections	7059 [ <i>R</i> <sub>int</sub> = 0.1210]	17412 [ <i>R</i> <sub>int</sub> = 0.0600]	4221 [ <i>R</i> <sub>int</sub> = 0.0748]
Data / restraints / parameters	7059 / 544 / 555	17412 / 620 / 1096	4221 / 86 / 286
Goodness on fit on <i>F</i> <sup>2</sup>	1.035	1.017	1.083
<i>R</i> <sub>1</sub> ( <i>I</i> > 2σ( <i>I</i> ))	0.0586	0.0400	0.0517
<i>wR</i> <sub>2</sub> (all data)	0.1474	0.0983	0.1325
Largest diff. peak and hole, e Å <sup>-3</sup>	0.602 / –0.322	0.701 / –0.429	0.604 / –0.409

Table 3: Crystal data and experimental details for [4a][BPh<sub>4</sub>]·CH<sub>2</sub>Cl<sub>2</sub>, [4c][BPh<sub>4</sub>]·0.5thf, [7a][CF<sub>3</sub>SO<sub>3</sub>], 13a, 13b and [14][BF<sub>4</sub>]·CH<sub>2</sub>Cl<sub>2</sub>.



<i>Complex</i>	<b>13a</b>	<b>13b</b>	<b>[14][BF<sub>4</sub>]·CH<sub>2</sub>Cl<sub>2</sub></b>
Formula	C <sub>19</sub> H <sub>18</sub> O <sub>4</sub> Ru <sub>2</sub>	C <sub>29</sub> H <sub>22</sub> O <sub>4</sub> Ru <sub>2</sub>	C <sub>24</sub> H <sub>30</sub> BCl <sub>2</sub> F <sub>4</sub> NO <sub>3</sub> Ru <sub>2</sub>
<i>F</i> <sub>w</sub>	512.47	636.61	740.34
T, K	295(2)	294(2)	295(2)
$\lambda$ , Å	0.71073	0.71073	0.71073
Crystal system	Orthorhombic	Monoclinic	Monoclinic
Space group	<i>P</i> 2 <sub>1</sub> 2 <sub>1</sub> 2 <sub>1</sub>	<i>P</i> 2 <sub>1</sub> / <i>c</i>	<i>P</i> 2 <sub>1</sub> / <i>n</i>
<i>a</i> , Å	9.9279(16)	10.5647(9)	16.280(3)
<i>b</i> , Å	11.5719(18)	14.6934(13)	10.5976(18)
<i>c</i> , Å	15.274(2)	16.2336(14)	16.662(3)
$\beta$ , °	90	105.4060(10)	92.275(2)
Cell Volume, Å <sup>3</sup>	1754.8(5)	2429.4(4)	2872.5(9)
<i>Z</i>	4	4	4
<i>D</i> <sub>c</sub> , g cm <sup>-3</sup>	1.940	1.741	1.712
$\mu$ , mm <sup>-1</sup>	1.741	1.277	1.290
<i>F</i> (000)	1008	1264	1472
Crystal size, mm	0.25×0.21×0.16	0.22×0.15×0.14	0.25×0.24×0.21
$\theta$ limits, °	2.21–26.00	1.90–28.00	1.72–27.00
Reflections collected	18166	27425	31061
Independent reflections	3457 [ <i>R</i> <sub>int</sub> = 0.0349]	5676 [ <i>R</i> <sub>int</sub> = 0.0200]	6266 [ <i>R</i> <sub>int</sub> = 0.0444]
Data / restraints / parameters	3457 / 98 / 234	5676 / 2 / 322	6266 / 134 / 344
Goodness on fit on <i>F</i> <sup>2</sup>	1.090	1.058	1.058
<i>R</i> <sub>1</sub> ( <i>I</i> > 2σ( <i>I</i> ))	0.0296	0.0202	0.0477
<i>wR</i> <sub>2</sub> (all data)	0.0774	0.0531	0.1422
Largest diff. peak and hole, e Å <sup>-3</sup>	0.878 / –0.363	0.286 / –0.584	1.017 / –0.725

Table 4: Crystal data and experimental details for **13a**, **13b** and **[14][BF<sub>4</sub>]·CH<sub>2</sub>Cl<sub>2</sub>**.

<i>Complex</i>	<b>16</b>	<b>18</b>
Formula	C <sub>48</sub> H <sub>48</sub> Fe <sub>4</sub> O <sub>6</sub>	C <sub>27</sub> H <sub>22</sub> Fe <sub>2</sub> O <sub>3</sub> S
<i>F</i> <sub>w</sub>	944.26	538.21
T, K	295(2)	296(2)
$\lambda$ , Å	0.71073	0.71073
Crystal system	Orthorhombic	Monoclinic
Space group	<i>P</i> 2 <sub>1</sub> 2 <sub>1</sub> 2 <sub>1</sub>	<i>P</i> 2 <sub>1</sub> / <i>c</i>
<i>a</i> , Å	10.815(3)	18.936(15)
<i>b</i> , Å	17.560(6)	8.902(5)
<i>c</i> , Å	23.070(7)	14.751(9)
$\beta$ , °	90	112.461(8)
Cell Volume, Å <sup>3</sup>	4381(2)	2298(3)
<i>Z</i>	4	4
<i>D</i> <sub>c</sub> , g cm <sup>-3</sup>	1.431	1.556
$\mu$ , mm <sup>-1</sup>	1.345	1.381
<i>F</i> (000)	1952	1104
Crystal size, mm	0.23×0.21×0.14	0.19×0.17×0.11
$\theta$ limits, °	1.46–25.20	1.49–25.02
Reflections collected	41987	20029
Independent reflections	7880 [ <i>R</i> <sub>int</sub> = 0.0588]	4034 [ <i>R</i> <sub>int</sub> = 0.1101]
Data / restraints / parameters	7880 / 240 / 493	20019 / 150 / 299
Goodness on fit on <i>F</i> <sup>2</sup>	1.084	1.868
<i>R</i> <sub>1</sub> ( <i>I</i> > 2σ( <i>I</i> ))	0.0503	0.1195
<i>wR</i> <sub>2</sub> (all data)	0.1414	0.3114
Largest diff. peak and hole, e Å <sup>-3</sup>	0.662/ –0.358	2.305/ –1.238

Table 5: Crystal data and experimental details for **16** and **18**.

<i>Complex</i>	<b>4a</b>	<b>4c (I)<sup>a</sup></b>	<b>4c (II)<sup>a</sup></b>	<b>7a</b>
M(1)–M(2)	2.7801(10)	2.7793(6)	2.7819(6)	2.6063(14)
M(1)–C(11)	2.187(14)	2.185(5)	2.175(5)	2.152(8)
M(2)–C(11)	1.946(12)	1.979(5)	1.972(5)	1.815(9)
M(1)–C(13)	1.829(13)	1.901(5)	1.895(5)	1.761(9)
M(2)–C(12)	1.845(13)	1.883(5)	1.875(5)	1.766(10)
M(1)–C(14)	2.138(9)	2.154(4)	2.168(4)	2.026(8)
M(2)–C(14)	2.015(11)	2.039(5)	2.049(4)	1.940(8)
M(1)–C(15)	2.199(10)	2.184(4)	2.182(4)	2.061(7)
C(11)–O(11)	1.200(12)	1.155(5)	1.156(5)	1.178(9)
C(12)–O(12)	1.159(12)	1.127(5)	1.138(5)	1.141(10)
C(13)–O(13)	1.184(12)	1.126(5)	1.124(5)	1.147(9)
C(14)–C(15)	1.390(13)	1.355(6)	1.360(6)	1.332(11)
C(15)–C(16)	1.328(13)	1.326(6)	1.329(5)	1.339(11)
M(1)–C(11)–M(2)	84.3(5)	83.6(2)	84.10(18)	81.7(3)
M(1)–C(11)–O(11)	130.0(10)	130.2(4)	129.6(4)	126.1(7)
M(2)–C(11)–O(11)	145.5(11)	146.0(4)	146.0(4)	152.2(8)
M(1)–C(14)–M(2)	84.0(4)	82.98(16)	82.50(15)	82.1(3)
M(2)–C(14)–C(15)	126.0(8)	126.4(4)	122.9(3)	124.7(6)
C(14)–C(15)–C(16)	154.8(10)	151.7(4)	151.5(4)	152.0(8)
C(14)–C(15)–M(1)	68.9(6)	70.6(3)	71.2(2)	69.6(5)
M(1)–C(15)–C(16) <sup>b</sup>	136.1(8)	137.7(3)	137.3(3)	137.7(6)

<sup>a</sup> Two independent molecules are present within the unit cell. <sup>b</sup> Sum angles at C(16): **4a**, 360.0(17); **4c (I)<sup>a</sup>**, 360.0(7); **4c (II)<sup>a</sup>**, 355.9(7); **7a**, 359.9(14)

Table 6: Selected bond lengths (Å) and angles (°) for **4a**, **4c** and **7a** in [**4a**][BPh<sub>4</sub>]·CH<sub>2</sub>Cl<sub>2</sub>, [**4c**][BPh<sub>4</sub>]·0.5thf, [**7a**][CF<sub>3</sub>SO<sub>3</sub>].

<i>Complex</i>	<b>13a</b>	<b>13b</b>	<b>14</b>
Ru(1)–Ru(2)	2.7544(6)	2.7375(3)	2.7386(6)
Ru(1)–C(11)	2.005(5)	2.020(2)	2.012(5)
Ru(2)–C(11)	2.049(5)	2.0628(19)	2.064(5)
Ru(2)–C(12)	1.871(5)	1.856(2)	1.855(6)
Ru(1)–C(13)	2.145(4)	2.1197(17)	2.149(5)
Ru(2)–C(13)	2.032(4)	2.0387(18)	2.043(5)
Ru(1)–C(14)	2.164(5)	2.1636(17)	2.169(4)
Ru(1)–C(15)	2.194(4)	2.1879(18)	2.189(4)
C(11)–O(11)	1.186(6)	1.172(2)	1.176(6)
C(12)–O(12)	1.124(6)	1.143(3)	1.148(7)
C(13)–C(14)	1.404(6)	1.406(2)	1.400(6)
C(14)–C(15)	1.411(7)	1.433(2)	1.429(6)
C(15)–C(16)	1.487(7)	1.461(3)	1.439(7)
C(16)–X(1)	1.205(6)	1.205(2)	1.313(6)
C(16)–O(2)	1.358(6)	1.376(3)	1.330(6)
C(17)–O(2)	1.479(6)	1.461(2)	1.502(6)
C(14)–C(17)	1.527(6)	1.533(2)	1.520(6)
Ru(1)–C(11)–Ru(2)	85.60(18)	84.20(7)	84.41(18)
Ru(1)–C(11)–O(11)	138.6(4)	139.37(17)	139.8(4)
Ru(2)–C(11)–O(11)	135.5(4)	136.14(17)	135.5(4)
Ru(1)–C(13)–Ru(2)	82.46(15)	82.32(6)	81.55(16)
C(13)–C(14)–C(15)	123.8(4)	122.82(16)	123.1(4)
C(14)–C(15)–C(16)	106.3(4)	106.91(17)	104.9(4)
C(15)–C(16)–O(2)	109.8(4)	109.98(16)	113.7(4)
C(16)–O(2)–C(17)	110.6(3)	110.65(14)	109.2(4)
O(2)–C(17)–C(14)	102.4(4)	103.35(14)	101.9(3)
C(17)–C(14)–C(15)	109.2(4)	107.65(15)	109.3(4)

<sup>a</sup> Sum angles at C(16): [**13a**], 360.0(3); [**13b**], 359.9(8); [**14**]<sup>+</sup>, 360.0(7).

Table 7: Selected bond lengths ( $\text{\AA}$ ) and angles ( $^\circ$ ) for **13a**, **13b** and **14** in [**14**][BF<sub>4</sub>] $\cdot$ CH<sub>2</sub>Cl<sub>2</sub>.<sup>a</sup>

<i>Complex</i>	<b>16</b>	<b>18</b>
	<i>Subunit I</i>	
Fe(1)–Fe(2)	2.513(12)	2.498(3)
Fe(1)–C(11)	1.737(5)	1.79(2)
Fe(2)–C(13)	1.732(6)	1.677(18)
Fe(1)–C(12)	1.893(5)	1.927(17)
Fe(2)–C(12)	1.929(5)	1.886(15)
Fe(1)–C(14)	2.021(5)	1.934(14)
Fe(2)–C(14)	1.992(5)	1.925(17)
C(11)–O(11)	1.159(7)	1.14(2)
C(12)–O(12)	1.179(6)	1.155(17)
C(13)–O(13)	1.169(7)	1.189(19)
C(14)–C(15)	1.539(7)	1.54(3)
C(15)–C(41)	1.520(8)	1.50(2)
C(15)–S(3)		1.810(17)
C(22)–S(3)		1.72(2)
Fe(1)–C(12)–Fe(2)	82.3(2)	81.8(6)
Fe(1)–C(14)–Fe(2)	77.54(17)	80.7(6)
C(14)–C(15)–C(16)	112.6(4)	109.3(16)
C(15)–S(3)–C(22)		107.5(8)
	<i>Subunit II</i>	
Fe(3)–Fe(4)	2.515(12)	
Fe(3)–C(31)	1.750(8)	
Fe(4)–C(33)	1.730(7)	
Fe(4)–C(32)	1.898(7)	
Fe(3)–C(32)	1.924(7)	
Fe(3)–C(17)	2.008(5)	
Fe(4)–C(17)	1.999(5)	
C(31)–O(31)	1.139(8)	
C(33)–O(33)	1.143(8)	
C(32)–O(32)	1.158(8)	
C(17)–C(16)	1.541(6)	
C(16)–C(47)	1.514(7)	
Fe(3)–C(32)–Fe(4)	82.3(3)	
Fe(3)–C(17)–Fe(4)	77.75(19)	
C(15)–C(16)–C(17)	110.5(4)	
C(15)–C(16)	1.583(7)	

Table 8: Selected bond lengths (Å) and angles (°) for **16** and **18**.

## 7. Bibliography

- 1 (a) Maitlis, P. M.; Zanotti, V. *Catal. Lett.* **2008**, *122*, 80. (b) Ritleng, V.; Chetcuti, M. J. *Chem. Rev.*, **2007**, *107*, 797. (c) Chiusoli, G. P.; Maitlis, P. M. (Eds.) *Industrial Organic Processes*, RSC Publishing, **2006**. (d) Larsen R. (Ed.) *Organometallics in Process Chemistry*, WILEY-VCH, Weinheim, **2004**. (e) Beller, M.; Bolm C. (Eds.) *Transition Metals for Organic Synthesis: Building Blocks and Fine Chemicals*, WILEY-VCH, Weinheim, **2004**. (f) Zhang, S.; Xu, Q.; Sun, J.; Chen, J. *Chem. Eur. J.* **2003**, *9*, 5111. (g) Cornils, B.; Herrmann W. A. (Eds.) *Applied Homogeneous Catalysis with Organometallic Compounds*, WILEY-VCH, Weinheim, **2002**.
- 2 (a) Busetto, L.; Maitlis, P. M.; Zanotti, V. *Coord. Chem. Rev.* **2010**, *254*, 470. (b) Busetto, L.; Zanotti, V. *Inorg. Chim. Acta* **2008**, *361*, 3004. (c) Albano, V. G.; Busetto, L.; Marchetti, F.; Monari, M.; Zacchini, S.; Zanotti, V. *Organometallics*, **2007**, *26*, 3448. (d) Dennett, J. N. L.; Knox, S. A. R.; Anderson, K. M.; Charmant, J. P. H.; Orpen, A. G. *Dalton Trans.* **2005**, 63. (e) Busetto, L.; Marchetti, F.; Zacchini, S.; Zanotti, V. *Eur. J. Inorg. Chem.*, **2005**, 3250. (f) Busetto, L.; Zanotti, V. *J. Organomet. Chem.* **2005**, *690*, 5430. (g) Dennet, J. N. L.; Knox, S. A. R.; Charmant, J. P. H.; Gillon, A. L.; Orpen, A. G. *Inorg. Chim. Acta* **2003**, *354*, 29. (h) King, P. J.; Knox, S. A. R.; McCormick, G. J.; Orpen, A. G. *J. Chem. Soc., Dalton Trans.* **2000**, 2975. (i) Akita, M.; Hua, R.; Knox, S. A. R.; Moro-oka, Y.; Nakanishi, S.; Yates, M. I. *Chem. Commun.* **1997**, 51.
- 3 (a) Saouma, C. T.; Müller, P.; Peters, J. C. *J. Am. Chem. Soc.* **2009**, *131*, 10358. (b) Patureau, F. W.; de Boer, S.; Kuil, M.; Meeuwissen, J.; Breuil, P.-A. R.; Siegler, M. A.; Spek, A. L.; Sandee, A. J.; de Bruin, B.; Reek, J. N. H. *J. Am. Chem. Soc.* **2009**, *131*, 6683. (c) Esswein, A. J.; Veige, A. S.; Piccoli, P. M. B.; Schultz, A. J.; Nocera, D. G. *Organometallics* **2008**, *27*, 1073. (d) Adams, R. D.; Captain, B. *J. Organomet. Chem.* **2004**, *689*, 4521. (e) Severin, K. *Chem. Eur. J.*, **2002**, *8*, 1514. (f) Gade, L. H.; Memmler, H.; Kauper, U.; Schneider, A.; Fabre, S.; Bezougli, I.; Lutz, M.; Galka, C.; Scowen, I. J.; McPartlin, M. *Chem. Eur. J.* **2000**, *6*, 692.
- 4 (a) Akita, M.; Hua, R.; Knox, S. A. R.; Moro-oka, Y.; Nakanishi, S.; Yates, M. I. *J. Organomet. Chem.* **1998**, *569*, 71. (b) Akita, M.; Hua, R.; Moro-oka, Y.; Nakanishi, S.; Tanaka, M. *Organometallics* **1997**, *16*, 5572.
- 5 (a) Busetto, L.; Marchetti, F.; Renili, F.; Zacchini, S.; Zanotti, V. *Organometallics*, **2010**, *29*, 1797. (b) Busetto, L.; Marchetti, F.; Zacchini, S.; Zanotti, V.; *Organometallics* **2008**, *27*, 5058. (c) Busetto, L.; Marchetti, F.; Zacchini, S.; Zanotti, V. *Organometallics*, **2007**, *26*, 3577. (d) Busetto, L.; Marchetti, F.; Zacchini, S.; Zanotti, V. *Organometallics*, **2006**, *25*, 4808. (e) Albano, V. G.; Busetto, L.; Marchetti, F.; Monari, M.; Zacchini, S.; Zanotti, V. *Organometallics*, **2003**, *22*, 1326.
- 6 (a) Gervasio, G.; Marabello, D.; Sappa, E.; Secco, A. *J. Organomet. Chem.* **2005**, *690*, 3755. (b) Bruce, M. I.; Zaitseva, N. N.; Skelton, B. W.; White, A. H. *J. Chem. Soc., Dalton Trans.* **2002**, 1678. (c) Wojcicki, A. *Inorg. Chem. Comm.* **2002**, *5*, 82, and references therein. (d) Ogoshi, S.; Nishida, T.; Tsutsumi, K.; Ooi, M.; Shinagawa, T.; Akasaka, T.; Yamane, M.; Kurosawa, H. *J. Am. Chem. Soc.* **2001**, *123*, 3223. (e) Doherty, S.; Hogarth, G.; Waugh, M.; Clegg, W.; Elsegood, M. R. *J. Organometallics* **2000**, *19*, 4557. (f) Doherty, S.; Hogarth, G.; Waugh, M.; Clegg, W.; Elsegood, M. R. *J. Organometallics* **2000**, *19*, 5696. (g) Willis, R. R.; Calligaris, M.; Faleschini, P.; Gallucci, J. C.; Wojcicki, A. *J. Organomet. Chem.* **2000**, *593-594*, 465. (h) Doherty, S.; Hogarth, G.; Waugh, M.; Scanlan, T. H.; Clegg, W.; Elsegood, M. R. *J.*

- 
- Organometallics* **1999**, *18*, 3178. (i) Doherty, S.; Waugh, M.; Scanlan, T. H.; Elsegood, M. R. J.; Clegg, W. *Organometallics* **1999**, *18*, 679. (j) Doherty, S.; Elsegood, M. R. J.; Clegg, W.; Ward, M. F.; Waugh, M. *Organometallics* **1997**, *16*, 4251. (k) Chen, J.-T.; Chen, Y.-K.; Chu, J.-B.; Lee, G.-H.; Wang, Y. *Organometallics* **1997**, *16*, 1476.
- 7 Kurosawa, H.; Ogoshi, S. *Bull. Chem. Soc. Jpn.* **1998**, *71*, 973.
  - 8 Feher, F. J.; Green, M.; Rodrigues, R. A. *J. Chem. Soc., Chem. Comm.* **1987**, 1206.
  - 9 Gamble, A. S.; Birdwhistle, K. R.; Templeton, J. L. *J. Am. Chem. Soc.* **1990**, *112*, 1818.
  - 10 Gotzig, J.; Otto, H.; Werner, H. *J. Organomet. Chem.* **1985**, 287, 247.
  - 11 Huang, T. S.; Chen, J. T.; Lee, G. H.; Wang, Y. *J. Am. Chem. Soc.* **1993**, *115*, 1170.
  - 12 (a) Young, G. H.; Wojcicki, A. *J. Am. Chem. Soc.* **1989**, *111*, 6890; (b) Young, G. H.; Raphael, M. V.; Wojcicki, A.; Calligaris, M.; Nardin, G.; Bresciani-Pahor, N. *Organometallics* **1991**, *10*, 1934.
  - 13 Nucciarone, D.; Taylor, N. J.; Carty, A. J. *Organometallics* **1986**, *5*, 1179.
  - 14 Carleton, N.; Corrigan, J. F.; Doherty, S.; Pixner, R.; Sun, Y.; Taylor, N. J.; Carty, A. J. *Organometallics* **1994**, *13*, 4179.
  - 15 (a) Wojcicki, A. *J. Cluster Sci.* **1993**, *4*, 59; (b) Doherty, S.; Corrigan, J. F.; Carty, A. J.; Sappa, E. *Adv. Organomet. Chem.* **1995**, 37 39.
  - 16 (a) Willis, R. R.; Shuchart, C. E.; Wojcicki, A.; Rheingold, A. L.; Haggerty, B. S. *Organometallics* **2000**, *19*, 3179. (b) Doherty, S.; Elsegood, M. R. J.; Clegg, W.; Rees, N. H.; Scanlan, T. H.; Waugh, M. *Organometallics* **1997**, *16*, 3221.
  - 17 Attali, S.; Dahan, F.; Mathieu, F. *Organometallics* **1986**, *5*, 1376.
  - 18 Wojcicki, A.; Shuchart, C. E. *Coord. Chem. Rev.* **1974**, *7*, 122.
  - 19 Seyferth, D.; Womack, G. B.; Archer, C. M.; Dewan, J. C. *Organometallics* **1997**, *16*, 3221.
  - 20 (a) Dyke, A. F.; Knox, S. A. R.; Naish, P. J.; Taylor, G. E. *J. Chem. Soc., Dalton Trans.* **1982**, 1297. (b) Gracey, B. P.; Knox, S. A. R.; MacPherson, K. A.; Orpeng, A. G.; Stobart, S. R. *J. Chem. Soc., Dalton Trans.* **1985**, 1935.
  - 21 McArdle, C.P. *PhD. Thesis* University of Bristol **1998**.
  - 22 Knox, S. A. R.; Marchetti, F. *J. Organomet. Chem.* **2007**, 692, 4119.
  - 23 (a) Shapley, J. R.; Richter, S. I.; Tachikawa, M.; Keister, J. B. *J. Organomet. Chem.* **1975**, *94*, C 43. (b) Xue, Z.; Sieber, W. J.; Knobler, C. B.; Kaesz, H. B. *J. Am. Chem. Soc.* **1990**, *112*, 1825. (c) Farrugia, L.; Chi, Y.; Tu, W.-C. *Organometallics* **1993**, *12*, 1616.
  - 24 Breckenridge, S. M.; Taylor, N. J.; Carty, A. J. *Organometallics* **1991**, *10*, 837.

- 
- 25 Blenkiron, P.; Corrigan, J. F.; Taylor, N. J.; Carty, A. J.; Doherty, S.; Elsegood, M. R. J.; Clegg, W. *Organometallics* **1997**, *16*, 297.
- 26 Shuchart, C. E.; Willis, R. R.; Wojcicki, A.; Rheingold, A. L.; Haggerty, B. S. *Inorg. Chim. Acta* **2000**, *307* 1.
- 27 (a) Doherty, S.; Elsegood, M. R. J.; Clegg, W.; Rees, N. H.; Waugh, M. *Organometallics* **1996**, *15*, 2688. (b) Doherty, S.; Hogarth, G.; Elsegood, M. R. J.; Clegg, W.; Rees, N. H.; Waugh, M. *Organometallics* **1998**, *17*, 3331.
- 28 Doherty, S.; Elsegood, M. R. J.; Clegg, W.; Mampe, D. *Organometallics* **1997**, *16*, 1186.
- 29 Doherty, S.; Hogarth, G.; Elsegood, M. R. J.; Clegg, W.; Scanlan, T. H.; Waugh, M. *Organometallics* **1997**, *16*, 3178.
- 30 Doherty, S.; Elsegood, M. R. J.; Clegg, W.; Mampe, D.; Rees, N. H. *Organometallics* **1996**, *15*, 5302.
- 31 (a) Boss, K.; Cox, M. G.; Dowling, C.; Manning, A. R. *J. Organomet. Chem.* **2000**, *18*, 612. (b) Albano, V. G.; Busetto, L.; Monari, M.; Zanotti, V. *J. Organomet. Chem.* **2000**, *606*, 163. (c) Busetto, L.; Marchetti, F.; Zacchini, S.; Zanotti, V. *J. Braz. Chem. Soc.* **2003**, *14*, 902. (d) Busetto, L.; Marchetti, F.; Zacchini, S.; Zanotti, V. *Inorg. Chim. Acta* **2005**, *358*, 1204. (e) Busetto, L.; Marchetti, F.; Zacchini, S.; Zanotti, V. *Z. Naturforsch. B* **2007**, *62b*, 427.
- 32 Willis, R. R.; Calligaris, M.; Faleschini, P.; Wojcicki, A. *J. Cluster Sci.* **2000**, *11*, 233.
- 33 (a) Hegedus, L. S. *Transition Metals in the Synthesis of Complex Organic Molecules*, University Science Books, Mill Valley, CA, **1994**. (b) Gates, B. C.; Katzer, J. R.; Schuit, G. C. A. *Chemistry of Catalytic Processes*, McGraw-Hill, NY, **1979**. (c) Parshall, G. W.; Ittel, S. D. *Homogeneous Catalysis*, Wiley-Interscience, NY, **1992**.
- 34 Martinez, J. M.; Adams, H.; Bailey, N. A.; Maitlis, P. M., *J. Chem. Soc., Chem. Commun.* **1989**, 286.
- 35 Frohnapfel, D. S.; Templeton, J. L. *Coord. Chem. Rev.* **2000**, *206-207*, 199.
- 36 Casey, C. P.; Brady, J. T.; Boller, T. M.; Weinhold, F.; Hayashi, R. K. *J. Am. Chem. Soc.* **1998**, *120*, 12500.
- 37 (a) Davidson, J. L.; Wilson, W. F.; Manojlovic-Muir, L.; Muir, K. W. *J. Organomet. Chem.* **1983**, *254*, C6. (b) Feng, S. G.; White, P. S.; Templeton, J. L. *J. Am. Chem. Soc.* **1992**, *114*, 2951.
- 38 Ros, J.; Mathieu, R. *Organometallics* **1983**, *2*, 771.
- 39 Werner, H.; Wolf, J.; Nessel, A.; Fries, A.; Stempfle, B.; Nürnberg, O. *Can. J. Chem.* **1995**, 1050.
- 40 Deeming, A. J.; Felix, M. S. B.; Nuel, D.; Powell, N. J.; Tocher, D. A. *J. Organomet. Chem.* **1990**, *384*, 181.



- 
- 41 Della Pergola, R.; Garlaschelli, L.; Martinengo, S.; Manassero, M.; Sansoni, M. *J. Organomet. Chem.* **2000**, 593, 63.
- 42 King, R. B.; Treichel, P. M.; Stone, F. G. A.; *J. Am. Chem. Soc.* **1961**, 83, 3600.
- 43 (a) Kruger, C.; Tsay, Y. H.; Grevels, F. –W.; Koerner von Gustorf, E. *Isr. J. Chem.* **1972**, 10, 201. (b) Grevels, F. –W.; Koerner von Gustorf, E. *Liebigs Ann. Chem.* **1975**, 547. (c) Grevels, F. –W.; Shulz, D.; Koerner von Gustorf, E.; Bunbury, D. St. P. *J. Organomet. Chem.* **1975**, 91, 341.
- 44 (a) Casey, C. P.; Marder, S. R.; Adams, B. R. *J. Am. Chem. Soc.* **1985**, 107, 7700. (b) Casey, C. P.; Meszaros, M. W.; Fagan, P. J.; Bly, R. K.; Colborn, R. E. *J. Am. Chem. Soc.* **1986**, 108, 4053.
- 45 (a) Dyke, A. F.; Knox, S. A. R.; Naish, P. J.; Orpen, A. G. *J. Chem. Soc., Chem. Commun.* **1980**, 441. (b) Kao, S. C.; Lu, P. P. Y.; Pettit, R. *Organometallics* **1982**, 1, 911.
- 46 Yañez, R.; Ros, J.; Mathieu, R. *J. Organomet. Chem.* **1991**, 414, 209.
- 47 (a) Beck, J. A.; Knox, S. A. R.; Riding, G. H.; Taylor, G. E.; Winter, M. J. *J. Organomet. Chem.* **1980**, 202, C49. (b) Dickson, R. S.; Mok, C.; Pain, G. N. *J. Organomet. Chem.* **1979**, 166, 385.
- 48 (a) Dyke, A. F.; Knox, S. A. R.; Morris, M. J.; Naish, P. J. *J. Chem. Soc., Dalton Trans.* **1983**, 1417. (b) Casey, C. P.; Cariño, R. S.; Sakaba, H. *Organometallics* **1997**, 16, 419.
- 49 Casey, C. P.; Fagan, P. J. *J. Am. Chem. Soc.* **1978**, 100, 3620.
- 50 Green, M. L. H.; Nagy, P. L. I. *J. Organomet. Chem.* **1963**, 1, 58.
- 51 (a) Brady, R. C.; Pettit, R. *J. Am. Chem. Soc.* **1980**, 102, 6181. (b) Herrmann, W. A. *Angew. Chem., Int. Ed. Engl.* **1982**, 21, 117.
- 52 Bruce, G. C.; Knox, S. A. R.; Phillips, A. J. *J. Chem. Soc., Chem. Comm.* **1990**, 716.
- 53 Bruce, C. G.; Gangnus, B.; Garner, S. E.; Knox, S. A. R.; Orpen, A. G.; Phillips, A. J. *J. Chem. Soc., Chem. Comm.* **1990**, 1360.
- 54 Doherty, N. M.; Howard, J. A. K.; Knox, S. A. R.; Terrill, N. J.; Yates, M. I. *J. Chem. Soc., Chem. Comm.* **1989**, 638.
- 55 (a) Batchelor, R. J.; Einstein, F. W. B.; Jones, C. H. W.; Sharma, R. D. *Organometallics* **1987**, 6, 2164. (b) Casey, C. P.; Marder, S. R.; Colborn, R. E.; Goodson, P. A. *Organometallics* **1986**, 5, 199.
- 56 Ros, J.; Mathieu, R. *Organometallics* **1983**, 2, 771.
- 57 (a) Love, R. A.; Koetzle, T. F.; Williams, G. J. B.; Andrews, L. C.; Bau, R. *Inorg. Chem.* **1975**, 14, 2653. (b) Guggenberger, L. J. *Inorg. Chem.* **1973**, 12, 499.
- 58 (a) Terada, M.; Masaki, Y.; Tanaka, M.; Akita, M.; Moro-oka, Y. *J. Chem. Soc., Chem. Commun.* **1995**, 1611. (b) Etienne, M.; Talarmin, J.; Toupet, L. *Organometallics* **1992**, 11, 2058. (c) Etienne, M.; Toupet, L. *J. Chem. Soc., Chem. Commun.* **1989**, 1110.

- 
- 59 Akita, M.; Kato, S.; Terada, M.; Masaki, Y.; Tanaka, M.; Moro-oka, Y. *Organometallics*, **1997**, *16*, 2392.
- 60 Adams, R. D.; Chen, G.; Chen L.; Yin, J. *Organometallics* **1993**, *12*, 2644.
- 61 Albano, V. G.; Busetto, L.; Marchetti, F.; Monari, M.; Zacchini, S.; Zanotti, V. *J. Organomet. Chem.* **2004**, *689*, 528.
- 62 Albano, V. G.; Busetto, L.; Marchetti, F.; Monari, M.; Zacchini, S.; Zanotti, V. *Organometallics* **2004**, *23*, 3348.
- 63 (a) Vigneron, J. P.; Méric, R.; Larchevêque, M.; Debal, A.; Kunesch, G.; Zagatti P.; Gallois, M. *Tetrahedron Lett.* **1982**, *23*, 5051. (b) Vigneron, J. P.; Méric, R.; Larchevêque, M.; Debal, A.; Lallemand, J. Y.; Kunesch, G.; Zagatti, P.; Gallois, M. *Tetrahedron* **1984**, *40*, 3529.
- 64 (a) Tomioka, K.; Ishiguro, T.; Koga, K. *J. Chem. Soc., Chem. Commun.* **1979**, 652. (b) Tomioka, K.; Ishiguro, T.; Iitaka Y.; Koga, K. *Tetrahedron* **1984**, *40*, 1303.
- 65 (a) Drew, M. G. B.; Mann, J.; Thomas, A. *J. Chem. Soc., Perkin Trans. 1* **1986**, 2279. (b) Mann, J.; Thomas, A. *J. Chem. Soc., Perkin Trans. 1* **1986**, 2287.
- 66 (a) Zhang, Q.; Cheng, M.; Hu, X.; Li, B.-G.; Ji, J.-X. *J. Amer. Chem. Soc.* **2010**, *132*, 7256. (b) Ugurchieva, T. M.; Veselovsky, V. V. *Russ. Chem. Rev.* **2009**, *78*, 337. (c) Casiraghi, G.; Zanardi, F.; Battistini, L.; Rassu, G. *Synlett* **2008**, 1525. (c) P. Langer, *Synlett* **2006**, 3369.
- 67 (a) El Kettani, S. E.-C.; Lazraq, M.; Ranaivonjatovo, H.; Escudié, J.; Gornitzka H.; Ouhsaine, F. *Organometallics* **2007**, *26*, 3729. (b) Shiu, Y.-T.; Madhushaw, R. J.; Li, W.-T.; Lin, Y.-C.; Lee, G.-H.; Peng, S.-M.; Liao, F.-L.; Wang, S.-L.; Liu, R.-S. *J. Am. Chem. Soc.* **1999**, *121*, 4066. (c) Saberi, S. P.; Salter, M. M.; Slawin, A. M. Z.; Thomas, S. E.; Williams, D. J. *J. Chem. Soc., Perkin Trans. 1* **1994**, 167. (d) Klimes J.; Weiss, E. *Angew. Chem. Int. Ed. Eng.*, **1982**, *21*, 205.
- 68 Bott, S. G.; Yang, K.; Richmond, M. G. *J. Organomet. Chem.*, **2006**, *691*, 3771.
- 69 (a) Ramazani, A.; Mahyari, A. T.; Rouhani, M.; Rezaei, A. *Tetrahedron Lett.* **2009**, *50*, 5625. (b) Ugurchieva, T. M.; Lozanova, A. V.; Zlokazov, M. V.; Veselovsky, V. *Russ. Chem. Bull., Int. Ed.* **2008**, *57*, 657. (c) Chen, Z.; Davies, E.; Miller, W. S.; Shan, S.; Valenzano, K. J.; Kyle, D. J. *Bioinorg. Med. Chem. Lett.* **2004**, *14*, 5275. (d) Sato, S.; Komoto, T.; Kanamaru, Y.; Kawamoto, N.; Okada, T.; Kaiho, T.; Mogi, K.; Morimoto, S.; Umehara, N.; Koda, T.; Miyashita, A.; Sakamoto, T.; Niino, Y.; Oka, T. *Chem. Pharm. Bull.* **2002**, *50*, 292.
- 70 Albano, V. G.; Busetto, L.; Marchetti, F.; Monari, M.; Zacchini, S.; Zanotti, V. *Organometallics* **2004**, *23*, 3348.
- 71 Paradies, J.; Fröhlich, R.; Kehr, G.; Erker, G. *Organometallics* **2006**, *25*, 3920.
- 72 Rogers, R. D.; Hrcir, D. C. *Acta Crystallogr., Sect. C* **1984**, *40*, 1160.
- 73 F. A. Cotton, G. Wilkinson, C. A. Murillo and M. Bochmann, *Advanced Inorganic Chemistry*, 6th Ed., Wiley, New York, **1999**.
- 74 Connelly, N. G.; Geiger, W. E. *Chem. Rev.* **1996**, *96*, 877.
- 75 Casey, C.P.; Austin, E.A. *Organometallics* **1987**, *6*, 2157.
- 76 Herrmann, W. A. *Adv. Organomet. Chem.* **1982**, *20*, 159.

- 
- 77 P. Zanello Inorganic Electrochemistry. Theory, Practice and Application; RSC:Cambridge, U.K., **2003**.
- 78 Gallo, E.; Solari, E.; Re, N.; Floriani, C.; Chiesi-Villa, A.; Rizzoli, C. *J. Am. Chem. Soc.* **1997**, *119*, 5144.
- 79 (a) Moinet, C.; Romkn, E.; Astruc, D. *J. Organomet. Chem.* **1977**, *128*, C45. (b) Nesmeyanov, A. N.; Vol'kenau, N. A.; Petrakova, V. A. *Bull. Acad. Sci. USSR* **1974**, 2083. (c) Nesmeyanov, A. N.; Vol'kenau, N. A.; Petrakova, V. A.; Kotova, L. S.; Denisovich, L. I. *Proceedings Acad. Sci. USSR*, **1975**, *217*, 475.
- 80 Busetto, L.; Marchetti, F.; Zacchini, S.; Zanotti, V. *Organometallics* **2005**, *24*, 2297.
- 81 Herrmann, W. A. *Adv. Organomet. Chem.* **1982**, *20*, 159.
- 82 Handbook of Chemistry and Physics, 81 st edition, CRC press.
- 83 Willker, W.; Leibfritz, D.; Kerssebaum R.; Bermel, W. *Magn. Reson. Chem.* **1993**, *31*, 287.
- 84 Ambrosetti, R.; Ricci, D. *Rev. Sci. Instrum.* **1991**, *62*, 2281.
- 85 Pinzino, C.; Forte, C. EPR-ENDOR, ICQEM-CNR Rome, Italy, **1992**.
- 86 Duling, D.R. *J. Magn. Reson. B* **1994**, *104*, 105.
- 87 Spartan '08, Wavefunction, Inc. 18401 Von Karman Avenue, Suite 370 Irvine, CA 92612 U.S.A.
- 88 Kim, K.; Jordan, K. D. *J. Phys. Chem.* **1994**, *98*, 10089.
- 89 Stephens, P.J.; Devlin, F. J.; Chabalowski, C. F.; Frisch, M. J. *J. Phys. Chem.* **1994**, *98*, 11623.
- 90 Becke, A. D. *Phys. Rev. A* **1988**, *38*, 3098.
- 91 Lee, C.; Yang, W.; Parr, R. G. *Phys. Rev. B* **1988**, *37*, 785.
- 92 Wilkinson, G. *Org. Syn.* **1956**, *36*, 31.
- 93 Doherty, N. M.; Knox, S. A. R. *Inorg. Synth.* **1989**, *25*, 179.